Geomech. Geophys. Geo-energ. Geo-resour. (2022) 8:211
https://doi.org/10.1007/s40948-022-00516-w

REVIEW

Hydraulic stimulation strategies in enhanced geothermal systems (EGS): a review

Yunzhong Jia · Chin-Fu Tsang · Axel Hammar · Auli Niemi

Received: 4 August 2022 / Accepted: 6 November 2022 / Published online: 28 November 2022

Abstract In enhanced geothermal systems (EGS), the natural permeability of deep rocks is normally not high enough and needs to be increased. Permeability increase can be achieved through various stimulation methods, such as hydraulic, chemical, and thermal stimulation. Among these, hydraulic stimulation is the most commonly used technique to increase both reservoir permeability and the specific area for heat exchange. A comprehensive understanding of the underlying processes towards an optimization of hydraulic stimulation performance while minimizing the potential of unwanted induced seismicity is a critical prerequisite for a successful development of any EGS site. In this paper, we review the hydraulic stimulation strategies that have been developed and implemented for EGS. We begin with a description of the underlying mechanisms through which the permeability and heat exchange area increases are achieved. We then discuss the mechanisms of fluid injection-induced seismicity during and after a hydraulic stimulation operation. After that, alternative hydraulic stimulation strategies, namely conventional hydraulic stimulation, multi-stage fracturing, and cyclic soft stimulation, are reviewed based on current research in theoretical studies as well as, laboratory, and in-situ field experiments. Finally, some representative EGS projects are reviewed, focusing on fluid injection strategies, seismic responses, and reservoir permeability enhancement performance. The review shows the importance and need of (a) a comprehensive geological characterization of the natural fracture system including the nearby fault zones as well as the in-situ stress conditions, prior to the development of the site, (b) a proper design of the well arrangement, such as the positioning of the injection and production wells, and (c) the selection of an appropriate fluid injection strategy for the system at hand.

Article highlights

- A comprehensive geological characterization of the natural fracture system and nearby fault zones is critical before the development of an EGS project.
- Proper design of the arrangement of the injection and production wells as well as the fluid injection

Y. Jia
State Key Laboratory of Coal Mine Disaster Dynamics and Control, Chongqing University, Chongqing 400044, China

Y. Jia · C.-F. Tsang · A. Niemi (✉)
Department of Earth Sciences, Uppsala University, Villavägen 16, 75236 Uppsala, Sweden
e-mail: auli.niemi@geo.uu.se

C.-F. Tsang
Earth Sciences Division, Lawrence Berkeley National Laboratory, 1 Cyclotron Rd, Berkeley, CA 94720, USA

A. Hammar
E. On Värme, Eriksfältsgatan 24, 21455 Malmö, Sweden

strategy are essential elements for successfully developing an EGS project.
- Further research in coupled thermo-hydro-mechanical-chemical processes during and after a fluid injection operation in EGS is needed, in particular for better understanding of the processes related to induced seismicity.

Keywords Hydraulic stimulation strategies · Reservoir permeability · Heat extraction · Seismic risks · Enhance geothermal systems (EGS)

1 Introduction

Geothermal energy is the thermal energy stored in the deep sub-surface of the earth. It is a potentially very important energy source because of its vast reserves and wide availability (Gong et al. 2020; Pan et al. 2019). One of the main obstacles that has been limiting the development of EGS is the low permeability of the deep rocks at the depths where most of the geothermal energy is stored. Thus, stimulation operations are commonly needed to enhance the reservoir permeability and to increase the specific area for heat exchange (Lu 2018; Olasolo et al. 2016). A system of developing geothermal energy through such stimulation operations is called an enhanced geothermal system (EGS).

Basic reservoir stimulation methods include hydraulic stimulation, chemical stimulation, and thermal stimulation. Of these, hydraulic stimulation is the most commonly used one in both conventional oil and gas industry and in unconventional gas or shale gas development. In this approach, a large amount of fluid is injected into the target reservoir from a packered-off section of a borehole, and the resulting high pressure cracks the rock creating new tensile fractures and, if a number of natural fractures are present, it may also cause opening and/or shear of these natural fractures (Ghassemi 2012; McClure and Horne 2014a, b; Elsworth et al. 2016; Lei et al. 2021). Increased permeability is a result from this tensile fracture aperture opening and the shear dilation of the existing fractures. Furthermore, fracture opening and shearing can also create fractures that connect to natural fractures further away, thereby significantly increasing the overall connectivity and permeability of the reservoir. At the same time, fracture surface areas are also increased, which is important for the heat exchange area and heat extraction from the surrounding rock. Chemical stimulation involves the injection of an acidic fluid into the formation while using a fluid pressure lower than the reservoir breakdown pressure. Permeability increase is then be realized through mineral dissolution, transport, and precipitation processes. This method has been commonly used in the oil and gas industry to enhance oil recovery (Economides and Nolte 1989; Portier et al. 2009; Smith and Hendrickson 1965), it can also be used in EGS, such as in Groß Schönebeck (Henninges et al. 2012), Desert Peak (Davatzes et al. 2012), and Soultz (Portier et al. 2009). For thermal stimulation, cold water is normally injected into the reservoir for a specific time, typically several weeks. Due to the large temperature difference between the injected low-temperature water and the high-temperature reservoir rock, the induced thermal stress causes deformation of in situ natural fractures and initiates new fractures (Liu et al. 2020). Among these three basic stimulation methods, hydraulic stimulation is the most commonly used in EGS to increase reservoir permeability and heat exchange extraction volume. Therefore, hydraulic stimulation is the focus of the present work.

In hydraulic stimulation, an optimal generation of a well-connected, high permeability fracture network with large heat exchange area towards the surrounding rock is critical for an optimal performance. For the design of such a system, a comprehensive understanding of the underlying mechanisms and the role of various factors, such as the existing natural fracture network, is essential. Extensive work has been carried out in this respect, on the related processes and effects (Bowker 2007; Brown 1989; Evans et al. 2005; Fisher et al. 2004; Gale et al. 2007; Ito 2003; Ito and Hayashi 2003; King 2010; Ledésert et al. 2010; Murphy and Fehler 1986; McClure and Horne 2014a, b; Pine and Batchelor 1984; Yin et al. 2019). However, work still remains to be done, especially concerning the role of the natural fracture network and fault zones with varying characteristics.

A specific challenge in hydraulic stimulation is the risk of injection-induced seismicity, both during and after the water injection (Ellsworth 2013; Elsworth et al. 2016). Even though the vast majority of the seismic events observed during the EGS developments have been of magnitudes less than 3.0, some cases

of damaging earthquakes have also been reported (Kim et al. 2018a; Knoblauch and Trutnevyte 2018). For instance, a series of earthquakes occurred at the Basel geothermal site in Switzerland from December 2006 and March 2007, with the maximum magnitude of M_w 3.4 (Evans et al. 2012), which led to the suspension of the Basel EGS project. More recently, an earthquake in the Pohang geothermal field in South Korea in November 2017, with a magnitude of M_w 5.5, also directly resulted in the suspension of the Pohang geothermal project (Grigoli et al. 2018). To mitigate seismic risks associated with EGS development, significant research effort has lately been invested into understanding the mechanisms related to fluid injection-induced seismicity (Atkinson et al. 2020; Schultz et al. 2020; Lei et al. 2021; Lei and Tsang 2022).

None of these reviews aims, however, to give a complete overview of all aspects of a hydraulic stimulation operation. In the present paper, we will present a review of hydraulic stimulation strategies for permeability and heat exchange area enhancement while limiting induced seismicity, with an emphasis on insight gained and lessons learned from previous projects. We will first briefly present the mechanisms behind permeability enhancement, heat exchange area increase, and fluid injection-induced seismicity during and after hydraulic stimulation. Next, some typical hydraulic stimulation methods are described, namely conventional hydraulic stimulation, multistage fracturing, and cyclic soft stimulations (CSS), based on findings from both theoretical studies and from laboratory and in-situ experiments. This is followed by summaries of some representative in-situ hydraulic stimulation in EGS projects with a focus on their fluid injection procedures, observed seismic response, and reservoir permeability enhancement performance. Lessons learned in each case are discussed, and some overall conclusions are then presented.

2 The mechanism of hydraulic stimulation and fluid injection-induced seismicity

In this section, we first present an overview of the basic mechanism of permeability enhancement during a hydraulic fracturing operation. Next, we discuss the mechanism of the heat exchange area enhancement. Finally, we review some recent studies on the mechanisms of fluid injection-induced seismicity.

2.1 The mechanism of permeability enhancement in EGS

The target reservoirs for EGS are most likely located at depths of several kilometers, where the subsurface is hot enough for heat extraction. Due to the great depths and the associated high in-situ stresses, the formations usually have very low permeability, which would need to be increased. Hydraulic stimulation is one of the most important methods used to increase the reservoir permeability as well as the heat exchange area of the reservoir (Tester et al. 2006; Kennedy et al. 2010; Meyer and Bazan 2011; Pan et al. 2019; Yin et al. 2020, 2021a).

Hydraulic stimulation is a relatively complicated coupled process involving fluid flow, new fracture creation, tensile and shear deformation of newly created and pre-existing natural fractures, and fluid leak-off from fractures to rock matrix at multiple space and time scales.The initial concept of hydraulic stimulation assumed that a single, planar tensile fracture was formed in the direction of the maximum stress, which appears to be what happens in oil and gas reservoirs (Brown et al. 2012), and this was named hydraulic fracturing. However, Willis-Richards et al. (1996) found that shearing slip of pre-existing natural fractures with shear dilation effect was actually the dominant stimulation mechanism, which was then named shear stimulation, hydraulic shearing, or hydroshearing (Cladouhos et al. 2011). Various numerical models have been developed to simulate the shear slip of pre-existing natural fractures (Bruel 2007; Dempsey et al. 2015; Kohl and Mégel 2007; McClure and Horne 2011, 2013a; Rachez and Gentier 2010; Riahi and Damjanac 2013; Tao 2010; Zhou and Ghassemi 2011). As for the dominant mechanism of hydraulic stimulation in EGS, early in-situ experiments at Fenton Hill, USA, found that some natural fractures were both opened and sheared during the hydraulic stimulation through an analysis of micro-seismicity data (Barton et al. 1988; Brown 1989; Brown et al. 2012; Brown and Duchane 1999; Fehler 1989; Moore and Pearson 1989; Norbeck et al. 2018; Pearson 1981; Pine and Batchelor 1984). The experience from the Soultz EGS project also indicated that both the newly created hydraulic fractures and the shear slip

of pre-existing natural fractures played a vital role in the permeability enhancement (Grecksch et al. 2003; Jung and Weidler 2000; McClure 2012; McClure and Horne 2013b, 2013c; Norbeck et al. 2018; Rinaldi and Rutqvist 2019). Thus, hydraulic stimulation in EGS combines hydraulic fracturing and hydroshearing, and this viewpoint is now commonly accepted in the EGS community.

Based on previous in-situ experiments and observations, McClure and Horne (2014a, b) summarized four potential mechanisms that may dominate during a hydraulic stimulation operation in EGS, as shown in Fig. 1. The first mechanism is the pure opening mode which is based on the conventional hydraulic fracturing concept, assuming no natural fractures within the reservoir. During stimulation, the injected fluid cracks the reservoir and creates newly opened propagating fractures, thus creating fluid channels and increasing permeability (Adachi et al. 2007; Economides and Nolte 1989; Geertsma and De Klerk 1969; Nordgren 1972; Perkins and Kern 1961). The second stimulation mechanism is the pure shear mode (hydroshearing), which means that permeability enhancement comes from the shear slip of pre-existing natural fractures. In this process, the injected fluid increases the pore pressure within the natural fractures, decreases the normal effective stress on fracture surfaces, and triggers shear slip under appropriate local stress conditions (effective normal and shear stresses). The third mode, defined as the primary fracturing with shear stimulation leak-off, represents a combination of new fracture opening (hydraulic fracturing) and induced shear slip of in-situ natural fractures (hydroshearing). This concept applies to low permeability rocks with a low density of natural fractures, and several numerical models have been developed to study this idea (Nagel et al. 2011; Palmer et al. 2007; Rogers et al. 2010; Warpinski et al. 2001). The fourth stimulation mechanism is called mixed-mechanism stimulation and is also a combination of hydraulic fracturing and hydroshearing. Under

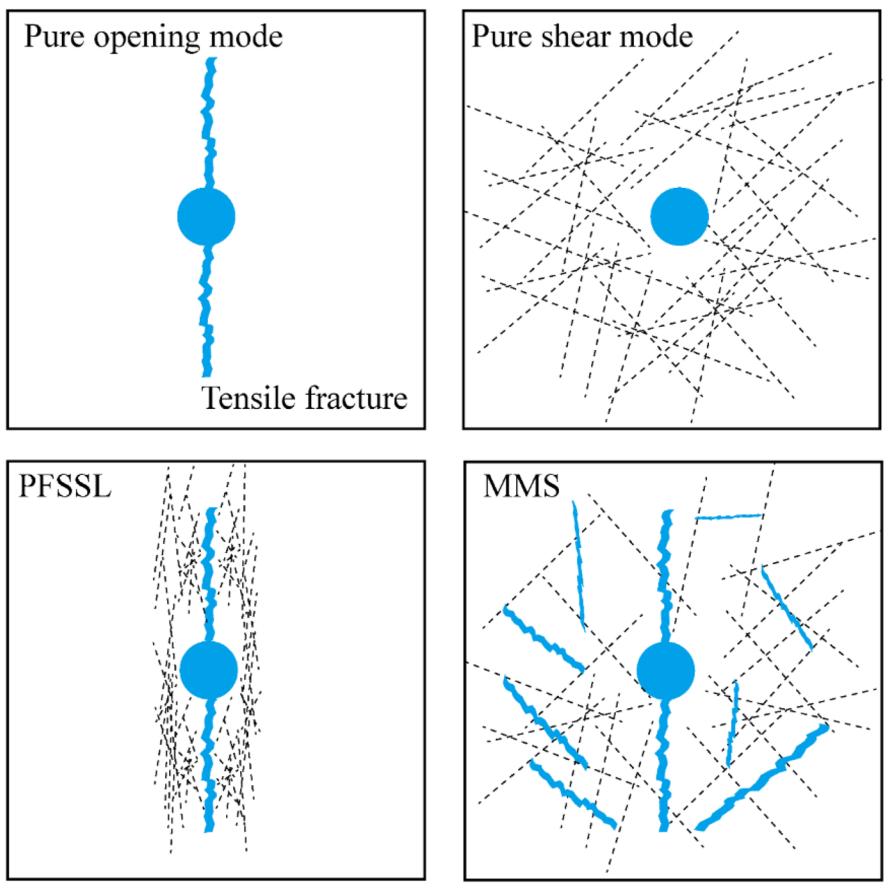

Fig. 1 The schematic presentation of the four potential mechanisms for hydraulic stimulation in EGS, including a) pure opening mode, pure shear mode, primary fracturing with shear stimulation leakoff (PFSSL), and mixed-mechanism stimulation (MMS) (modified from McClure and Horne 2014a, b)

this mechanism, high-pressure fluid first cracks the reservoir around the injection point, creates tensile fractures, and drives fracture propagation. When encountering natural fractures, the hydraulic fractures may terminate and then propagate along the direction of natural fractures or cross the natural fractures, depending on the angle between the natural fractures and the hydraulically propagating fractures, the fluid pressure, in-situ stress state, and other geological parameters.

Based on the above four potential mechanisms, research has been carried out to identify the critical parameters that determine which mechanisms may dominates during hydraulic stimulation in an EGS site. These parameters include:

(i) *Reservoir's initial transmissivity and transmissivity heterogeneity*. Numerical simulations indicate that if the initial transmissivity is very low near the borehole because of the sparse presence of natural fractures or their very small fracture hydraulic apertures, tensile fracture may be opened near the injection borehole when the injection pressure exceeds rock breakdown pressure. On the other hand, if the transmissivity is high, representing the presence of connected hydraulically conducting fractures, a lower injection pressure would be required to cause shear displacement and dilation on these natural fractures.

(ii) *The storativity of the pre-existing natural fracture systems*. Numerical simulation results indicate that if the natural fractures are closed and have low storativity, fluid injection will induce very rapid natural fractures propagations. In this case, the closed natural fractures cannot contain much fluid, and pressure buildup is relatively fast. Moreover, the experience from Soultz geothermal site indicated that if there is a large fault zone near the injection borehole, the high storativity of the fault zone can accommodate a large injection fluid volume (Cuenot et al. 2008, 2010; Dezayes and Genter 2008). In that case only shearing fractures were observed, but no tensile fracture opening. Hence, we may conclude that fracture tensile opening tends to take place in regions of low fracture storativity and shear displacement in regions of high fracture storativity.

(iii) *The development degree of the fault zone*. The development degree indicates the fracture density in the target reservoir. A well-developed or mature natural fracture system with high fracture density and/or a fault zone with reasonable thickness increases the tendency for the shear slip of natural fractures. Moreover, optimally oriented critical fractures intersecting the borehole have large possibility for shearing. Similarly fault zones with large transmissivity and storativity have a higher potential for shear slip initiation, assuming a sufficiently large injection pressure is imposed. However, after the initiation of the shear slip of natural fractures, the resulting increase in the permeability quickly lowers the pressure and hence the probability of large tensile fracture formation within the reservoir (Lei et al. 2021; McClure and Horne 2011, 2014a, b).

(iv) *Fluid injection rate and borehole bottom-hole pressure*. Evidence from the GPK2 well at Soultz, France, indicated that if the bottom-hole fluid pressure remained substantially below the minimum principal stress due to the low fluid injection rate, the shear slip of pre-existing fractures would be the dominant mechanism and many seismic events with the magnitude less than 2.0 were observed (Valley and Evans 2006). A similar phenomenon was observed at Cooper Basin EGS sites in Australia, where the shear slip was the dominant stimulation mechanism (Baisch et al. 2006, 2009). Conversely, if the fluid was injected into the reservoir with a high injection rate and high bottom-hole pressure, a main hydraulic fracture would be created, which was found to be the case behind the permeability increase of GPK1 and GPK4 wells in Soultz, France (Tischner et al. 2007).

2.2 The mechanism of heat extraction volume increase in EGS

Another objective of hydraulic stimulation is to increase the heat extraction volume and heat exchange surface area, as the effectiveness of heat exchange between the working fluid and the rock is critical in determining whether the EGS site is successful or not.

Research indicates that water circulation in EGS is primarily dominated by flow in the fractures (a single fracture or fracture network), rather than the rock matrix (Baisch et al. 2006; Brown 1997, 2009; Brown and Duchane 1999; Genter et al. 2012; Koh et al. 2011). Therefore, the flow characteristics through the fractures and the heat exchange efficiency between circulating fluid and the surrounding rocks will determine the heat production efficiency (Guo et al. 2016). Thus, it is highly desirable that fluid flow is in contact with a large area of fracture surfaces and that fractures with such flow cover a large rock volume. Spatial heterogeneity in flow will be created during a hydraulic stimulation operation due to the target reservoir's complicated geological setting (Kosakowski et al. 2001; Méheust and Schmittbuhl 2000; Neretnieks 1987). When fluid flow takes place through a fracture network with fractures of variable permeability values and if, further, individual fractures have a heterogeneous aperture distribution, channelized preferential flow paths would likely be formed (Moreno and Tsang 1994; Tsang and Neretnieks 1998; Tsang and Tsang 1989). Channelized flow is not optimal for heat extraction as the interface between the rock and the circulating flow is reduced. In addition, the phenomenon may be self-enhancing. Rock matrix near the preferential flow paths cools faster than those farther from the flow paths and the cooled rock body could then induce thermal stress and decrease the effective compressive stress near the preferential flow paths, with the possibility of increased local hydraulic permeability, which will make the fluid flow even more channelized along those preferential paths. This phenomenon is not desirable as these preferential paths would carry an increasing portion of the fluid flow, thus leading to early production temperature decline.

The above discussion is illustrated in Fig. 2. Chen and Jiang (2016) presented the following equations to describe the heat conduction in the rock matrix and heat convection and advection for the fluid within the fractures, respectively:

$$\frac{\partial[\varepsilon(\rho C_p)_f T_f]}{\partial t} + \mathrm{u}\cdot\nabla[(\rho C_p)_f T_f] = \nabla\cdot(k_f^{eff}\nabla T_f) + ha(T_s - T_f) \quad (1)$$

$$\frac{\partial[(1-\varepsilon)(\rho C_p)_s T_s]}{\partial t} = \nabla\cdot(k_s^{eff}\nabla T_s) - ha(T_s - T_f) \quad (2)$$

In these equations, ρ [kg/m^3] is the density; ε [dimensionless] is the porosity; C_p [J/kg/K] is the heat capacity; the subscript f denotes the property of the working fluid and s denotes the property of the solid (rock matrix); **u** [m/s] is the superficial velocity vector; T [K] is the temperature; a [1/m] is the specific surface area of the fractures; h [W/m^2/K] is the convective heat transfer coefficient. The term $ha(T_s$-$T_f)$ appears in both equations. It describes the heat exchange between the rock matrix and the working fluid in the fractures. The specific surface area represents the rock-fluid heat exchange area per unit reservoir volume. This parameter is a purely geometrical parameter with its value associated with the fracture morphology (Jiang et al. 2014). The heat transfer rate is directly proportional to the specific surface area based on the effective medium theory. It is a direct reflection of the fact that with a larger specific surface area of the fractures, the heat exchange will be more efficient.

Finally, it is useful to highlight the difference between permeability enhancement and specific surface area improvement for heat extraction due to hydraulic stimulation. After a successful hydraulic stimulation, the permeability is enhanced. This permeability enhancement may be due to the creation of one main fracture between the injection well and the production well (Case I in Fig. 2b), or due to the creation of N fractures between the two wells (Case II in Fig. 2b). For the same permeability enhancement, with the flow rate Q between the injection and production wells in the two cases being kept equal, then based on the cubic law, the apertures of the fractures in the two cases can be related through $e_1^3/12 = Ne_2^3/12$, so that $e_2 = e_1/N^{1/3}$. Now, for Case I, the porosity is e_1/L, and the specific surface area for heat exchange as defined by Chen and Jiang (2016) is $1/L$, where L is the length of the reservoir along the well. As for case II, with N fractures the porosity is $Ne_2/\mathrm{L} = N^{2/3}e_1/\mathrm{L}$, much larger than that of Case I and thus resulting in a slower flow velocity as compared with Case I. Further, in Case II, the specific surface area for heat exchange is N/L, which is N times larger than the specific surface area in case I. Hence, even though the flow in Case I and in Case II are the same (meaning a similar permeability enhancement due to hydraulic fracturing stimulation), Case II provides a significantly better condition for heat transfer in EGS.

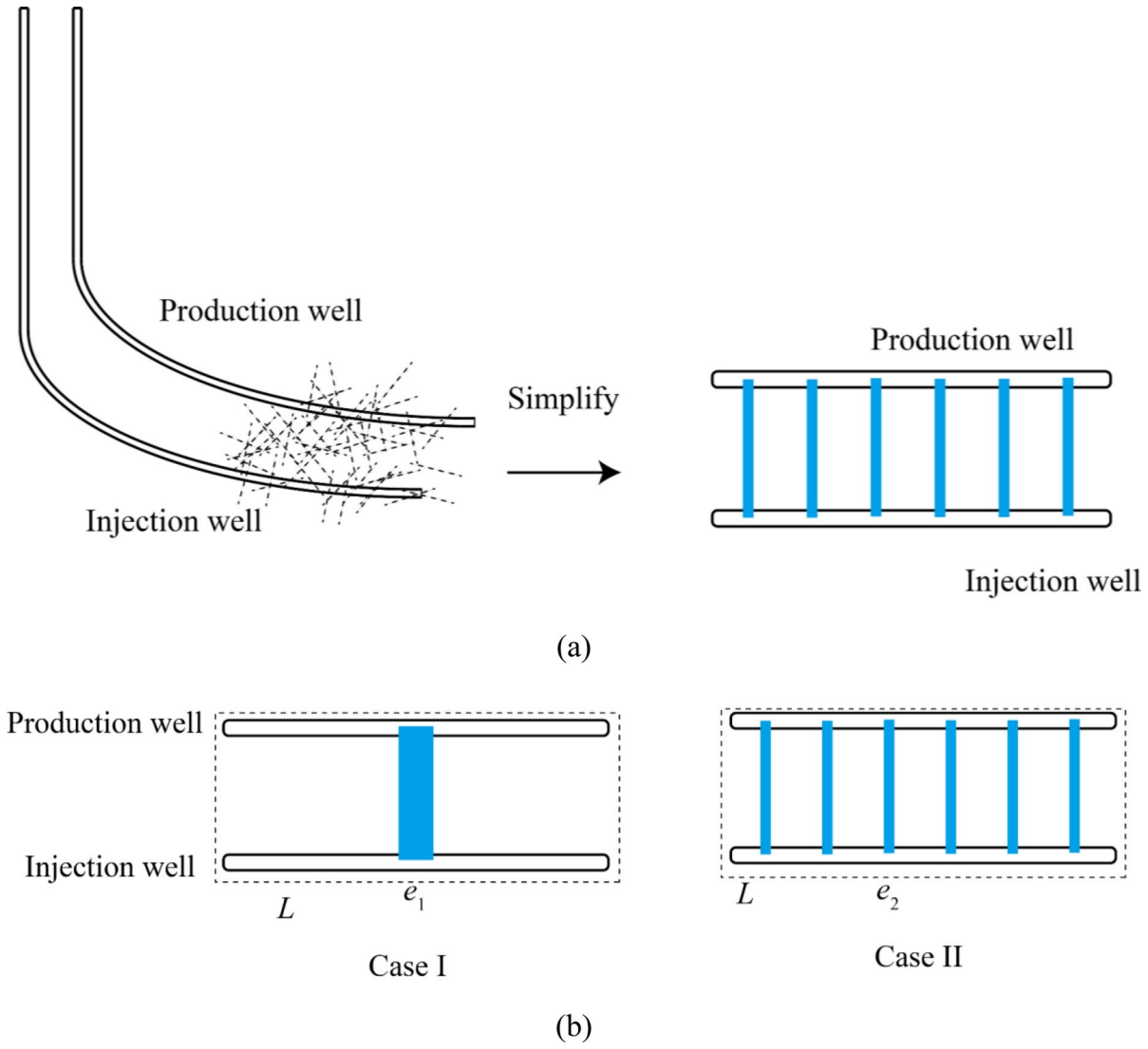

Fig. 2 **a** A schematic simplification of a fracture network for heat extraction between fluid and rock in EGS. **b** Two extreme cases illustrate the difference in permeability enhancement and heat exchange surface area increase: with the same total permeability, Case I has a smaller heat exchange surface area and heat extraction volume than Case II

As discussed above, it is easy to conclude that the aim of hydraulic stimulation in EGS is not the same as in oil and gas reservoirs. In EGS reservoirs, apart from solely increasing the permeability/transmissivity, it is also important to increase the heat exchange area. That is to say, more fluid channels for heat exchange will benefit the heat production. Thus, in EGS, creating more fractures with smaller hydraulic apertures may be better than fewer fractures with larger hydraulic apertures.

2.3 The mechanism of fluid injection-induced seismicity

A number of recent review papers have summarized the activation mechanisms of fluid injection-induced seismic events (Atkinson et al. 2020; Kang et al. 2019; Rathnaweera et al. 2020; Schultz et al. 2020). McGarr et al. (2015) listed five main industrial operations that may cause fluid injection-induced seismicity, namely (a) wastewater disposal; (b) massive

fluid injection to enhance oil recovery; (c) hydraulic fracturing operations; (d) deep injection of CO_2; and (e) EGS development. Bommer et al. (2006), Bruhn et al. (2011), Suckale (2009), and Davies et al. (2013) reviewed the fluid injection-induced seismicity in the different applications. Warpinski et al. (2012) examined the induced seismicity specifically related to hydraulic fracturing in shale gas development. Evans et al. (2012) summarized 41 European cases of fluid injection-induced seismicity in the EGS and CO_2 storage projects. The review by Ellsworth (2013) focused on earthquakes caused by wastewater injection, especially in the USA. Rubinstein and Mahani (2015) summarized fluid injection-induced seismicity cases associated with wastewater injection, hydraulic stimulation, and enhanced oil recovery. Schultz et al. (2020) reviewed the reported cases of hydraulic fracturing induced seismicity in Canada, USA, UK, and China, during oil and gas exploration, with analysis of earthquake swarms and their proximity to the injection locations. Atkinson et al. (2020) summarized six key issues associated with hydraulic fracturing induced seismicity, including the triggering mechanisms, the effect of the tectonic environment, commonalities and differences between induced and natural earthquakes, damage potential, prediction, and relative hazards evaluation.

Table 1 gives a summary of reported fluid injection-induced earthquakes in geothermal systems. Majer et al. (2007) proposed four possible mechanisms to understand the injection-induced seismicity during EGS development, namely (a) pore pressure increase; (b) fluid temperature decrease; (c) fluid injection/withdrawal-induced fluid volume

Table 1 A summary of fluid injection-induced earthquakes in geothermal systems

Project	Location	Time	Maximum magnitude	Remarks	Reference
The Southeast Geysers	USA	1982	4.6		Breede et al. (2013)
Rosemanowes	UK	1987	2.0		Breede et al. (2013), Evans et al. (2012)
Fjällbacka	Sweden	1989	−0.2	Felt event during fluid circulation	Breede et al. (2013), Evans et al. (2012)
Soultz-sous-Forêts	France	1993	1.9	During the fluid injection stage	Charléty et al. (2007), Cuenot et al. (2008), Dorbath et al. (2009)
		2003	2.9	Post-injection stage, about 300 events were above M_w 2.0	
KTB	Germany	1994	1.2		Evans et al. (2012)
Krafla	Iceland	2002	< 2.0		Evans et al. (2012)
Bad Urach	Germany	2002	1.8	The injection rate dropped from 50 to 10 L/s in several hours	Zang et al. (2014)
Genesys Horstberg	Germany	2003	< 0		Evans et al. (2012)
Cooper Basin	Australia	2003	3.7	More than 50,000 events occurred	Breede et al. 2013
Hellisheidi	Iceland	2003	2.4		Breede et al. (2013), Evans et al. (2012)
Basel	Switzerland	2006	3.4		Breede et al. (2013), Evans et al. (2012)
Berlin	EI Salvador	2003	4.4		Breede et al. (2013), Evans et al. (2012)
Landau	Germany	2007	2.7	During fluid circulation, due to the wells intersected with faults	Zang et al. (2014)
Unterhaching	Germany	2007	2.4	During fluid circulation; both wells intersect faults	Zang et al. (2014)
Groß Schönebeck	Germany	2007	−1.1	Data from stimulation of the second well	Rathnaweera et al. (2020)
Pohang	South Korea	2017	5.5	Largest known induced earthquake in EGS	Rathnaweera et al. (2020)

alternation, and (d) chemical changes in fractures. Ghassemi (2012) in turn summarized the rock mechanics-related issues in fluid injection-induced seismicity, including how coupled thermo-hydro-mechanical-chemical (T-H-M-C) processes affect seismic events during EGS development as well as the role of strain localization, fluid flow and diffusion, and heat exchange during earthquake nucleation. Zang et al. (2014) discussed the relationship between fluid injectivity, fluid volume, in-situ stress conditions, and the occurrence of large seismic events in time and space during hydraulic stimulation in a specific EGS site. Their results indicated that long-term injection had a higher potential to induce earthquakes with large magnitudes than short-time injection.

As shown in Fig. 3, Eyre et al. (2019) summarized three commonly accepted, potential mechanisms that induce seismic events during hydraulic stimulation, including (1) direct effect from increased pore pressure on fault; (2) change of fault-loading conditions, and (3) fault loading by aseismic slip. However, underlying these mechanisms are some critical factors that will determine if and how a seismic event will be initiated, such as the total fluid injection volume, fluid injection rate, fluid temperature, reservoir original pore pressure, reservoir permeability, reservoir temperature, and the orientations of pre-existing faults (Dinske and Shapiro 2013; Shapiro and Dinske 2009; Zoback 2010, 2012). Moreover, whether a seismic event with a large magnitude can occur after the activation of the natural fractures/faults depends also on the frictional strength evolution of the faults. Seismologists use rate- and state-friction law to describe the frictional strength evolution as a function of slip velocity and slip history (Dieterich 1978; Marone et al. 1990; Ruina 1983). It has been shown that the so-called frictional stability parameter will determine whether a fracture/fault has velocity strengthening or velocity weakening behavior. The factors that affect the frictional stability of faults include the mineralogical compositions of fault gouges, fluid pressure, and temperature (Kang et al. 2019). Experimental and in-situ results indicate that faults with high content of brittle and hard mineral particles, such as quartz and feldspar, can be expected to have higher frictional strength but lower frictional stability, with a higher tendency for potential seismic slip events (Boulton et al. 2012; Byerlee and Brace 1968; Carpenter et al. 2009; Fang et al. 2017; Ikari et al. 2007, 2011; Moore and Lockner 2004; Morrow et al. 2000; Niemeijer and Collettini 2013; Shimamoto and Logan 1981; Summers and Byerlee 1977; Tembe et al. 2010). Moreover, these results indicate that fluid pressure may enhance or hinder the potential for seismic events for different rocks (De Barros et al. 2016; Jia et al. 2020; Guglielmi et al. 2015; Scuderi and Collettini 2016). Finally, temperature also affects the frictional stability evolution, especially during EGS development where the target reservoir is commonly under a high temperature gradient due to the significant difference in temperature between injected fluid and in-situ fluid (Den Hartog et al. 2012a, 2012b; McClure and Horne 2014a, b; Niemeijer and Collettini 2013; Rutqvist et al. 2008; Verberne et al. 2010, 2015). With a decrease of temperature, the faults' frictional strength increases dramatically, and the rock may evolve from plastic to semi-brittle deformation behavior, which increases the tendency for seismic events (Blanpied et al. 1995; He et al. 2006). Thus generally, during the EGS development, cold water injection could decrease the temperature of fault gouges, induce more brittle failure, and increase the seismic risks.

Although it is impossible to predict natural earthquakes accurately at this stage, researchers have attempted to estimate the maximum seismic magnitude of fluid injection-induced seismicity (Foulger et al. 2018). Representative methods include statistical, physical, and hybrid approaches (Cloetingh et al. 2010; Luginbuhl et al. 2019; Gaucher et al. 2015; Schoenball et al. 2012). Some representative models and empirical relationships have been summarised by Shapiro et al. (2011), McGarr (2014), Van der Elst et al. (2016), and Galis et al. (2017). Current results indicate the injected fluid volume to be the main control on the magnitude of the fluid injection-induced seismicity. In Fig. 4, a summary of observed magnitudes of fluid injection-induced seismicity as a function of injected fluid volume in various EGS projects is shown, along with the model predictions by McGarr (2014) and Galis et al. (2017). However, the results also show that some seismic events may significantly deviate from the general model predictions, including a number with much larger magnitudes. This may especially happen if the rupture is a runaway/unarrested rupture (Grigoli et al. 2018). An important example is the Pohang earthquake, where the earthquake sequences cannot be predicted based on the net

fluid injection volume (Lee et al. 2019). In general, without the consideration of specific in-situ tectonic stresses and local fault rupture physics, the estimation of the particular extent of seismic events will be difficult.

Another important phenomenon that has been under intense study is post-stimulation seismic events. Parotidis et al. (2004) indicated that the pore pressure diffusion was the dominant triggering mechanism for the post-fracturing induced seismicity. Baisch et al. (2010) found that pore pressure at a nearby fault can dramatically increase after shut-in, bringing the fault to the critically stressed state. Later, Segall and Lu (2015) suggested that the poro-elastic effect is the main reason for the seismic events after shut-in. De Simone et al. (2017) emphasized that during the analysis of the effect of fluid on the post-fracturing induced seismicity, various time scales and distances to the injection borehole should be considered. Mukuhira et al. (2017) further analyzed the distribution of pore pressures after the hydraulic stimulation, concluding that the pore pressure distribution after the shut-in indeed could destabilize a larger portion of a fault, resulting in localized shear slip with the potential of triggering a seismic event with large magnitudes. In addition to these considerations, some other processes may also be important for the post-fracturing induced seismicity; for example, thermal stress associated with the temperature difference between injected fluid and in-situ fluid may also facilitate the triggering of fault slips (Gan and Lei 2020).

As we summarised above, the mechanisms causing post-injection seismicity are under extensive studies and are still very much an open research topic. One possible mechanism could be pore pressure diffusion, in which fluid injection pressure will still diffuse outwards even after the shut-in and subsequently reaches an area under pre-existing critical stress condition. Another possible mechanism is the normal closure of an initially injection-induced opening of fractures in a fault zone near the injection well after shut-in. The opening and closure of the fractures in a fault zone under particular local stress conditions may induce changes in stress, deformation and water pressure in a fault zone that create new critical stress conditions and their disruptions. The post-injection induced seismicity is a coupled hydromechanical process in a fault zone with complex network of fractures which need to be further investigated.

3 Typical hydraulic stimulation techniques

This section reviews the most common hydraulic stimulation techniques used to enhance reservoir permeability. These methods include conventional hydraulic stimulation, multi-stage fracturing, and the so-called cyclic soft stimulations (CCS), which combines cyclic injection protocols and a traffic light system. While the emphasis of this section is on EGS, information and references on hydraulic stimulation methods from related fields are also included, since they form part of the knowledge base for stimulation design for EGS projects and may help to convey a broader view of stimulation approaches and techniques.

3.1 Conventional hydraulic stimulation

Conventional hydraulic stimulation technique is commonly used in the oil and gas industry (Agarwal et al. 1979; Veatch 1983). It generally refers to hydraulic stimulation operation involving a large amount of water and proppant injected into the reservoir. This technique was first used in the oil and gas industry to enhance the permeability of tight sandstone formations, including the Denver Basin and Piceance Basin (Chancellor, 1977; Fast et al. 1977). Due to the high fluid injection rate, fluid pressure will increase quickly at the injection borehole. When the fluid pressure reaches a certain value, rock breakdown occurs, and tensile fractures are created near the injection borehole interval. The fluid pressure at which rock breakdown occurs is defined as the reservoir breakdown pressure, which can be calculated based on the in-situ stress state and tensile strength of reservoir rock (Detournay 2016). After the reservoir rock breakdown, injection fluid pressure also acts as the driving force to further open the generated tensile fracture and to propagate it further. However, after the injection stops, the hydraulic fractures may close again due to in-situ compressive stress. Thus, a combination of slickwater fracturing and proppant injection is commonly used to keep the fracture open (Barati and Liang 2014). After creating long and narrow fractures by slickwater, proppants are then injected into the reservoir as the second step, aiming to keep the hydraulic fractures open. The common materials used as proppants include silica sand as well as resin-coated and ceramic proppants.

3.2 Multi-stage fracturing

Multi-stage fracturing is a more complex hydraulic stimulation technique developed with the advance of horizontal drilling technology. In this approach, horizontal wells (with lengths of hundreds to a few thousand meters) are firstly drilled. Then, packers are used to isolate sections along the borehole, and fluid is injected into those sections simultaneously or in a certain time sequence. Through this process, multiple fractures can be created along the borehole, and a larger rock volume is stimulated with increased permeability (Tang et al. 2016; Yao et al. 2012).

In recent years, the possibility of replacing conventional hydraulic stimulation with multi-stage fracturing has become of interest to the EGS community. In multi-stage fracturing, the stress shadow effect is a critical phenomenon that needs to be addressed. The stress shadow effect refers to the effect of stress redistribution in the region near a generated hydraulic fracture. Then, if a second hydraulic fracture is to be created at the next time stage in its vicinity or in its shadow, a higher fluid pressure may be required. Moreover, the second fracture may have a more limited length, narrower width, and its propagation direction may also deviate from the maximum stress direction, because of the directional change of the local stress field (Taghichian et al. 2014; Zangeneh et al. 2015).

Sneddon and Elliot (1946) presented an analytical solution for stress distribution around a 2D vertical fracture extended from a horizontal borehole. In their derivation, the rock material was assumed to be homogeneous and isotropic, the fracture was open, i.e., unfilled, and the presence of the borehole was neglected. The equations below can be used to describe the stress changes around a created hydraulic fracture (Geertsma and De Klerk 1969; Perkins and Kern 1961):

$$\begin{aligned}\Delta\sigma_{\mathrm{x}} &= P_n \cdot \left[1 - \frac{x^3}{(h_f^2/4 + x^2)^{3/2}}\right] \\ \Delta\sigma_z &= P_n \cdot \left[1 - \frac{xh_f^2/2 + x^3}{(h_f^2/4 + x^2)^{3/2}}\right] \\ \Delta\sigma_y &= \nu(\Delta\sigma_{\mathrm{x}} + \Delta\sigma_z)\end{aligned} \tag{3}$$

where $\Delta\sigma_{\mathrm{x}}$ [MPa], $\Delta\sigma_{\mathrm{y}}$ [MPa] and $\Delta\sigma_{\mathrm{z}}$ [MPa] are stress changes caused by the hydraulic fracture in X, Y and Z direction, respectively. P_{n} [MPa] is the fluid pressure within the fracture, x [m] is the distance to the fracture center, h_{f} [m] is the vertical extent of the fracture, and ν is the Poisson' ratio. Studies have also been conducted for the case where several fractures are initiated simultaneously from several isolated sections in the horizontal well. The propagating fractures are found to interfere with each other, resulting in complicated fracturing geometries and uneven fracture distribution (Di and Tang 2018; Tang et al. 2016).

Laboratory experiments have been conducted to investigate the role of the stress shadow effect on multi-stage hydraulic fracturing. Geyer and Nemat-Nasser (1982) observed the uneven propagation of fractures and the apparent compression of two long simultaneously propagating fractures. Zhou et al. (2018) found that the stress shadow effect restrained the fracture propagation of adjacent fractures and caused a divergence of adjacent fractures in shale. Gai et al. (2020) found that multiple hydraulic fractures with small spacing would coalesce even under high horizontal stress differences. Moreover, the needed initiation pressure of later hydraulic fracture increases with increased fluid pressure within the earlier fractures. A later fracture would also deviate from the ideal direction perpendicular to the horizontal wellbore and deflect towards the earlier hydraulic fracture.

Due to the limited sample size that can be investigated in the laboratory, numerical simulations were also used to investigate the stress shadow effect. Wong et al. (2013) observed that the stress shadow effect could make fractures diverge outwards from the created group of fractures, and the inside fractures may be closed due to the compression effect of outer factures. Analyses confirmed that an increase in fracture spacing would result in a reduced stress shadow effect and prevent the directional deviation of later fractures (Morrill and Miskimins 2012; Roussel and Sharma 2011; Singh and Miskimins 2010).

Moreover, perhaps the most significant multi-stage hydraulic stimulation tests were performed in the Bedretto Underground Laboratory for Geosciences and Geoenergies (BULGG) to evaluate its capability to improve the quality of the granite rocks reservoir. In this experiment the borehole ST1 was divided into

14 injection intervals by means of a multi-packer system. Results and details can be found in Bröker et al. (2022) and Castilla et al. (2022).

In summary, the stress shadow effect may cause the following drawbacks: (a) the alteration of local in-situ stress states due to the pressurization of earlier fractures (Cheng 2009; Nagel and Sanchez-Nagel 2011; Olson 2008; Roussel and Sharma 2011); (b) a subsequent fracture may propagate towards the previous fracture regime or terminate due to fracture intersection (Olson 2008; Roussel and Sharma 2011); and (c) the compression effect of outer fractures may decrease the width of inner fractures (Olson 2008). Thus, approaches have been developed to limit the negative effects of stress shadow, and these techniques can be divided into two categories: (a) multi-stage fracturing in space, which means the optimization on fracturing spacing, and (b) multi-stage fracturing in time, which means that fracturing operations are performed sequentially rather than simultaneously.

3.2.1 Multi-stage fracturing in space

One practical idea to eliminate the stress shadow effect is the optimal design of spacings of fracturing intervals based on in-situ stress states and geomechanical properties of the target reservoir. The main point of fracturing stage optimization is to understand how the adjacent parallel fractures interfere with each other as a function of spacing. Yamamoto et al. (2004) developed a three-dimensional simulator, which could effectively describe the paralleled fracture propagation with mechanical interactions between fractures. Olson (2008) used a pseudo-3D model to simulate paralleled fracture propagation, which dramatically decreased the calculation time for obtaining the optimal fracture spacing. Meyer and Bazan (2011) also developed a DFN model to investigate paralleled fracture propagation, which could predict the mechanical interaction impact on the fracture aperture growth for evenly spaced fractures. These techniques can be applied to design optimal spacing based on rock mechanical properties, fluid properties, and geological conditions.

3.2.2 Multi-stage fracturing in time

Another practice to minimize the stress shadow effect is to perform hydraulic fracturing in well-spaced borehole sections according to a certain time sequence. Waters et al. (2009) considered two parallel horizontal wells, where the sections in the two wells opposite each other are stimulated simultaneously in successive time stages when moving towards to the ends of the wells, Fig. 5a. The next modification in the stimulation procedure was to differentiate the timing of the stimulation stages in the two wells, so that the hydraulic fracturing in the two wells follows a particular time sequence, Fig. 5b. This method is referred to as zipper fracturing. Later, a modified zipper fracturing was further introduced by placing the stimulation sections of the two wells not directly opposite to each other, Fig. 5c. In this case, the stress shadow effect was further reduced. Rafiee et al. (2012) found that the modified zipper fracturing technique creates a more complex fracture network in shale in a case where the two parallel wellbores have a distance between 150 and 300 m. A limitation of the method is that the generated fracture network was concentrated in between the two wells, and thus the stimulated volume may be limited. Vermylen and Zoback (2011) investigated the stress shadow effect in multiple lateral wells in Barnett shale, and their results indicated that the zipper fracturing was more effective than the simultaneous fracturing in generating hydraulic fractures with a longer length. Nagel et al. (2013) found that by drilling multiple lateral wells and performing hydraulic fracturing in sequence, the reservoir permeability could be significantly enhanced. Izadi et al. (2015) modeled the hydraulic fracture propagation and found the largest stimulated volume was achieved by the modified zipper fracturing method compared with simultaneous hydraulic fracturing. While most of the work on this stimulation approach is for shale formation, Kumar and Ghassemi (2016, 2019) also conducted three-dimensional numerical simulations to explore the multi-stage fracturing in horizontal wells for EGS design. The results indicated that the modified zipper fracturing could be used for more closely spaced horizontal wells to generate more complicated fracture networks than by the use of simultaneous hydraulic fracturing method. Zangeneh et al. (2015) compared the fracturing performance between conventional hydraulic fracturing, simultaneous fracturing, and zipper fracturing. They found both the maximum hydraulic fracture aperture and length to increase when the stimulation method moves from conventional fracturing to simultaneous

fracturing and to zipper fracturing, the latter being the most effective.

It should be remarked here that many factors, such as local stress state, pre-existing natural fracture systems (length, density, and hydraulic properties), will strongly influence the performance of a hydraulic fracturing stimulation. Hence, for any given site, site-specific data should be used in numerical modeling to obtain a comprehensive understanding and prediction of the hydraulic fracture propagation prior to a stimulation operation.

3.3 Cyclic soft stimulation (CSS)

The cyclic soft stimulation (CSS) is a hydraulic stimulation strategy that combines (a) cyclic fluid injection and (b) a so-called traffic light system (TLS). CSS's two major objectives are to enhance the reservoir permeability and to mitigate the fluid injection-induced seismicity caused by hydraulic stimulation (Zang et al. 2013, 2017).

3.3.1 Cyclic fluid injection fracturing

Kiel (1977) first proposed the cyclic injection fracturing concept for increasing the hydraulic conductivity of reservoir rocks. Over the past few years, laboratory-scale as well as in-situ field experiments have been conducted to investigate the breakdown process of the reservoir under cyclic fluid injection (including breakdown pressure, fracture propagation, and distribution), the associated seismic behaviors, and induced fracture permeability, with the goal of understanding the basic mechanism underlying these processes (Hofmann et al. 2018; Zang et al. 2019). More recently, the cyclic injection protocol has been proposed for various applications, including EGS (Zimmermann et al. 2010), shale gas hydraulic fracturing (Jia et al. 2021), and coalbed methane (Xu et al. 2017).

To relate this approach to other methods, Zhuang et al. (2020) and Li et al (2022) presented a summary of several fluid injection schemes, both injection-rate controlled and pressurization controlled, as shown in Fig. 6. Continuous injection with a constant rate is commonly used in massive hydraulic fracturing, as shown in Fig. 6a. Figure 6b shows the stepwise rate injection with increasing injection rates. Figure 6c shows cyclic progressive injection, where high and low injection rates alternate in each cycle, with the high injection rates increasing in successive cycles. Figure 6d shows the stepwise pressurization scheme, in which the fluid injection pressure increases to successively higher pressure in several steps. Figure 6e is a modification of stepwise pressurization with each step maintained through pulsed pressurization. Figure 6f is the cyclic pulsed pressurization, in which the injection pressure is decreased after the pulse pressurization step after each cycle and before the next pressurization cycle.

The injection schemes in Fig. 6b–f could be regarded as the cyclic injection, which is also known as the fatigue hydraulic fracturing method (Zang et al. 2017). Fatigue failure occurs after a series of successive loadings at a load smaller than the load required to fail a material by static loading. It may result in a violent failure without early warning. The micromechanisms of fatigue failure have been well studied in metal materials but are less investigated for rock materials. The Paris-Erdogan law is commonly used to describe the fatigue-based failure in fracture mechanics and expressed as (Zang et al. 2019):

$$\frac{dc}{dN} = A \cdot (\Delta k)^m \tag{4}$$

where dc/dN is the fracture growth per cycle; Δk is the stress intensity factor; N is the loading cycles; A and m are two constants. This equation defines the power-law relationship between fracture growth rate and stress intensity factor. Based on this concept, experiments in the laboratory with rock samples have been performed with cyclic loading (Haimson and Kim 1991; Erarslan and Williams 2012; Yin et al. 2021b). More details on mechanical fatigue failure can be found in a review paper by Cerfontaine and Collin (2017). It is worth mentioning that there are two significant differences between cyclic mechanical loading and cyclic hydraulic fracturing in rocks, namely: (a) fluid pressure may affect the rock strength, and (b) potential chemical reactions may occur between fluid and silicate minerals in rocks (Atkinson 1984).

Generally, during cyclic fluid injection into the reservoir, a high-frequency water pulse could dismantle and remove weak minerals from fracture surfaces while decreasing the rock strength locally (Fig. 7a). Through these processes, the fatigue hydraulic fracturing could achieve three goals: (a) lowering the breakdown pressure of the reservoir; (b) generating a

more complicated fracture network with higher permeability and heat-transfer surface area of the reservoir and (c) minimizing the potential for large earthquakes by inducing smaller seismic events with the cyclic injection of a smaller amount of fluid.

A number of laboratory experiments have been performed to validate whether CSS is an effective technique to increase reservoir permeability while mitigating seismic risks. Zang et al. (2000, 2002) conducted laboratory experiments with granites and sandstones, and the results indicated that cyclic mechanical loadings could form a damaged zone with different widths. Later experiments with tuff and monzonite gave similar findings indicating that cyclic mechanical loading produced a smaller but more intense fracture zone than static failure loading (Ghamgosar and Erarslan 2016). Experiments on Pocheon granites with X-ray CT technology indicated that cyclic hydraulic fracturing reduced the breakdown pressure by about 20% compared to conventional hydraulic stimulation with a constant injection rate. Moreover, cyclic hydraulic fracturing was found to produce complex and branched fractures, whereas the conventional hydraulic fracturing tended to create a single main fracture. However, the induced fracture aperture was smaller for cyclic injection, resulting in a limited permeability enhancement, as shown in CT images (Zhuang et al. 2016). Similar experiments with sandstone samples indicated that the breakdown pressure is lowered by about 16% compared with conventional hydraulic fracturing. Moreover, BSE-SEM images showed that cyclic injection could create a damaged zone around the induced fractures that is twice as wide as the fracture zone created by continuous fluid injection (Patel et al. 2017).

3.3.2 *Traffic light systems (TLS)*

Another component of cyclic soft stimulation (CSS) is the traffic light system (TLS) (Hofmann et al. 2018). The TLS involves careful monitoring of seismic events over the duration of the stimulation procedure and adjusting operation accordingly, such as decreasing injection flow rate, reducing fluid pressure, shutting-in, or flowing-back, when the seismic magnitude or the peak ground velocity reaches a specific threshold, or when other unexpected observations occur. The oil and gas industry has adopted the TLS as part of a hydraulic stimulation operation (Bommer et al. 2015).

A typical TLS proposed by Hofmann et al. (2018) for hydraulic fracturing stimulation in EGS is shown in Fig. 7b. The threshold of each stage is calculated based on the maximum tolerable seismic moment magnitude (M_{wmax}) and magnitude increase (ΔM_{w}). Details could be found in Hofmann et al. (2018). A challenge is that seismic events with increased magnitudes have been observed in a period of time after injection shut-in (Majer et al. 2007), and the question exists whether the TLS can effectively mitigate such post-injection seismic risks.

In-situ experiments have been carried out to investigate the potential of using fatigue hydraulic fracturing for EGS, by combing CSS and TLS. An example is the experiments conducted at Äspö Hard Rock Laboratory, Sweden (Lopez-Comino et al. 2017; Zang et al. 2017; Zimmermann et al. 2019). In these experiments, three different injection procedures were investigated: (a) conventional hydraulic fracturing with a constant injection rate, (b) an approach where injection flow rate was gradually increased in a cycle of alternating high and low pressures, and (c) an additional pressure pulsation imposed on each step of the cyclic injection. The results indicated that a lower breakdown pressure was observed for the cyclic pulse injection protocols (c). Moreover, both the number and magnitudes of the seismic events were lower in this case. However, the authors pointed out that further investigations are needed to understand the parameters influencing the number and magnitude of seismic events during and after fluid injection (Zang et al. 2017). The fluid injection strategy was instructed to follow a cyclic protocol to dissipate hydraulic energy at Espoo near Helsinki, Finland, in 2018 and 2020 (Hillers et al. 2020; Kwiatek et al. 2019; Leonhardt et al. 2021). Five hydraulic stimulations were conducted in 2018 in well OTN-3 at this site, and the CSS method was deployed with a total of 18,160 m^3 freshwater injected into the target reservoir over 49 days (Ader et al. 2020; Kwiatek et al. 2019). The results indicated that the reservoir conductivity increased, and no seismic events were recorded with magnitudes higher than 2.0 (Kwiatek et al. 2019; Kukkonen and Pentti 2021). Hydraulic stimulations were also performed in another well, OTN-2, with ~ 7000 m^3 fluid injection through a 1.3 km open hole section. Even though details of those hydraulic

stimulations have not yet been published, the experience at this site illustrates the possibility of CSS to increase the reservoir permeability while mitigating seismic risks in EGS. Another hydraulic stimulation project has also been proposed, combining cyclic injection, TLS, and risk analysis system in a well RV-43 near Reykjavik, Iceland, at a depth from 1001 to 1750 m (Broccardo et al. 2020). Furthermore, CSS hydraulic stimulation was also applied to an EGS project in Pohang, South Korea (Park et al. 2020), which will be discussed in more detail in Sect. 4.3.2.

4 Examples of EGS hydraulic stimulation projects and some lessons learned

In this section, we present some representative EGS projects around the world during the last few decades. Many ways of grouping these projects can be used, but in this study, we group them into three categories: (a) experimental EGS projects intended basically for scientific research; (b) commercial EGS projects that have been led by industrial companies, aiming at electricity generation or heat production; and (c) EGS projects which have been suspended or terminated due to certain reasons such as borehole damage or seismic risks. These three categories of projects are summarized in Tables 2, 3 and 4, with information on their locations, years of activity, reservoir rock types, well depths, stimulation methods, and some remarks. We then select two representative sites from each category (indicated by ** in the tables) for a more detailed review in the following subsections with a focus on the implemented hydraulic stimulation strategy, the resulting permeability enhancement performance, and induced seismicity. Some lessons learned and insights gained from each case are summarized.

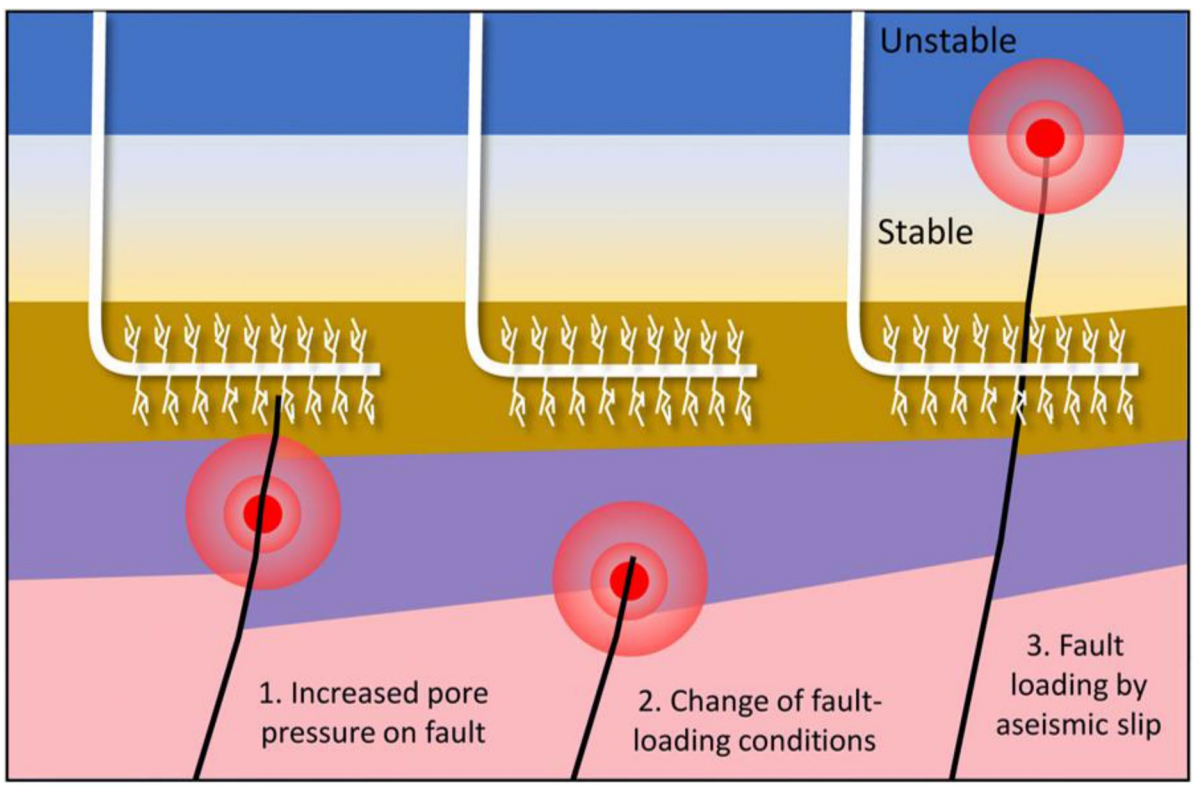

Fig. 3 Three potential mechanisms for fluid injection-induced seismicity. (1) Direct effect from increased pore pressure on fault; (2) Change of fault-loading conditions; and (3) Fault loading by aseismic slip (Eyre et al. 2019)

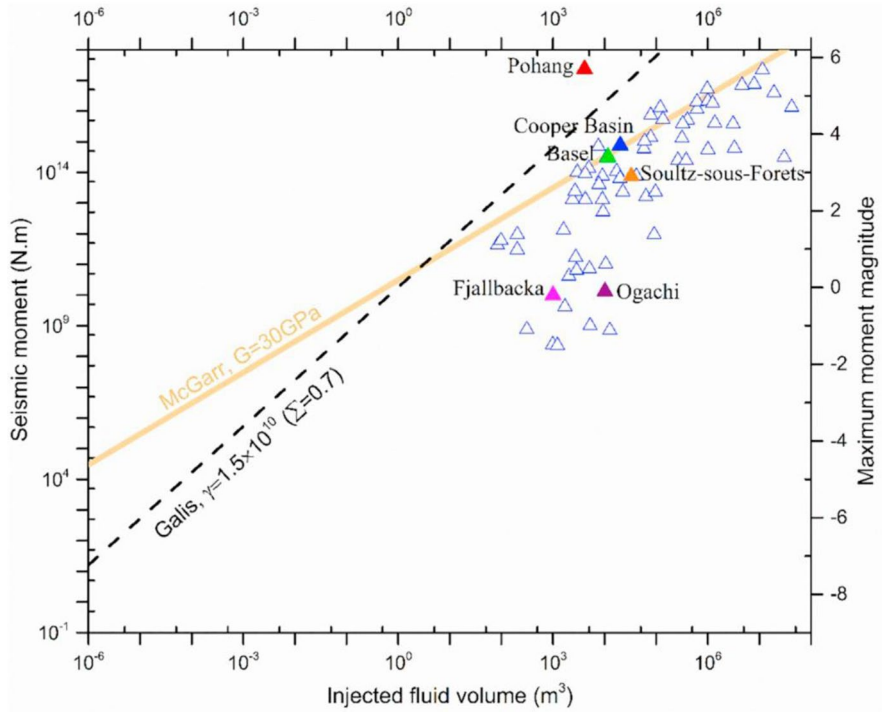

Fig. 4 Seismic moment and maximum moment magnitude as a function of injected fluid volume as estimated by McGarr (2014) and Galis et al. (2017) (modified from Rathnaweera et al. 2020)

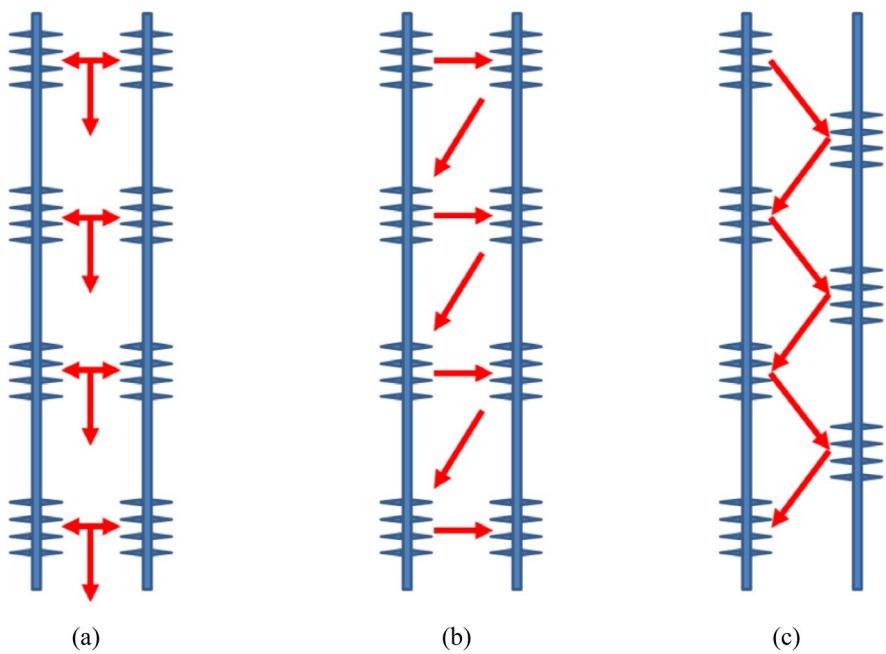

Fig. 5 **a** Simultaneous hydraulic fracturing, **b** Sequential hydraulic fracturing (Zipper fracturing), and **c** Modified Zipper fracturing. (modified from Cuss et al. 2015). In these figures, two-headed arrows (found only in **a**) indicate simultaneous fracturing, while single-headed arrows indicate a step delay in time

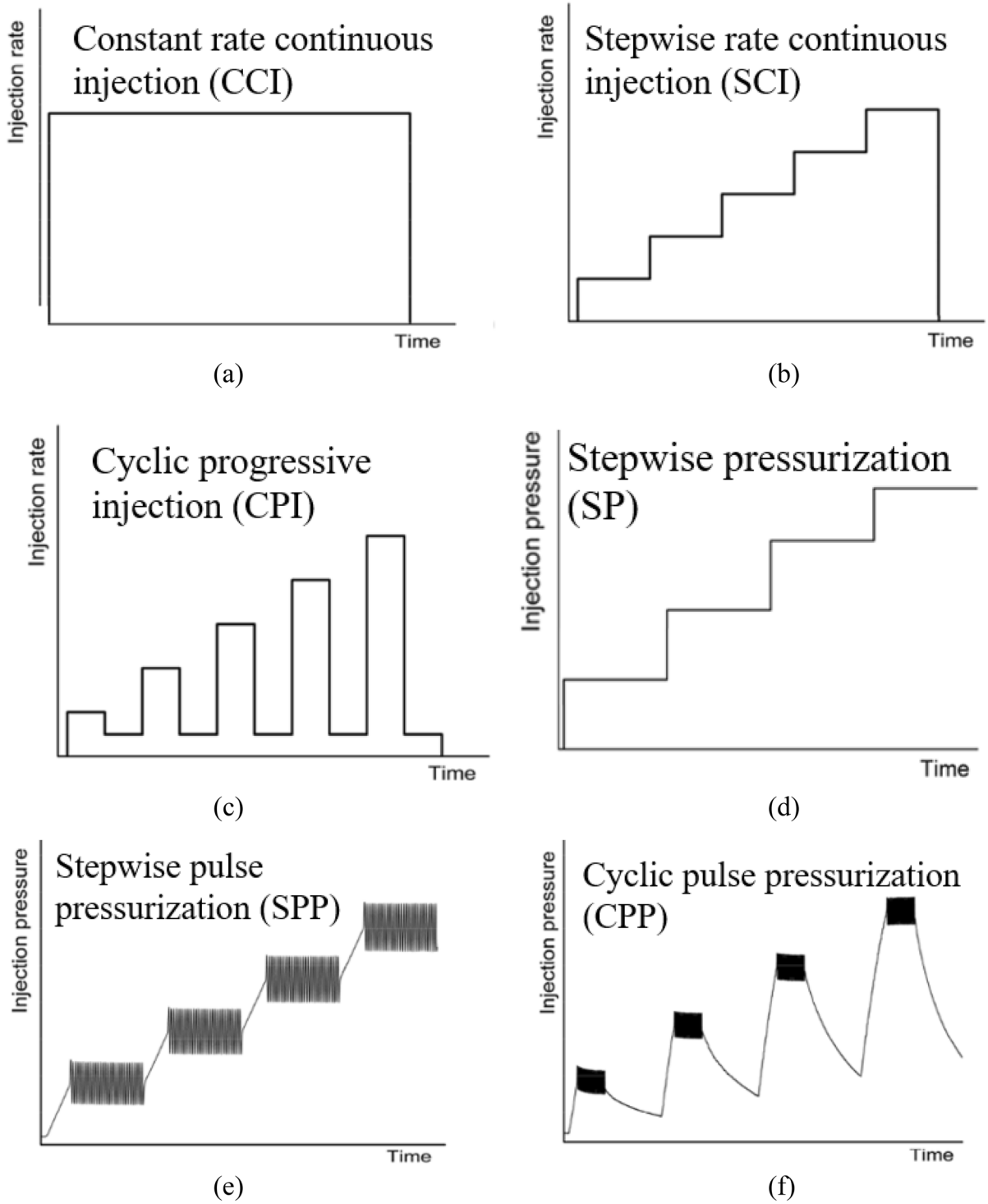

Fig. 6 Six different injection schemes of hydraulic fracturing. **a** Constant rate continuous injection (CCI), **b** stepwise rate continuous injection (SCI), **c** cyclic progressive injection (CPI), **d** stepwise pressurization (SP), **e** stepwise pulse pressurization (SPP) and **f** cyclic pulse pressurization (CPP). (Modified from Zhuang et al. 2020)

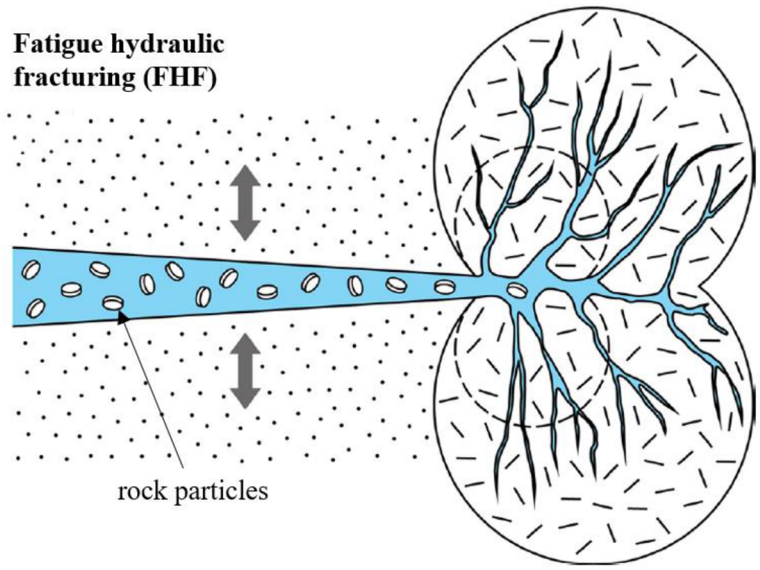

(a)

M_w	Stage	Injection rate (Event @ HIR)	Injection rate (Event @ LIR)	Adjusted injection rates for next LTC
≥ M_{wmax}	5	Flowback	Flowback	Flowback
≥ M_{wmax} – ΔM_w	4	Flowback	Flowback	Flowback
≥ M_{wmax} - $2\Delta M_w$	3	★	★	★ Flowback
≥ M_{wmax} - $3\Delta M_w$	2	★	★	
< M_{wmax} - $3\Delta M_w$	1	★	★	⇧

Legend: ★ Induced seismic event — adjusted injection rate --- planned injection rate
M_{wmax} ... maximum tolerable seismic moment magnitude
ΔM_w ... expected magnitude increase
HIR ... high injection rate
LIR ... low injection rate
LTC ... long-term cycle

(b)

Fig. 7 **a** In fatigue hydraulic fracturing, rock particles are removed from fracture faces through high-frequency vibrations and reached the fracture tip. A fracture process zone is created during fatigue hydraulic fracturing. (modified from Zang et al. 2019). **b** The traffic light system for cyclic fluid injection schemes (modified from Hofmann et al. 2018)

Table 2 EGS projects for in-situ experiments (research purposes)

Project	Location	Year	Rock type	Well depth	Reservoir temperature (°C)	Stimulation method	Remarks	Reference
Fenton Hill**	USA	1974–1993	Crystalline rock	2932–4390 m	235	Hydraulic fracturing	First EGS in the world	Brown (2009), Tester et al. (2006), Tenzer (2001)
Rosemanowes	UK	1977–1992	Granite	2000–2600 m	79–100	Hydraulic fracturing; Viscous gel stimulation		Parker (1999)
Falkenberg	Germany	1977–1986	Granite	500 m	13.5	Hydraulic fracturing	Shallow depth	Schaefer and Heinig (2011)
Le Mayeta	France	1978	Granite	200–800 m	22	Hydraulic fracturing with and without proppant		Portier et al. (2007)
Northwest Geysers	USA	1980s	Metasedimentary rocks	3396 m	400	Thermal fracturing		Romero et al. (1995)
Fjällbacka	Sweden	1984–1995	Granite	70–500 m	16	Hydraulic fracturing; Acid fracturing	The first EGS experiments in Sweden	Jupe et al. (1992)
Ogachi	Japan	1989–2002	Granodiorite	400–1100 m	160	Multiple wells with multiple fracture zones		Kaieda et al. (2005, 2010)
Hunter valley	Australia	1999	Granite	1946 m (PPHR1)	~61	Hydraulic stimulation		Burns et al. (2000)
Groß Schönebeck**	Germany	2000	volcanic rocks	4309 m	145	Hydraulic fracturing; Thermal and chemical stimulations	In situ geothermal laboratory for EGS research	Breede et al. (2013)
Lund	Sweden	2001	Gneiss, granite	3701.8 m	85		The temperature (85℃) was low	Rosberg and Erlström (2019)
Genesys Horstberg	Germany	2003–2007	Sedimentary	3800 m	115	Hydraulic fracturing	Using an existing abandoned gas well	Schaefer and Heinig (2011)
Genesys Hannover	Germany	2009	sandstone	3900 m	160	Hydraulic fracturing	Single-well concepts	Schaefer and Heinig (2011)

Table 2 (continued)

Project	Location	Year	Rock type	Well depth	Reservoir temperature (°C)	Stimulation method	Remarks	Reference
Newberry	USA	2010	Volcanic rocks	3066 m	315	Hydroshearing, multi-zone isolated stimulation techniques		Cladouhos et al. (2011)

Projects with ** will be summarized in more details in Sect. 4.1

4.1 Experimental EGS sites

4.1.1 Fenton Hill, USA

The first extensive in-situ experiments aimed to study the extraction of heat from "hot dry rock" (HDR) started in 1975 at Fenton Hill, on the western flank of Valles Caldera, USA (Fig. 8a). The whole project could be divided into three stages: (a) The early stage (1970–1973) aimed to develop the basic concept and to conduct some preliminary tests; (b) Phase I (1974–1980), which involved borehole drilling, hydraulic stimulation and flow experiments; (c) Phase II (1981–1995) which involved a further development in drilling and testing operations (Brown 1997, 2009).

Figure 8b shows the well distribution of the Fenton Hill geothermal project. More information about the drilling history can be found in Tester et al. (1986, 1989). In Phase I, the first injection borehole (GT2) was drilled to the final depth of 2932 m in host rock consisting of jointed granodiorite. After that, a second borehole (EE-1) was directionally drilled below the bottom of the GT-2 borehole (Duchane and Brown 2002). In Phase II, wells EE-2 and EE-3 were drilled to depths of approximately 3500 m. Conventional hydraulic fracturing was performed in the EE-2 well aiming at creating a penny-shaped fracture propagating upwards to intersect the EE-3 borehole above. During a 2.5-day period, about 21,000 m^3 water was injected into well EE-2 with an average fluid pressure of about 48.0 MPa at the surface (Kennedy et al. 2010). Figure 8c shows the flow rate and fluid pressure evolution with time. It could be observed that the fluid pressure curve followed a similar shape with injection rate evolution, and no pressure drop was observed. This means that no fluid flow channels had been created to connect EE-2 and EE-3 wells. In Fig. 8d, the microseismic activity map also supports this interpretation since the seismic clouds were located near the EE-2 borehole, and not penetrated by borehole EE-3. The conventional hydraulic fracturing test ended with a high-pressure flange failure, so that the wellhead pressure could not be controlled, and the EE-2 borehole experienced sustained severe damage. Subsequently, an additional larger stimulation test was performed in the EE-3 borehole (May 1984), but the results were still unsatisfactory (Tester et al. 2006). As shown in Fig. 8e, the microseismic events caused by EE-3 stimulation are concentrated near and above the injection well EE-3, and do not overlap with EE-2 seismic clouds. It was concluded that the hydraulic fractures created by these experiments did not grow in the direction predicted, probably due to an unanticipated shift in the stress field in the deeper part of the formation (Brown 1997). To provide an adequate connection between the two wells (EE-2 and EE-3), a branch borehole EE-3A was drilled, in September 1985, off from the EE-3 well at 2830 m to a depth of 4018 m. The relative position of EE-3A and EE-3 is shown in Fig. 8f. EE-3A intersected several of the fractures created by the previous hydraulic stimulations (Dash et al. 1989), and in January 1986, another hydraulic stimulation was conducted in well EE-3A to further enhance the reservoir permeability, and a good connection between EE-2 and EE-3A was finally established. More details could be found in Dash et al. (1989).

The Fenton Hill geothermal project reached the granite reservoir with a temperature of 300 °C at 4.4 km depth and provided heat energy to a 60-kW binary cycle power generator. Even though the project was terminated in 1995 due to its inability to reach the expected capacity, it provided critical lessons for later deep geothermal development. The most important

Table 3 EGS projects for commercial purpose

Project	Location	Year	Reservoir rock ty pe	Well depth	Reservoir temperature (°C)	Stimulation method	Remarks	Reference
Bouillante	France	1963	Volcanic lavas and tuffs	1000–2500 m	250–260	Thermal cracking		Portier et al. (2007)
Lardarello	Italy	1970	Metamorphic rocks	2500–4000 m	300–350	Hydraulic and thermal stimulation		Portier et al. (2007)
Bruchsal	Germany	1983	Bunter Sandstone	1874–2542 m	123	N/A		Schaefer and Heinig (2011)
Neustadt-Glewe	Germany	1984	Sandstone	2320 m	99	N/A	Pilot power plant for utilizing low enthalpy geothermal	
Hijiori	Japan	1985	Granodiorite	1805–1910 m	190	Hydraulic fracturing		Kaieda et al. (2005, 2010)
Soultz-sous-Forêts**	France	1987	Granite	5093 m	165	Hydraulic fracturing and acidizing		Portier et al. (2007)
Altheim	Austria	1989	Limestone	2165–2306 m	106	Acidizing hydraulic stimulation		Tester et al. (2006)
Berlín	El Salvador	2001	Volcanic rocks	2000–2380 m	183	Hydraulic fracturing and chemical		Portier et al. (2007)
Coso	USA	2002	Diorite, granodiorite, granite	2430–2956 m	≥300	Hydraulic, thermal and chemical		Breede et al. (2013)
Desert Peak	USA	2002	Volcanic and metamorphic rocks	1067 m	179–196	Shear, chemical, hydraulic		Chabora et al. (2012)
Raft River	USA	2002	Quartz monzonite, schist, quartzite, and siltstone	1750 m	135–146	Hydraulic stimulation		Bradford et al. (2017)
Landau	Germany	2003	Granite	3170 to 3300 m	159	Hydraulic stimulation		Portier et al. (2007)
Cooper Basin**	Australia	2003	Granite	4421 m	242–278	Hydraulic stimulation	Largest demonstration project	Tester et al. (2006)
Unterhaching	Germany	2004	Limestone	3350–3580 m	123	Acid fracturing	First Kalina cycle power plant in Germany	Schaefer and Heinig (2011)
Paralana	Australia	2005	Metasediments, granite	4003 m	171	Hydraulic stimulation		Tester et al. (2006)

Table 3 (continued)

Project	Location	Year	Reservoir rock ty pe	Well depth	Reservoir temperature (°C)	Stimulation method	Remarks	Reference
Insheim	Germany	2007	Sandstone and Granite	3600–3800 m	165	Hydraulic stimulation	Drilling side-leg for injection well	Portier et al. (2007)
Bradys	USA	2008	Rhyolite, tuff	1320 m	180–193	Hydraulic stimulation		Lutz et al. (2011)
Otaniemi project	Finland	2015	Granite	Two wells: one is 6.4 km and the other one is 3.3 km	130 (expected)	Hydraulic stimulation phase just finished; results not published yet	The first deep geothermal project in Nordics	Hillers et al. (2020)
Rittershoffen	France	2005	Granite	GTR-1: 2500 m GTR-2: 2700 m	177	Hydraulic stimulation	First European EGS providing industrial heat	Baujard et al. (2017)
South Hungarian EGS	Hungary	2012	Igneous granite	3500–4000 m (planned)	225 (expected)	Hydraulic stimulation (planned)	Planned four production and two injection wells	Horváth et al. (2015)
United Downs Project	UK	2018	Granite	2393 m for injection well and 5275 m for production well	190 (expected)	N/A	First geothermal power plant in the UK	Ledingham et al. (2019)

Projects with ** will be summarized in more details in Sect. 4.2

References: Breede et al. (2013); Schaefer and Heinig (2011); Tenzer (2001); Tester et al. (2006)

lesson learned is that due to the in-situ stress complexity, hydraulic fractures may not propagate as predicted. In particular, a vertical penny-shaped fracture was not observed; rather, fractures occurred around the stimulated borehole as indicated by the observed microseismic clouds. The experiments suggested that the most direct way for EGS development may be one in which one well is drilled first to conduct hydraulic stimulation, and then a second well is drilled and specifically directed to the created fracture zone, as indicated by data on the location of the microseismic event clouds. This would then result in a hydraulic conductivity (permeability) between the two wells high enough to enable a significant flow rate between them (Brown 2009). Results from this case also suggest the following points: (a) for the development of an EGS site, comprehensive seismic surveys and downhole logging and testing should be performed to acquire data about the in-situ stress states and existing natural fracture network (density, orientation, permeability, and spatial distribution); (b) during the hydraulic stimulation, microseismic activities should be monitored and comprehensively recorded, and (c) tracer and hydraulic tests could also be used at detecting the reservoir connectivity, and these test data may be important for evaluation of permeability enhancement and heat extraction performance.

4.1.2 Groß Schönebeck, Germany

The research EGS site at Groß Schönebeck, Germany, was established in 2001 to investigate various techniques for extracting geothermal energy (Huenges et al. 2002). The site was located in the North German

Table 4 Representative suspended or terminated EGS projects due to technical reasons

Project	Location	Year	Reservoir rock type	Well depth (m)	Reservoir temperature (°C)	Stimulation method	Reasons for termination	Reference
Bad Urach	Germany	1977–1981	Gneiss	3334–4445	172	Hydraulic fracturing	Torn off bore rods in the borehole	Rathnaweera et al. (2020)
Basel**	Switzerland	1996–2009	Granite	5000	~200	Hydraulic fracturing	Induced seismicity exceeding acceptable levels	Ladner and Häring (2009), Giardini (2009)
The Southeast Geysers	USA	2008–2009	Greywacke	1341	240	Multiple fracture zones in wells	Wellbore collapsing and seismic risks	Romero et al. (1995)
Pohang**	South Korea	2010–2017	Crystalline rocks	4340	> 140	Hydraulic fracturing	Induced a M_w 5.5 earthquake	Rathnaweera et al. (2020)

Projects with ** will be summarized in more details in Sect. 4.3

Basin, and two wells were drilled into the Lower Permian sedimentary and volcanic layers. The first well "E GrSk 3/90" served as an injection well, and it was a previously abandoned gas exploration well (Zimmermann et al. 2011). The second well Gt GrSk 4/05, was drilled in 2006 to a depth of 4404.4 m. The well path was designed with a deviation between 37° to 49° inclination and reached 48° at the well bottom. This well was designed as a production well, and the bottom distance to the injection well (E GrSk 3/90) was 475 m. The geological conditions of Groß Schönebeck EGS site are shown in Fig. 9a. After the well completion, three consecutive hydraulic stimulations were performed in various depth intervals (Zimmermann and Reinicke 2010; Zimmermann et al. 2010), resulting in a productivity index increase from 4.25 to 10.10 m^3/h/MPa in the injection well.

In 2007, the Fatigue Hydraulic Fracturing (FHF) method was applied by cyclic injection in the second well Gt GrSk 4/05 to test its feasibility (Zimmermann et al. 2010). The target reservoir was volcanic rock, and its permeability was mainly fracture-dominated. The proposed plan was to form a hydraulic fracture with a half-length of 150–200 m, fracture height of 80–100 m, and average effective hydraulic aperture of 5–10 mm. The detailed wellhead pressure and flow rate curves are shown in Fig. 9b. During the cyclic injection, the fracture propagation and final distribution were influenced by the flow rate, wellhead pressure, and cycle duration. Horizontal fracture propagation was found to be dominant during high flow rate injections, while low injection rate periods led to an increased fracture aperture. During high flow rate injections, low concentrations of quartz sand were also injected to support the fracture aperture, and a friction-reducing agent was used to avoid high wellhead pressure. In total, 13,170 m^3 of water was injected into the reservoir, and results indicated a maximum wellhead pressure of 58.6 MPa when the injection rate reached its maximum value. Figure 9c shows the seismic monitoring result, indicating extremely low seismicity during and after the stimulation. Only 80 events were observed during the six-day fluid injection, with magnitudes ranging from -1.8 to -1.0. Moreover, an estimated fracture distribution after the hydraulic stimulation was calculated by numerical modeling, as shown in Fig. 9d. The simulation results indicated that the final mean fracture aperture was 19.5 mm, and the length and width were 190 m and 90 m, respectively. More details about the numerical simulation can also be found in Zimmermann and Reinicke (2010). The cyclic injection test in well Gt GrSk 4/05 at Groß Schönebeck is a successful attempt to use this advanced injection protocol

to increase the reservoir permeability while mitigating the seismic risks. Through a series of in-situ test, cyclic injection may decrease the reservoir breakdown pressure compared to conventional hydraulic fracturing. The total number of seismic events is smaller and the magnitudes of those events are also lower. Moreover, based on production tests after several hydraulic stimulations with gel/proppant, the productivity of Gt GrSk4/05 was found to be lower than expected. It was suggested that this could be the result of a filter cake near the open-hole section caused by drilling fluid, and hence acid stimulation was recommended in the near-wellbore region to improve the performance of well productivity. Finally, the hydraulic stimulation methods and fluid injection protocols should be designed based on site-specific conditions, including the reservoir properties and geological conditions. Moreover, if the natural fractures are not well-developed before the hydraulic fracturing stimulation and the created fracture networks are dominated by tensile fractures, then proppant sand should be added to keep the fracture open in order to maintain a good flow rate in the reservoir.

4.2 Commercial sites

4.2.1 Soultz-sous-Forêts, France

Soultz-sous-Forêts EGS could be regarded as the most successful commercial EGS projects to date. By 2019, the annual electricity production is about 11 GWh/year (Ravier et al. 2019). The site is located in the upper Rhine Graben, as shown in Fig. 10a.

In 1987, the first well GPK1 was drilled to the depth of 2002 m, with a number of challenging issues, including direction control, circulation loss, pipe stuck, and an overrun budget. The temperature at 2000 m was only about 140 °C, which was lower than expected (Baria et al. 2005). In 1990, an existing oil well EPS1 was deepened from 930 to 2227 m, where the temperature was measured to be near 150 °C (Genter and Traineau 1996). This well was used to characterize the natural fracture systems in the area. Figure 10b shows the cross-sectional map of the Soultz geothermal system (Dezayes and Genter 2008; Hébert et al. 2011; Ledésert and Hébert 2012). Details of the drilling work and the development history of the Soultz EGS project can be found in Baria et al. (1999, 2005), Gérard et al. (1997), and Jung et al. (1996). Since the present review has a focus on hydraulic stimulation strategies, we shall summarize the three stimulation operations that were conducted at Soultz:

(a) After the re-drilling of the GPK2 well in 2000, a hydraulic stimulation operation was performed. A total of 23,400 m^3 fluid was injected into the reservoir with the flow rate ranged from 30 to 50 kg/s, and the maximum wellhead pressure reached 14.5 MPa. The detailed injection rate, wellhead pressure, and seismic event rates were shown in Fig. 10c (Baria et al. 2005; Gérard et al. 1997). Results of acoustic events mapping indicated that hydraulic fracturing was well developed over a region 500 m in width and 1000 m in length. Additionally, geophysical logging results indicated a major fracture set, oriented towards N160E, and two secondary fracture sets oriented in N140E and N20E, which contributed to a significant permeability enhancement (Moriya et al. 2003).

(b) From 2001, the GPK3 well was drilled to the depth of 5093 m to reach the fractured zone, which had been previously created by stimulation of well GPK2 in 2000. The distance between the GPK2 and the GPK3 well bottoms was 600 m. An injection test was performed with the GPK3 as the injection well and GPK2 as the production well. The results indicated a productivity index of 3.5 kg/s/MPa, implying an excellent connection between the two wells. Thus, in 2003, hydraulic stimulation was conducted in GPK3 with the injection of ~ 37,000 m^3 water into the reservoir. The wellhead pressure, injection rate, and seismic event evolution are shown in Fig. 10c.

(c) An inclined well GPK4 was drilled from 2003 to 2004, reaching 5105 m depth, at a bottom-hole distance of 650 m from the GPK3 well. After the well completion, the GPK4 well was stimulated by injection of heavy brine as the working fluid. However, the results of the stimulation operation were not as good as expected, explainable by the possible presence of a linear aseismic zone separating GPK4 from the two wells, GPK2 and GPK3. Even though acid fracturing was further used, the connection was still limited. The total fluid volume injected into the GPK4 was 22,000

m^3. The hydraulic stimulation results of the GPK4 well are shown in Fig. 10c.

Based on the fluid injection history, we can see that conventional hydraulic fracturing was generally used at the Soultz site. For some stimulation operations in GPK2 and GPK3 wells, hydraulic stimulations were successful in creating new fractures connecting the wells as shown by results from acoustic mapping monitoring. However, in some cases, such as the two consecutive hydraulic fracturing stimulation in GPK4, the permeability enhancement was limited. Nevertheless, the Soultz EGS project can perhaps be regarded as one of the most successful EGS system commercially, and furthermore the project provided data from more than 30 years of scientific/technical research, covering petrogeology investigation, well-drilling design, hydraulic fracturing optimization, and seismic monitoring. One important lesson learned is that proper site selection and characterization should be an essential element for the development of an EGS site. The natural fracture system was found to be well-developed in one area (GPK2 and GPK3), where significant permeability enhancement and well connections were accomplished through hydraulic stimulation, while the absence of large critically stressed faults near the site decreased the potential of large earthquakes. However, in some other areas (e.g., near GPK4), the natural fractures are not well-connected, in which case hydraulic stimulation was found to be not so effective and some other stimulation methods would need to be applied to enhance the reservoir permeability.

4.2.2 Cooper Basin, Australia

Inspired by oil and gas drilling results that the temperature at a depth of 4 km reached 250 °C in the Cooper Basin area in Australia (Fig. 11a), the Cooper Basin EGS project was initiated in 2002 (Mills and Humphreys, 2013). The target reservoir was identified as composed of radiogenic granites and uranium-rich rocks (Meixner et al. 2000). The objective of the project was to investigate the EGS feasibility in this area.

The well distribution is shown in Fig. 11b. Well Habanero-1 was finished at a depth of 4421 m, with the bottom-hole temperature of 250 °C. It intersected the granite at a depth of 3668 m and was located near the McLeod-1 well, an oil-exploration well that had previously penetrated the granitic basement. Data indicated that the granite was critically stressed for shear failure, and some of these fractures intersected Habanero-1 with a fluid pressure of 35 MPa. During well drilling, heavy-weight fluids were used to avoid potential mud loss. However, fracture permeability was higher than expected and some fractures slipped, which resulted in massive mud loss during well drilling. Details of the drilling history can be found in Humphreys et al. (2014).

After completing Habanero-1, hydraulic stimulations were performed in the well from November to December 2003 (Garcia-Aristizabal, 2018). The wellhead pressure, flow rate, and injectivity are shown in Fig. 11c. Conventional hydraulic fracturing technique with step injection pulses was used to enhance the reservoir permeability. A total of 20,000 m^3 of water was injected into the reservoir at a depth of 4250 m, with the flow rate first increasing from 8.0 L/s to 24.0 L/s, and then, in the third and fourth steps, the wellhead pressure was maintained between 31.0 MPa and 35.0 MPa. The wellhead pressure was found to increase quicker than the injection rate, which indicated that the injectivity decreased, and the permeability enhancement was poor. A total of 10,436 seismic events larger than the magnitude of -0.8 were recorded during this hydraulic stimulation, and they formed a large planar cloud dipping at 10° to the west direction, with an area of 1000 m times 2000 m and a thickness over 150 m (Kumano et al. 2005; Soma et al. 2004). It was suggested that all these events occurred in a single large fault, which was later confirmed and the fault was named Habanero Fault (Baisch et al. 2006; Bendall et al. 2014).

Besides this hydraulic stimulation in Habanero-1, some other stimulations were performed in other wells in the Cooper Basin (Hogarth et al. 2013a, 2013b; Holl and Barton 2015). Moreover, some injection tests and close-loop flow tests were performed before production operation and more details and results about close-loop and injection tests can be found in the references (Hogarth et al. 2013a, 2013b; Holl and Barton 2015; Hogarth and Bour 2015).

After almost 20 years of planning, drilling, testing, and scientific research concerning the Cooper Basin EGS project, some lessons were summarized by Hogarth and Holl (2017). They pointed out that the natural fracture systems in these granite rocks were likely to be closed, which means that the natural fractures are isolated from the general fluid flow in the domain.

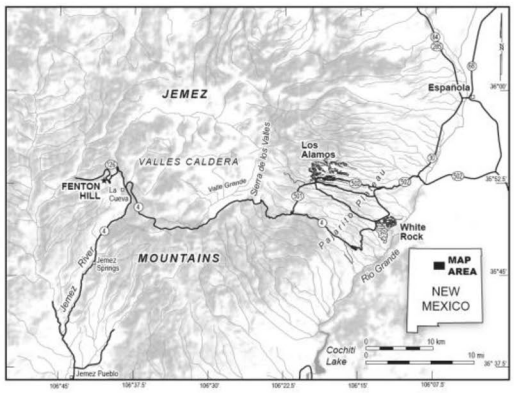
JEMEZ
VALLES CALDERA
MOUNTAINS
FENTON HILL
Los Alamos
Española
White Rock
Jemez Springs
Jemez Pueblo
Cochiti Lake
MAP AREA
NEW MEXICO

(a)

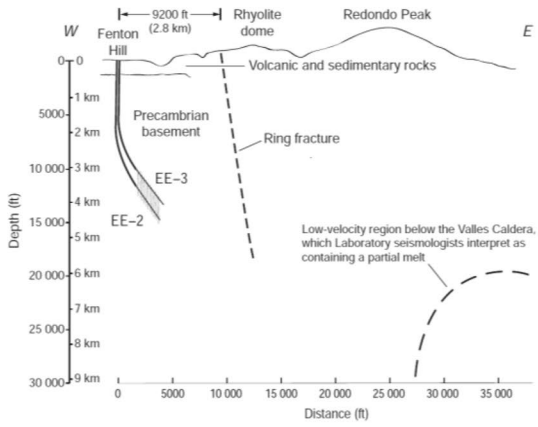
W
E
9200 ft (2.8 km)
Fenton Hill
Rhyolite dome
Redondo Peak
Volcanic and sedimentary rocks
Precambrian basement
Ring fracture
EE–3
EE–2
Low-velocity region below the Valles Caldera, which Laboratory seismologists interpret as containing a partial melt
Depth (ft)
Distance (ft)

(b)

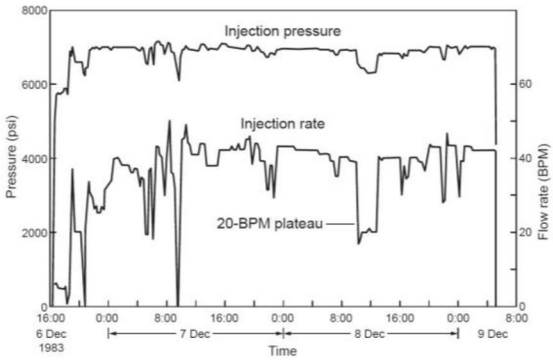
Injection pressure
Injection rate
20-BPM plateau
Pressure (psi)
Flow rate (BPM)
6 Dec 1983
7 Dec
8 Dec
9 Dec
Time

(c)

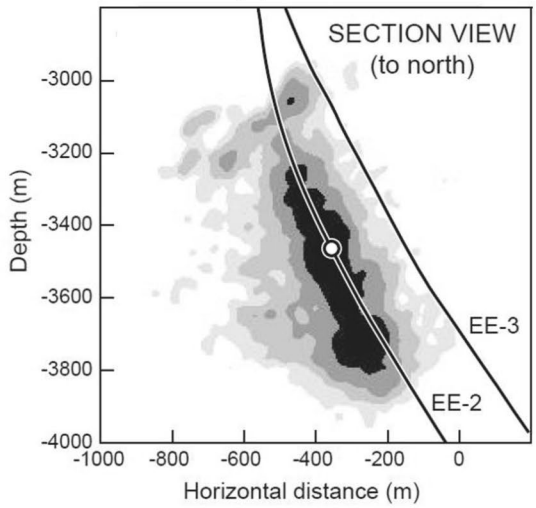
SECTION VIEW
(to north)
Depth (m)
EE-3
EE-2
Horizontal distance (m)

(d)

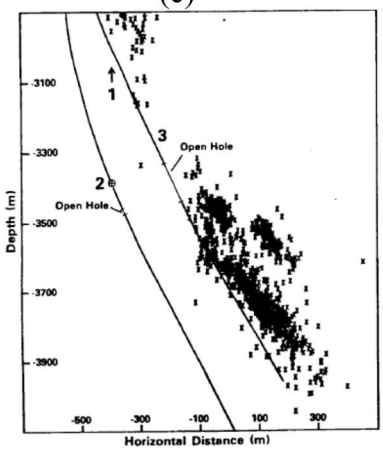
Depth (m)
Open Hole
Open Hole
Horizontal Distance (m)

(e)

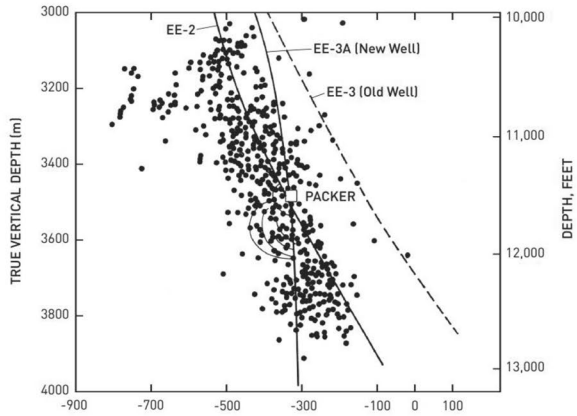
EE-2
EE-3A (New Well)
EE-3 (Old Well)
PACKER
TRUE VERTICAL DEPTH (m)
DEPTH, FEET

(f)

◂**Fig. 8** **a** The location of the Fenton Hill geothermal project. **b** The well location and basic geological condition. **c** The injection rate, pressure at the surface during the conventional hydraulic fracturing test in EE-2 wellbore. **d** The section-view of microseismic activities cloud map of EE-2 and EE-3 borehole. **a** to **d** are extracted from Kennedy et al. (2010). **e** The microseismic map after the hydraulic fracturing in well EE-3 (Dash et al. 1985). **f** The position of well EE-3A after re-drilling (Tester et al. 2006)

However, upon hydraulic stimulation, they were hydraulically connected and thus the reservoir permeability was enhanced. Moreover, the pre-existing natural fractures/faults that experienced high slip during the stimulation stage may serve as the main fluid channels and paths. It is suggested that, for a potential EGS site, the in-situ stress state should be carefully investigated since it plays a dominant role in hydraulic fracture propagation. Also, a comprehensive identification of critically stressed fractures/faults is important for efforts to mitigate induced seismic risks. Finally, it is suggested that induced seismicity cannot be totally avoided during long-term hydraulic stimulation and fluid circulation in a successful EGS project. Thus, a proper design of fluid injection strategy is crucial in reducing seismic potential and lowering the maximum magnitude of seismic events.

4.3 Suspended (or terminated) EGS sites

4.3.1 Basel, Switzerland

The Basel EGS project is located at the south-eastern end of the Rhine Graben, Switzerland, as shown in Fig. 12a. Geological investigation indicated a north-northwest trending compression and a west-northwest extension making this area a seismically active environment (Dèzes et al. 2004; Laubscher 2001). The first exploration well, Otterbach2, was drilled to the depth of 2755 m to be used for recording regional seismic events (Hölker and Graf 2005). Then, Basel 1 well was drilled from May to October 2006 to the depth of 5000 m, and it crossed the sedimentary rocks at a depth of 2400 m and the granitic basement at a depth of 2600 m. The bottom of the wellbore reached a temperature of about 200 °C (Wyss and Rybach, 2010). An acoustic borehole imager was used to identify natural fractures from 2557 to 5000 m depth, and a total of 984 natural fractures were found near the borehole (Vidal and Genter 2018; Ziegler et al. 2015). Before hydraulic stimulation of Basel 1 well, an injection test was performed to characterize the hydraulic properties of pre-existing natural fractures. The results yielded a value of effective permeability of 1×10^{-17} m^2 (Bourdet 2002), and the reservoir permeability was found to be dominated by a few major fractures in the open hole section.

The first hydraulic stimulation was performed in Basel 1 over the open hole section below 4629 m, as shown in Fig. 12b (Häring et al. 2008; Ladner and Häring 2009). The detailed injection rate, wellhead pressure, triggered event rate, and magnitudes of the seismic events are shown in Fig. 12c (Ladner and Häring 2009). The fluid was injected into the formation with a stepwise increasing flow rate. During the first 16 h of fluid injection, the flow rate was increased from 0 to 100 L/min, and the wellhead pressure reached about 11.0 MPa. During the subsequent fluid injection, the injection rate was increased stepwise to 3300 L/min, and the maximum wellhead pressure reached 29.6 MPa (296 bars). The seismic event rate increased with the rise of wellhead pressure and fluid injection rate. Later, due to the large number of seismic events observed, with some events having a magnitude near 3.0, the flow rate was decreased in the early morning of 8 December 2006. In total, the injection lasted for almost six days. However, the decrease in flow rate did not directly result in a decrease in the number and magnitude of the seismic events, and it was decided to bleed off the well. However, an earthquake with a magnitude of 3.4 occurred just before the bleed-off operation. With the bleed-off operation, the wellhead pressure dropped to the hydrostatic fluid pressure after four days. After that, the well remained open, and 3400 m^3 water flowed back over a period of 14 months.

During the injection operation, when the injection pressure was below 8.0 MPa (80 bars), the wellhead pressure showed a large increase with increasing injection flow rate, indicating that the reservoir's injectivity was relatively low. However, when the fluid pressure was higher than 8.0 MPa, the reservoir's injectivity increased, i.e., a smaller pressure rise was observed with an increase in injection rate (Krietsch et al. 2020; Pandey et al. 2018). Moreover, with further stepwise increase of injection rate, some wellhead pressure drops were observed, which indicated the occurrence of sudden permeability increases due to shear slip of optimally oriented pre-existing

natural fractures (Rutqvist and Stephansson 2003). When the wellhead pressure reached 23.5 MPa (235 bars), the pressure response with injection flow rate became more erratic. This could be regarded as a sign of shear-induced permeability enhancement together with elastic response of fractures caused by local changes in normal effective stress, which contribute to the reservoir permeability enhancement (Häring et al. 2008). Analysis showed that the reservoir transmissibility was increased almost 400 times, and this enhancement may have been irreversible during the bleed-off process (Jung and Ortiz 2007).

The Basel earthquake magnitude numbers were provided by the Swiss Seismological Service, as shown in Fig. 12c (Hölker and Graf 2005), which was complemented by seismic modeling with optimized network resolution (Dyer et al. 2008). The results indicated the occurrence of a large event (M_L 3.4) on 8 December 2006, followed by three aftershocks with a magnitude larger than 3. These aftershocks occurred 29 (M_w 3.1), 39 (M_w 3.2), and 56 (M_w 3.2) days after injection termination. The focal mechanism for these events was investigated, and more details could be found in the references (Deichmann et al. 2014; Deichmann and Giardini 2009; Kraft and Deichmann, 2014; Mukuhira et al. 2013). These results indicated that the induced seismic events did not originate from a single rupture and strain release among pre-existing faults. The root cause of seismic events in the Basel EGS project appears to be multiple shearing of obliquely oriented fractures in the fractured zone.

In summary, even though the project was terminated because of the large seismic events, the Basel EGS project is influential in history because it was the first attempt to extract deep geothermal energy under a modern urban environment. Based on data analysis, the seismic events induced by hydraulic stimulation at the site appear to have resulted from multiple hydraulic shearing of obliquely oriented fractures in the fractured zone, which suggests that, before hydraulic fracturing stimulation, the natural fracture systems should be comprehensively mapped for an assessment of potential seismic risks.

4.3.2 Pohang, South Korea

The Pohang EGS site is located in the Heunghae Basin, shown in Fig. 13a (Park et al. 2020). The target reservoir is a granodiorite at about 4.2 km depth, overburdened by tertiary sedimentary rocks and quaternary alluvium. Based on geological investigation, the Pohang area is a high heat-flow area, with a temperature higher than 140 °C at a depth of 4200 m (Lee et al. 2010).

Prior to the Pohang EGS project, four wells named BH-1 to BH-4 were drilled down to a maximum depth of 2300 m between 2003 and 2008. They were used for a low-temperature geothermal application in this area (Lee and Song 2008). Also, a 1000-m borehole nearby (EXP-1) was used for in-situ stress measurements (Kim et al. 2017). Two deep boreholes were then drilled for the main Pohang EGS project, named PX-1 and PX-2 wells. The arrangements of the two wells are shown in Fig. 13b. The vertical well PX-2 was drilled to a depth of 4340 m, with a 140-m open hole section at the borehole bottom. The borehole PX-1 was drilled vertically to a depth of 2419 m before the drilling of PX-2, and then after PX-2 was drilled, PX-1 was extended directionally inclined approximately 20° from the vertical direction, in the 304° mean azimuth, to the depth of 4215 m, with a 313 m open-hole section at the bottom. The distance between the two boreholes PX-1 and PX-2, was 6 m on the surface and 600 m at the well bottom, forming a geothermal fluid circulation system (Park et al. 2020).

The timeline for the Pohang EGS project could be found in Park et al. (2020).A total of five hydraulic stimulation operations (P1–P5) were performed and general information on seismic events and accumulative injection volume is shown in Fig. 14c.

The first hydraulic stimulation P1 was performed in the PX-2 well, aiming to enhance the reservoir permeability and to characterize reservoir hydromechanical properties at the same time. During a total of 23 days of fluid injection from 29 January 2016 to 20 February 2016, several injections were performed without a packer (Fig. 14-a1). A cyclic injection protocol, combined with a traffic light system (TLS), was designed and implemented to mitigate the seismic

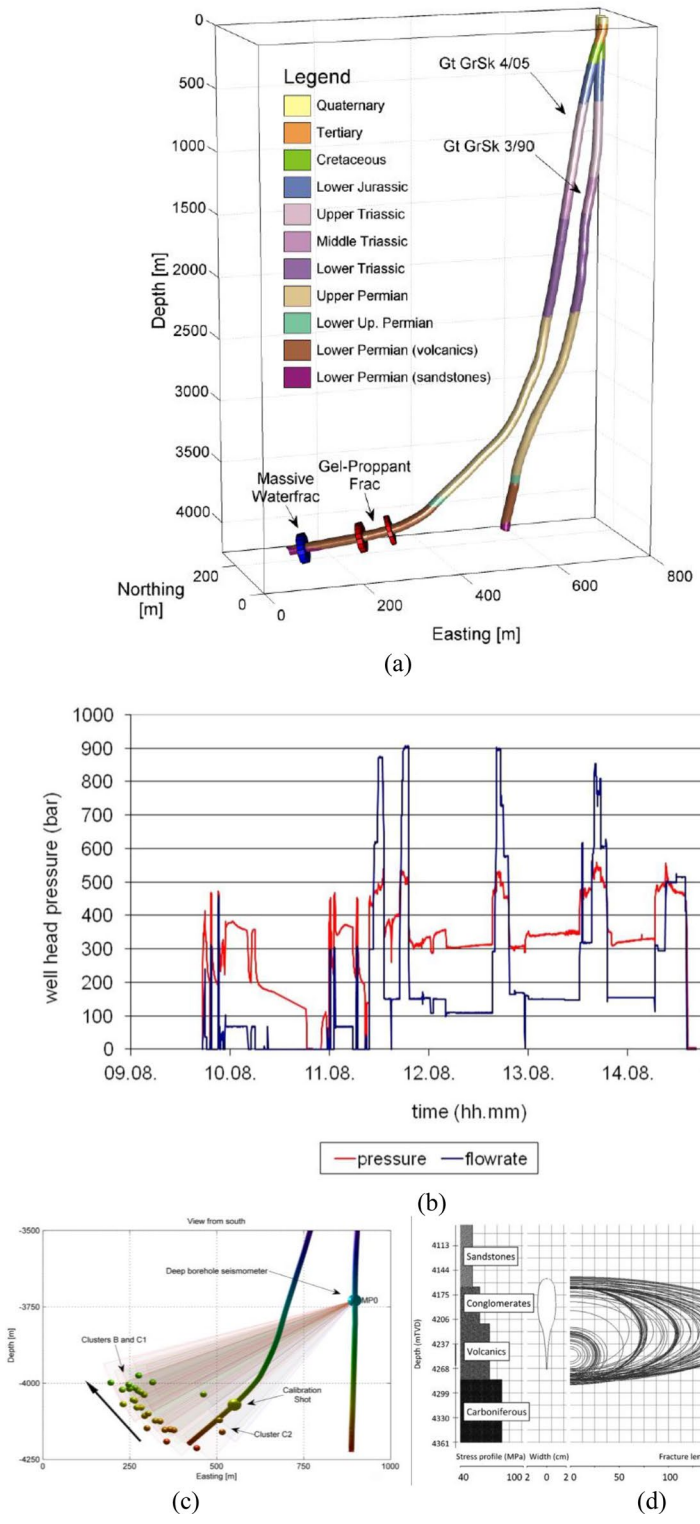

Fig. 9 **a** The schematic map of the Groß Schönebeck site (modified from Zimmermann et al. 2008); **b** The wellhead pressure and flow rate evolution with time for cyclic injection in Gt GrSk 4/05 well. (modified from Zimmermann et al. 2008); **c** The monitoring seismic events associated with the hydraulic stimulation in Groß Schönebeck geothermal site. (modified from Kwiatek et al. 2010). The MP0 represents the location of the deep borehole seismometer. The color reflects the hypocentral depth of events. The black arrow shows the migration of seismic events with time. **d** The calculated fracture distribution after the hydraulic stimulation is based on numerical simulation results. Each curve represented one hour of fracture propagation, and the stress profile was the minimum principal stress. (modified from Zimmermann et al. 2010)

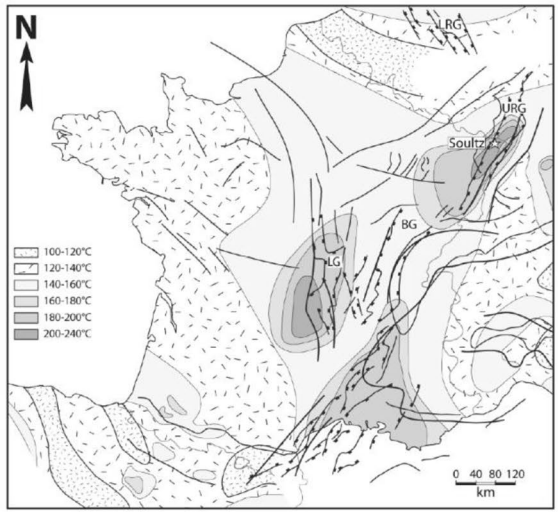
N
LRG
URG
Soultz
BG
LG
100-120°C
120-140°C
140-160°C
160-180°C
180-200°C
200-240°C
0 40 80 120
km

928

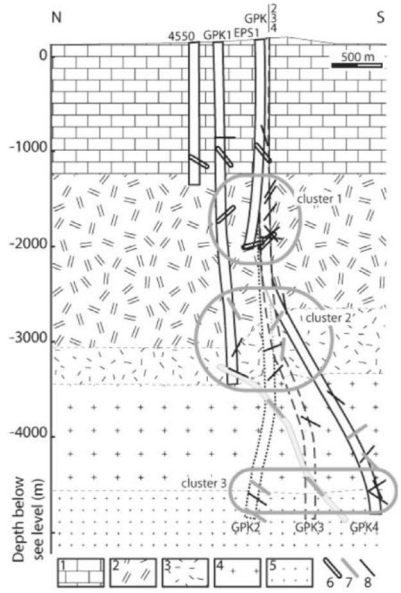
N
S
GPK 2 3 4
4550 GPK1 EPS1
500 m
0
-1000
-2000
-3000
-4000
cluster 1
cluster 2
cluster 3
Depth below see level (m)
GPK2
GPK3
GPK4
1 2 3 4 5 6 7 8

(a) (b)

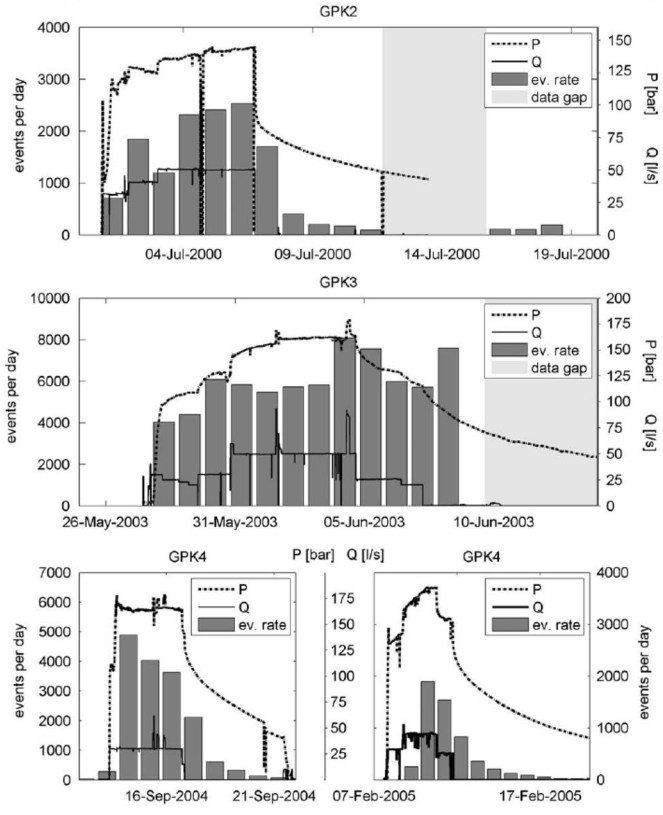
GPK2
events per day
P [bar]
Q [l/s]
P
Q
ev. rate
data gap
04-Jul-2000
09-Jul-2000
14-Jul-2000
19-Jul-2000
GPK3
26-May-2003
31-May-2003
05-Jun-2003
10-Jun-2003
GPK4
16-Sep-2004
21-Sep-2004
07-Feb-2005
17-Feb-2005

(c)

◂**Fig. 10** **a** The location of Soultz geothermal site (modified from Dèzes et al. 2004); **b** The cross-section map of the Soultz geothermal system (modified from Dezayes and Genter 2008; Hébert et al. 2011; Ledésert and Hébert 2012); **c** The wellhead pressure (dotted line), the fluid injection rate (solid line), and the rate of induced seismic events (vertical bars) evolution with time for four main hydraulic fracturing stimulation operations in the Soultz EGS project (modified from Baisch et al. 2010)

risks (Kim et al. 2018b). A total of 1970 m^3 of water was injected in pulses with a maximum flow rate of 46.8 L/s. Correspondingly, the wellhead pressure displayed peaks at times of injection pulses with a maximum peak at 89.2 MPa (Fig. 14-a1), which was equivalent to 131.7 MPa bottom-hole pressure. More detailed data from the first day (29 January 2016) of fluid injection are shown in Fig. 14-a3 as an example of the reservoir response to the cyclic injection. The wellhead pressure increased quickly under the first injection pulse and then stabilized at around 60–70 MPa over the following 11 injection pulses. The pressure decreased after each of the later pulses and also after the last pulse, indicating the opening of a flow channel for water leakage at about 50 MPa (Fig. 14-a3). Figure 14-a2 shows a weak positive relationship between injection volume and seismic magnitude up to the injection volume of 1500 m^3, beyond which the maximum magnitude of the seismic events of each day seemed to stay below 1.8. It can be seen that more seismic events were observed during the shut-in periods (red rectangles) than during the injection periods (blue triangles), and the occurrence of seismic events seemed to persist even when pumping was stopped for a long time (one week). It is interesting to note that similar magnitudes and numbers of seismic events during the shut-in period were also observed in the hydraulic stimulations at Basel, Switzerland, and at Soultz-sous-Forets, France (Charléty et al. 2007; Schill et al. 2017). The mechanism of this phenomenon has been discussed in terms of the pore pressure diffusion, poroelastic effects, and hydromechanical response (Baisch et al. 2010; De Simone et al. 2017; McClure 2015; Mukuhira et al. 2017). An important lesson from these observations is that the injection-induced seismic events after injection, during shut-in stages, must be given enough attention and carefully investigated in planning hydraulic stimulation in EGS since a number of them have large magnitudes.

The second hydraulic stimulation P2 was performed in the directionally extended well PX-1. This hydraulic fracturing stimulation was divided into two stages: (a) test stimulation and (b) main stimulation, which lasted from 15 to 28 December 2016 (Fig. 14b). The test stimulation aimed to evaluate the reservoir's initial transmissivity and monitor the seismic responses to design the traffic light system (TLS). A total of 3907 m^3 of water was injected into the reservoir, and a total of 2164 m^3 of water was bled off during and after the conclusion of the injection operation on 28 of December, see Fig. 14-b2. The timeline of the second hydraulic stimulation is shown in Fig. 14-b1, including information on injection rate (red line) and wellhead pressure (blue line). It is interesting to observe that the wellhead pressure (27.7 MPa) during the second hydraulic stimulation in PX-1 was much lower than the peak wellhead pressure during the first hydraulic stimulation (P1) in PX-2 (64.0–89.0 MPa), and different stimulation mechanisms may have dominated the two stimulations (Park et al. 2020). The seismic events during the second hydraulic stimulation are shown in Fig. 14-b2, categorized into injection phase (blue triangles), shut-in phase (red rectangles), and bleed-off phase (green circles). The black line represents the injection volume, and the dashed line represents the net volume (injection minus bleed-off). A earthquake occurred on 23 December, with a local magnitude of 2.2. After that, the bleed-off decreased the occurrences of seismic events in the short term (green circles). However, once the fluid injection re-started on 26 December, seismic events occurred again, and two large events with magnitudes more than 2.0 occurred during the shut-in on 29 December. After that, more bleed off was conducted, and the seismic activities decreased.

The later three hydraulic fracturing operations, P3, P4, and P5 were performed in the PX-1 and PX-2 wells in 2017. Details on the injection rate, injection volume, and wellhead pressure of these stimulation operations could be found in Yeo et al. (2020). The third hydraulic stimulation P3 was conducted in the PX-2 well, with cyclic injection protocol from 16 March to 14 April 2017. It is worth mentioning that a M_w 3.2 earthquake occurred on 15 April during the shut-in period (Korean Government Commission 2019). The fourth hydraulic stimulation, P4, was performed from 7 to 14 August 2017, with a total

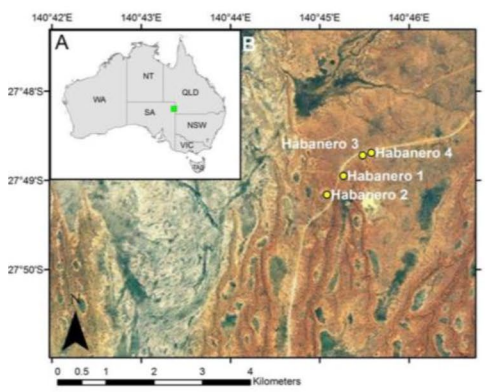
140°42'E
140°43'E
140°44'E
140°45'E
140°46'E
27°48'S
27°49'S
27°50'S
A
B
NT
QLD
WA
SA
NSW
VIC
Habanero 3
Habanero 4
Habanero 1
Habanero 2
0 0.5 1 2 3 4
Kilometers

(a)

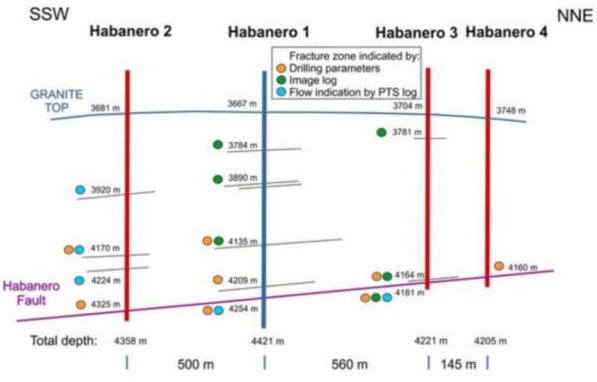
SSW
NNE
Habanero 2
Habanero 1
Habanero 3
Habanero 4
Fracture zone indicated by:
Drilling parameters
Image log
Flow indication by PTS log
GRANITE TOP
3681 m
3667 m
3704 m
3748 m
3784 m
3781 m
3920 m
3890 m
4170 m
4135 m
4224 m
4209 m
4164 m
4160 m
4325 m
4254 m
4181 m
Habanero Fault
Total depth:
4358 m
4421 m
4221 m
4205 m
500 m
560 m
145 m

(b)

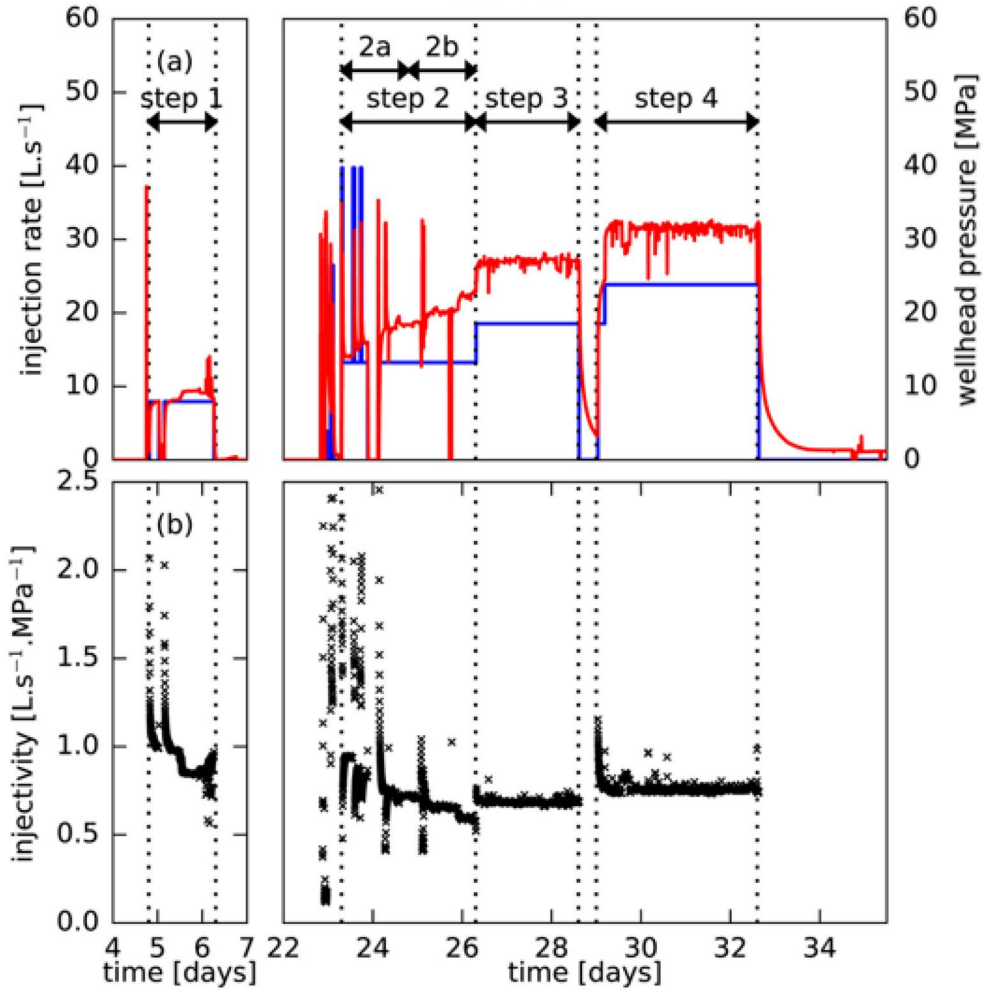
(a)
step 1
2a
2b
step 2
step 3
step 4
injection rate [L.s^{-1}]
wellhead pressure [MPa]
(b)
injectivity [L.s^{-1}.MPa^{-1}]
time [days]
time [days]

(c)

◂**Fig. 11** **a** Location of the Cooper Basin EGS site. (modified from Ayling et al. 2016); **b** The schematic map of the cross-section of the Habanero wells (modified from Holl and Barton 2015); **c** The wellhead pressure, injection rate, and injectivity evolution with time for the hydraulic fracturing stimulation in Habanero-1 well. (modified from Riffault et al. 2018). The blue line is injection rate and red line is wellhead pressure

of 1756 m^3 water injected into the PX-1 well. This hydraulic stimulation was a validation study of the soft cyclic injection with the flow rates periodically alternating between 1.0 and 10.0 L/s. There were only 52 seismic events recorded, and the largest magnitude was M_w 1.9. However, no significant permanent reservoir permeability enhancement was observed in the fourth hydraulic stimulation (Farkas et al. 2021; Hofmann et al. 2019). The final hydraulic simulation P5 was performed again in PX-2 well from 30 August to 14 September, also with cyclic injection protocol. This hydraulic stimulation only produced a modest seismic response, similar to the first stimulation P1 at PX-2 well, with a maximum magnitude event of M_w 2.0 (Korean Government Commission 2019). In total, 5663 m^3 and 7135 m^3 of water was injected into PX-1 and PX-2 wells, respectively, 3968 m^3 and 2989 m^2 water flowed back from PX-1 and PX-2 wells, and a net volume of 5841 m^3 remained in the reservoir after the five hydraulic stimulations at Pohang geothermal site. Over the period of the five hydraulic stimulations, only one damaging earthquake occurred. This was during the shut-in stages of the third hydraulic stimulation P3 and had a magnitude of 3.2. All other seismic events were modest and with magnitudes less than 2.0, and thus it was believed that the cyclic injection protocol could be an effective technique to mitigate seismic risk on the site (Hofmann et al. 2019). However, 58 days after the last hydraulic stimulation P5, a M_w 5.5 earthquake hit this area on 15 November 2017, and shook Pohang city, injuring over 100 people, causing $300 million worth of damage, and requiring more than 1700 residents to move to emergency housing (Grigoli et al. 2018; Lim et al. 2020). Therefore, the government suspended the Pohang EGS project and invited domestic and international researchers to investigate the origin of this earthquake. The committee concluded that the main shock was triggered by fluid injection-induced fracturing in a previously unmapped fault zone that grew quickly and released the local tectonic strain. The activated unmapped fault plane is shown in Fig. 14c. It extends from 2.5 to 6.0 km and intersects the PX-2 well at 3.8 km (Korean Government Commission 2019). More researches to explore the reasons for Pohang earthquake could be found in Hong et al. (2022), Kim et al. (2022), McGarr et al. (2018, 2019), Westaway and Burnside (2019), and Woo et al. (2019).

Two major lessons may be learned from the Pohang EGS project.: Firstly, the CSS, which combines cyclic fluid injection and seismic monitoring with the traffic light system (TLS) (see Sect. 3.3.2), was shown to have effectively increased the reservoir permeability and mitigated seismic risks in the crystalline rock reservoir. However, its possible connection with the 5.5 magnitude earthquake that occurred 58 days afterwards needs to be investigated in depth. Secondly, the hydraulic stimulation of the PX-1 well in December 2016 produced a fracture network as planned, while injection in the PX-2 well in February and September 2017 appears to have activated an unmapped fault, resulting in an earthquake in November 2017. During the drilling of the PX-2 well, a large-scale mud loss occurred, but it did not attract enough attention to the possible existence of a large-scale fault. If this critically stressed fault could have been mapped before the hydraulic fracturing stimulation and appropriate actions taken, there would have been a possibility that the earthquake could have been avoided (Ellsworth et al. 2019). Thus, before fluid injection, the local natural fracture systems and large faults should be comprehensively mapped. Moreover, all the drilling and seismic data should be timely analyzed and interpreted during well drilling and hydraulic stimulation operations. These data will form an important or even critical part of the effort in assessing potential seismic risks of the EGS during the process of development.

In this part, we summarised representative EGS sites globally and selected six of them for a detailed review of the hydraulic stimulation strategy, permeability enhancement performance, and induced seismicity. However, there are some other recent important field projects, such as the Espoo project in Finland (Hillers et al. 2020; Kwiatek et al. 2019; Leonhardt et al. 2021), Eden project in the UK (Abesser et al. 2020; Baumgärtner 2022; Fink et al. 2022) and projects under the Frontier Observatory for Research in Geothermal Energy (FORGE) in the

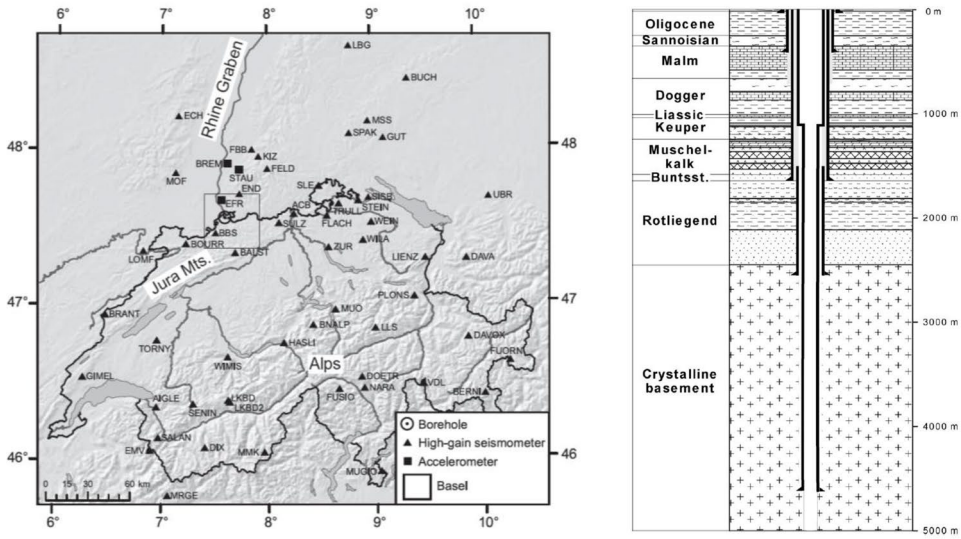
Rhine Graben
Jura Mts.
Alps
Borehole
High-gain seismometer
Accelerometer
Basel
Oligocene
Sannoisian
Malm
Dogger
Liassic
Keuper
Muschel-
kalk
Buntsst.
Rotliegend
Crystalline
basement
0 m
1000 m
2000 m
3000 m
4000 m
5000 m

(a) (b)

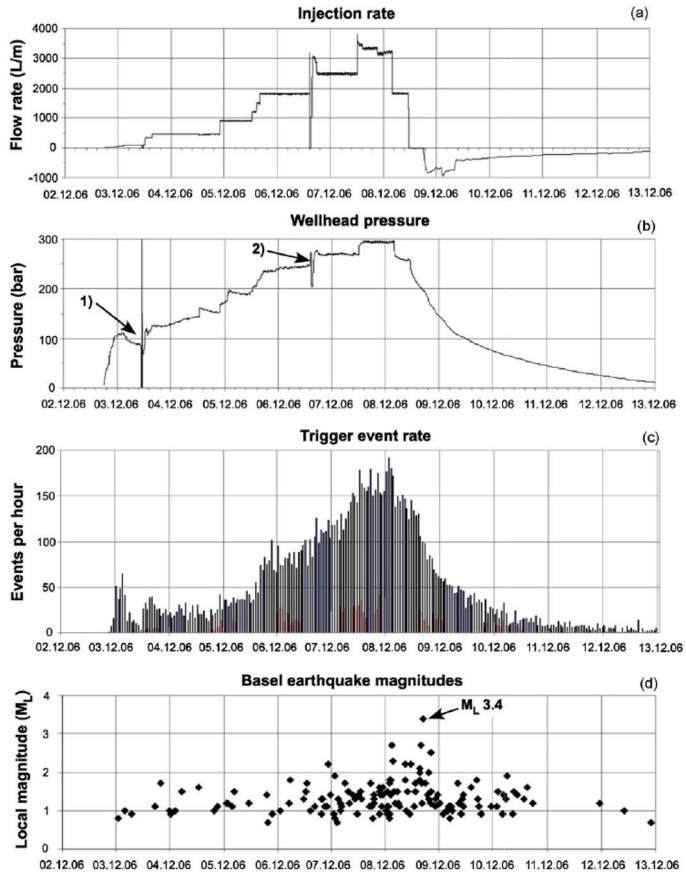
Injection rate
(a)
Flow rate (L/m)
Wellhead pressure
(b)
Pressure (bar)
1)
2)
Trigger event rate
(c)
Events per hour
Basel earthquake magnitudes
(d)
Local magnitude (M_L)
M_L 3.4
02.12.06 03.12.06 04.12.06 05.12.06 06.12.06 07.12.06 08.12.06 09.12.06 10.12.06 11.12.06 12.12.06 13.12.06

(c)

◂**Fig. 12** **a** The location of Basel EGS site and topographic map of Switzerland and surrounding regional seismic stations. (modified from Deichmann and Giardini 2009); **b** Lithological sequence along the Basel-1 borehole modified after c The evolution of injection rates, wellhead pressure, triggered event rates, and earthquake magnitude during hydraulic stimulation. (modified from Ladner and Häring 2009; Häring et al. 2008).

USA (Moore et al. 2018, 2019; Xing et al. 2022). More details concerning these projects can be found in the references, and we expect that many interesting results and lessons learned will emerge from these projects.

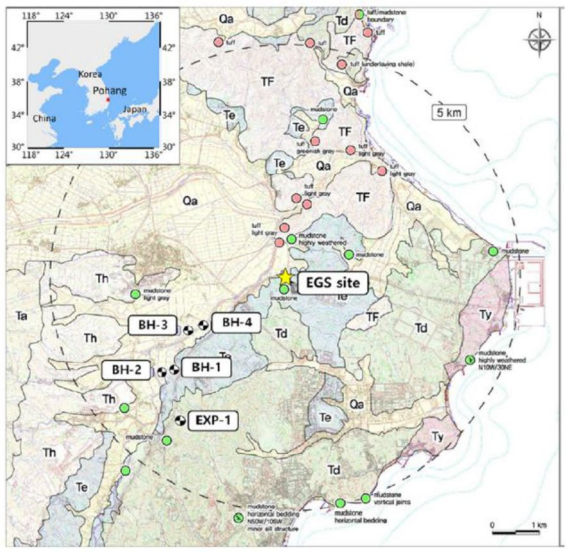

(a)

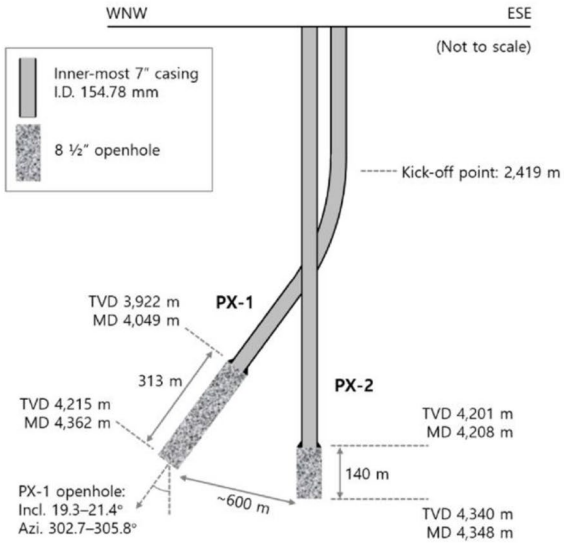

(b)

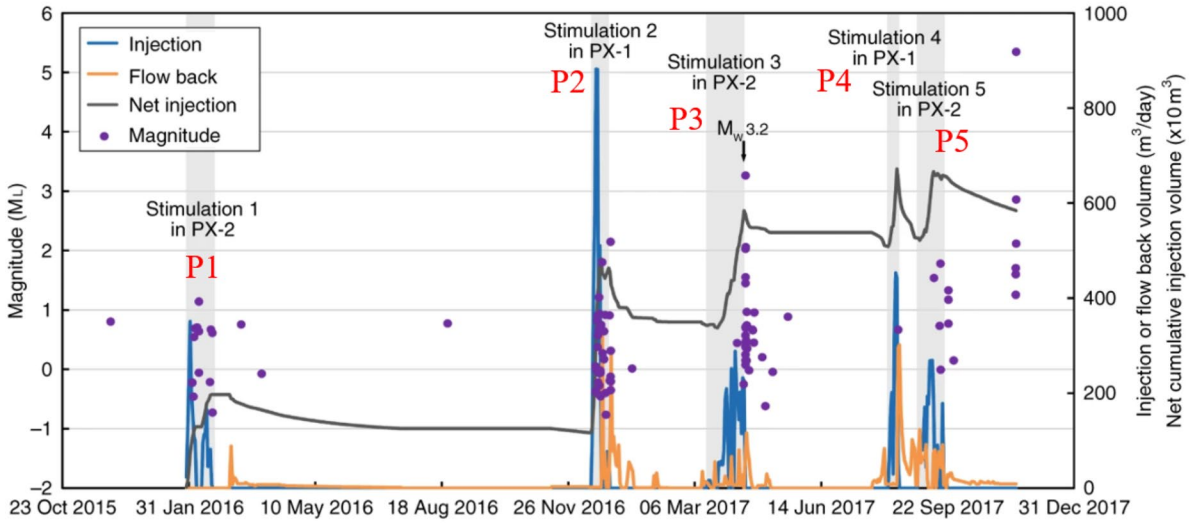

(c)

Fig. 13 **a** Geologic maps of the Pohang region, including the locations of the EGS site and the five nearby wells; **b** The simplified well dimension at the Pohang EGS site (Park et al. 2020); **c** The hydraulic fracturing operations at Pohang EGS sites (injection rate (blue line), flow back rate (orange line), and net injection volume (dark gray line). Five stages of hydraulic fracturing operations were named P1 to P5, and P1, P3, and P5 were performed in the PX-2 well, while P2 and P4 were performed in the PX-1 well. The seismic events were represented by purple circles (modified from Yeo et al. 2020)

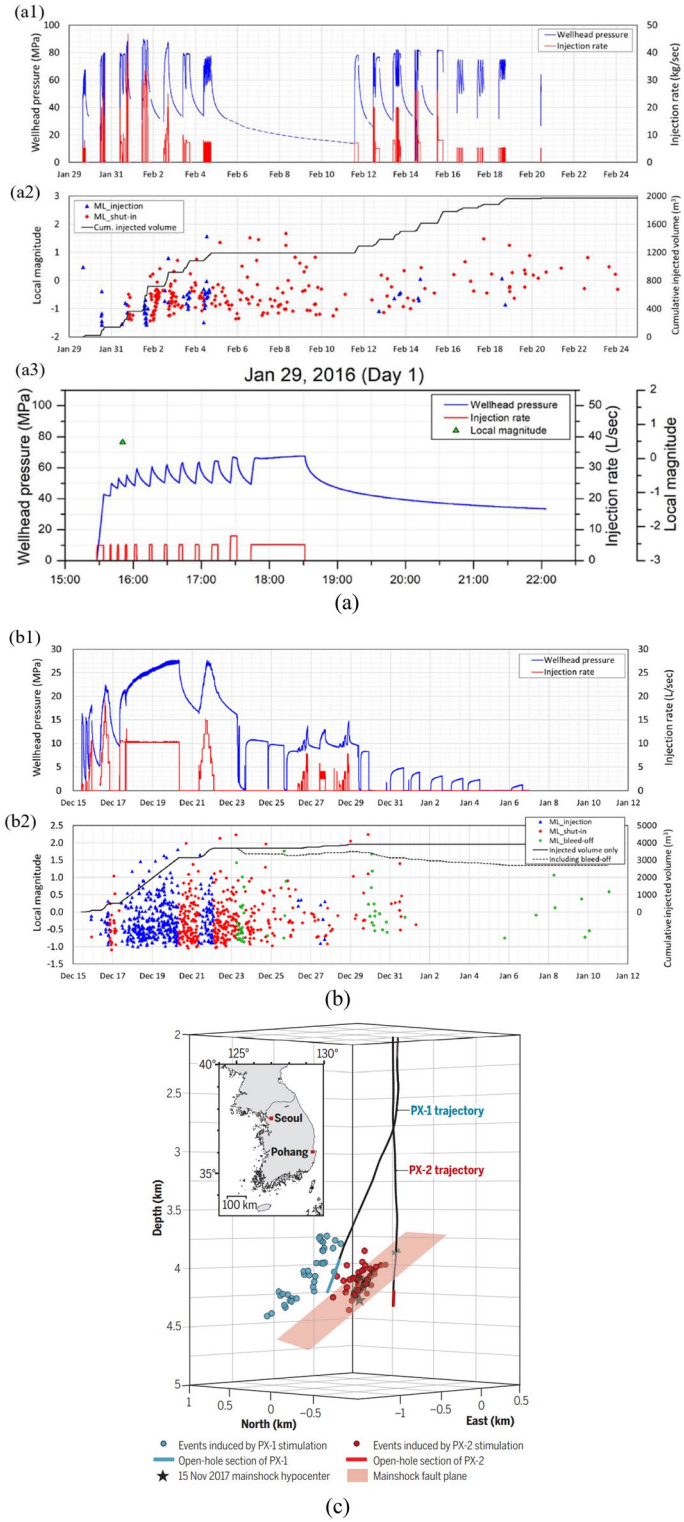

Fig. 14 **a** The hydraulic fracturing stimulation history for first stimulation in the PX-2 well (Modified from Park et al. 2020): **a1** The wellhead pressure and injection flow rate evolution for the whole period; **a2** the corresponding seismic response and cumulative injection volume; **a3** the injection rate, wellhead pressure, and the one seismic event on 29 January 2016. **b** Second stimulation in PX-1 well (Modified from Park et al. 2020) with **b1** injection rate and wellhead pressure evolution and **b2** corresponding seismic events and cumulative volume. **c** Schematic illustration of the relationship between the seismicity and the Pohang earthquake's rupture plane. The blue dots were the seismic events related to stimulation of the PX-1 well, and the red dots were the seismic events induced by PX-2 well stimulation. The mainshock fault plane extended from 2.5 km to 6 km and intersected the PX-2 well at 3.8 km (Lee et al. 2019)

5 Concluding remarks

In this review, we first discuss the hydraulic stimulation mechanisms underlying the enhancement of reservoir permeability and increase of the heat extraction area, and to understand the potential for fluid injection-induced seismicity during an EGS development. Then, some representative hydraulic stimulation designs and fluid injection strategies are reviewed, including conventional hydraulic fracturing, multi-stage fracturing, and cyclic soft stimulation. Finally, some typical EGS sites are reviewed by addressing two representative cases from the following three categories of sites: experimental field sites, successfully operating commercial sites, and currently suspended/terminated projects. Based on the review, we identify a number of critical components that should be considered for an optimal design of a hydraulic stimulation as well as highlight some areas that should be further researched:

(a) Comprehensive geological survey and evaluation of the natural fracture system and nearby fault zones prior to the site development

The natural fracture system and nearby faults are important for two critical aspects of an EGS site, namely (i) the hydraulic fracture propagation, shear dilation and new fracture network formation and (ii) the fluid injection-induced seismicity. Thus, the characterization of the natural fracture system and the major nearby faults as well as an understanding of thermo-hydro-mechanical-chemical processes that may be operating in them is critical in determining whether an EGS site will be successful. The role of the natural fracture system in hydraulic fracture propagation has been reviewed in Sect. 2.2. The interaction between natural fractures and hydraulically induced fractures determines the final topography of the generated fracture networks and thus the resulting hydraulic conductivity and heat exchange area. For instance, if the natural fracture system is not well developed within the reservoir, conventional hydraulic fracturing with a high injection rate needs to be performed to create open tensile fractures. In contrast, if the natural fracture networks are relatively well developed before the hydraulic stimulation, low-rate cyclic injection may be preferred to drive the shear slip of natural fractures for increasing reservoir permeability. Thus, a sufficiently comprehensive understanding of natural fracture distribution (size, orientation, density) within the target reservoir near the injection well is needed for a successful hydraulic stimulation design and optimization.

Large critically-stressed active faults should be avoided in the selection of EGS sites. As reviewed in Sect. 4.3, the Basel site's seismic events mainly came from multiple hydraulic shearing of obliquely oriented fractures in the fractured zone, while the Pohang earthquake appears to be a result of triggering a large critically-stressed fault by hydraulic stimulation. Thus, before the fluid injection, the natural fracture systems and large faults should be comprehensively mapped and evaluated to assess potential seismic risks.

(b) Proper design of the well arrangement and fluid injection strategy

The conventional concept of an EGS site includes one vertical injection well and one vertical production well, connected through one or a few major fractures created by massive fluid injection. However, as discussed in Sect. 3.2, this usually results in limited stimulated volume and early cold injection water breakthrough with significant heat production decay. Hence, the combination of horizontal drilling and multi-stage fracturing is proposed and may allow the EGS to reach a larger stimulation rock volume. The spacing of stimulation stages or intervals plays a vital role in determining the heat production efficiency and life expectancy of the operation. If the spacing is too small, the cost will be high, and the stress shadow effect may adversely affect the fracture propagation. On the other hand, if the stage spacing is too large, the reservoir may be under-stimulated, resulting in poor hydraulic conductivity between injection and production wells. Another point that should be highlighted is that the positioning of the active sections in the injection and production boreholes need to be optimized. This may be accomplished by drilling the two wells sequentially; that is, drilling the second well after the drilling and stimulation of the first well is completed, to ensure that the second well is drilled into the microseismic clouds produced by the stimulation of the first well. This is

an important lesson drawn from the Fenton Hill project in which, after some initial unsuccessful attempts, the production well was drilled directly into a hydraulically induced fracture region (microseismic cluster area) around the injection well. Only in this circumstance, the hydraulic conductivity between injection and production wells became high enough to allow the desired flow rate. Moreover, in recent years, besides the traditional doublet well layout, some new well layouts have been proposed, including the triplet well layout or quintuplet well layout (Chen and Jiang 2015). Hence, the well layout and arrangement of EGS are another area of consideration in an EGS project.

(c) Evaluating the fluid injection-induced seismicity, including post-stimulation seismicity

As discussed in Sect. 2.3, it is a challenging task to estimate the fluid injection-induced seismicity during an EGS site development, both during and after a hydraulic stimulation operation. The fluid injection-induced seismicity is a complicated thermo-hydro-mechanical-chemical (T-H-M-C) coupled process rather than a purely mechanical process. During fluid injection, some critical processes may affect the earthquake nucleation process, including the fluid diffusion within the reservoir and within faults, in-situ effective stress changes due to fluid pressure, thermomechanical changes due to cold water injection, and water–rock chemical interactions. Thus, a deeper understanding of the coupled T-H-M-C process of hydraulic stimulation is needed in the evaluation of the underlying mechanisms of fluid injection-induced seismicity, where geothermal heat, injected fluid, geologic structures and local in-situ stress conditions concurrently control fault instability behaviors.

One important observation is that seismic events with high magnitudes have been found to occur sometime after the termination of fluid injection. Examples have been reviewed in Sect. 4.3 for the Basel and Pohang EGS sites. Some possible mechanisms for post-stimulation seismicity have been pointed out in Sect. 2.3. We believe that profound research is essential on the understanding and modeling of post-stimulation seismic activities and on the development of control methods to mitigate such seismic risks.

Acknowledgements We acknowledge funding from E. On Värme, Malmö, Sweden.

Funding Open access funding provided by Uppsala University.

Declarations

Conflict of interest The authors declare that there are no known competing financial interests or personal relationships that could have influenced the work reported herein.

References

Abesser C, Busby J P, Pharaoh TC, Bloodworth AJ, Ward R S (2020) Unlocking the potential of geothermal energy in the UK

Adachi J, Siebrit E, Peirce A, Desroches J (2007) Computer simulation of hydraulic fractures. Int J Rock Mech Min Sci 44(5):739–757. https://doi.org/10.1016/j.ijrmms.2006.11.006

Ader T, Chendorain M, Free M, Saarno T, Heikkinen P, Malin PE et al (2020) Design and implementation of a traffic light system for deep geothermal well stimulation in Finland. J Seismol 24(5):991–1014. https://doi.org/10.1007/s10950-019-09853-y

Agarwal RG, Carter RD, Pollock CB (1979) Evaluation and performance prediction of low-permeability gas wells stimulated by massive hydraulic fracturing. J Pet Technol 31(3):362–372. https://doi.org/10.2118/6838-PA

Atkinson BK (1984) Subcritical crack growth in geological materials. J Geophys Res Solid Earth 89(B6):4077–4114. https://doi.org/10.1029/JB089iB06p04077

Atkinson GM, Eaton DW, Igonin N (2020) Developments in understanding seismicity triggered by hydraulic fracturing. Nat Rev Earth Environ 1(5):264–277. https://doi.org/10.1038/s43017-020-0049-7

Ayling BF, Hogarth RA, Rose PE (2016) Tracer testing at the Habanero EGS site, central Australia. Geothermics 63:15–26. https://doi.org/10.1016/j.geothermics.2015.03.008

Baisch S, Weidler R, Vörös R, Wyborn D, Graaf L (2006) Induced seismicity during the stimulation of a

geothermal HFR reservoir in the Cooper Basin, Australia. Seismol Soc Am Bull 96(6):2242–2256. https://doi.org/10.1785/0120050255

Baisch S, Vörös R, Weidler R, Wyborn D (2009) Investigation of fault mechanisms during geothermal reservoir stimulation experiments in the Cooper Basin, Australia. Seismol Soc Am Bull 99(1):148–158. https://doi.org/10.1785/0120080055

Baisch S, Vörös R, Rothert E, Stang H, Jung R, Schellschmidt R (2010) A numerical model for fluid injection induced seismicity at Soultz-sous-Forêts. Int J Rock Mech Min Sci 47:405–413. https://doi.org/10.1016/j.ijrmms.2009.10.001

Barati R, Liang JT (2014) A review of fracturing fluid systems used for hydraulic fracturing of oil and gas wells. J Appl Polym Sci 131:40735. https://doi.org/10.1002/app.40735

Baria R, Baumgärtner J, Gérard A, Jung R, Garnish J (1999) European HDR research programme at Soultz-sous-Forêts (France) 1987–1996. Geothermics 28(4–5):655–669. https://doi.org/10.1016/S0375-6505(99)00036-X

Baria R, Michelet S, Baumgärtner J, Dyer B, Nicholls J, Hettkamp T, Teza D, Soma N, Asanuma H, Garnish J, Megel T (2005) Creation and mapping of 5000 m deep HDR/HFR reservoir to produce electricity. In: Proceedings of the world geothermal congress, vol 1627

Barton CA, Zoback MD, Burns KL (1988) In-situ stress orientation and magnitude at the Fenton Geothermal Site, New Mexico, determined from wellbore breakouts. Geophys Res Lett 15(5):467–470. https://doi.org/10.1029/GL015i005p00467

Baujard C, Genter A, Dalmais E, Maurer V, Hehn R, Rosillette R, Vidal J, Schmittbuhl J (2017) Hydrothermal characterization of wells GRT-1 and GRT-2 in Rittershoffen, France: Implications on the understanding of natural flow systems in the Rhine Graben. Geothermics 65:255–268. https://doi.org/10.1016/j.geothermics.2016.11.001

J Baumgärtner 2022 The Eden Geothermal Project: Eden's (UK) hot rocks project hits target with successful drilling of first deep well. GeoTHERM Abstracts

Bendall B, Hogarth R, Holl H, McMahon A, Larking A, Reid P (2014) Australian experiences in EGS permeability enhancement-A review of 3 case studies. Paper presented at 39th Workshop on Geothermal Reservoir Engineering, Stanford University, Stanford, CA, USA

Blanpied ML, Lockner DA, Byerlee JD (1995) Frictional slip of granite at hydrothermal conditions. J Geophys Res Solid Earth 100(B7):13045–13064. https://doi.org/10.1029/95JB00862

Bommer JJ, Oates S, Cepeda JM, Lindholm C, Bird J, Torres R et al (2006) Control of hazard due to seismicity induced by a hot fractured rock geothermal project. Eng Geol 83(4):287–306. https://doi.org/10.1016/j.enggeo.2005.11.002

Bommer JJ, Crowley H, Pinho R (2015) A risk-mitigation approach to the management of induced seismicity. J Seismol 19(2):623–646. https://doi.org/10.1007/s10950-015-9478-z

Boulton C, Carpenter BM, Toy V, Marone C (2012) Physical properties of surface outcrop cataclastic fault rocks, Alpine Fault, New Zealand. Geochem Geophys Geosyst 13(1):01018. https://doi.org/10.1029/2011GC003872

Bourdet D (2002) Well test analysis: the use of advanced interpretation models. Elsevier, Amsterdam

Bowker KA (2007) Barnett Shale gas production, Fort Worth Basin: issues and discussion. Am Assoc Pet Geol Bull 91(4):523–533. https://doi.org/10.1306/06190606018

Bradford J, McLennan J, Moore J, Podgorney R, Plummer M, Nash G (2017) Analysis of the thermal and hydraulic stimulation program at Raft River, Idaho. Rock Mech Rock Eng 50(5):1279–1287. https://doi.org/10.1007/s00603-016-1156-0

Breede K, Dzebisashvili K, Liu X, Falcone G (2013) A systematic review of enhanced (or engineered) geothermal systems: past, present and future. Geotherm Energy 1:4. https://doi.org/10.1186/2195-9706-1-4

Broccardo M, Mignan A, Grigoli F, Karvounis D, Rinaldi AP, Danciu L et al (2020) Induced seismicity risk analysis of the hydraulic stimulation of a geothermal well on Geldinganes, Iceland. Nat Hazards Earth Syst Sci 20(6):1573–1593. https://doi.org/10.5194/nhess-20-1573-2020

Bröker K, Ma X, Gholizadeh DN, Wenning Q et al (2022) Multistage hydraulic stimulation at the Bedretto Underground Laboratory, Switzerland: First results from a geomechanical perspective. In: 13th European Geothermal PhD Days (EGPD 2022). ETH Zurich, Institute of Geophysics

Brown DW (1989) The potential for large errors in the inferred minimum earth stress when using incomplete hydraulic fracturing results. Int J Rock Mech Min Sci Geomech Abstr 26(6):573–577. https://doi.org/10.1016/0148-9062(89)91437-X

Brown DW, Duchane DV (1999) Scientific progress on the Fenton Hill HDR project since 1983. Geothermics 28(4–5):591–601. https://doi.org/10.1016/S0375-6505(99)00030-9

Brown DW, Duchane DV, Heiken G, Hriscu VT (2012) Mining the Earth's heat: Hot Dry Rock geothermal energy. Springer, Berlin

Brown D (1997) Review of Fenton Hill HDR Test Results. No. LA-UR-97-434; CONF-970371-1. Los Alamos National Lab. NM (United States)

Brown DW (2009) Hot dry rock geothermal energy: important lessons from Fenton Hill. In: Proceedings of the 34th Workshop on Geothermal Reservoir Engineering. Stanford University, CA, USA

Bruel D (2007) Using the migration of the induced seismicity as a constraint for fractured Hot Dry Rock reservoir modelling. Int J Rock Mech Min Sci 44(8):1106–1117. https://doi.org/10.1016/j.ijrmms.2007.07.001

Bruhn D, Huenges E, Ágústsson K, Zang A, Kwiatek G, Rachez X et al (2011) Geothermal engineering integrating mitigation of induced seismicity in reservoirs-The European GEISER Project. Geotherm Res Council Trans 35:1623

Burns KL, Weber C, Perry J, Harrington HJ (2000) Status of the geothermal industry in Australia. World Geothermal Congress 2000, Japan

Byerlee JD, Brace WF (1968) Stick slip, stable sliding, and earthquakes-effect of rock type, pressure, strain rate, and

stiffness. J Geophys Res 73(18):6031–6037. https://doi.org/10.1029/JB073i018p06031
Carpenter BM, Marone C, Saffer DM (2009) Frictional behavior of materials in the 3D SAFOD volume. Geophys Res Lett 36(5):277–291. https://doi.org/10.1029/2008GL036660
Castilla R, Serbeto F, Christe F, Meier P et al (2022) Data Integration and Model Updating in a Multi-Stage Stimulation in the Bedretto Lab, Switzerland. In: 56th US Rock Mechanics/Geomechanics Symposium
Cerfontaine B, Collin F (2017) Cyclic and fatigue behaviour of rock materials: review, interpretation and research perspectives. Rock Mech Rock Eng 51(2):391–414. https://doi.org/10.1007/s00603-017-1337-5
Chabora E, Zemach E, Spielman P, Drakos P, Hickman S, Lutz S et al. (2012) Hydraulic stimulation of well 27-15, desert Peak geothermal field, Nevada, USA. In: Proceedings of thirty-seventh workshop on geothermal reservoir engineering, vol 30
Chancellor R (1977) Mesaverde Hydraulic Fracture Stimulation, Northern Picenace Basin-Progress Report
Charléty J, Cuenot N, Dorbath L, Dorbath C, Haessler H, Frogneux M (2007) Large earthquakes during hydraulic stimulations at the geothermal site of Soultz-sous-Forêts. Int J Rock Mech Min Sci 44(8):1091–1105. https://doi.org/10.1016/j.ijrmms.2007.06.003
Chen J, Jiang F (2015) Designing multi-well layout for enhanced geothermal system to better exploit hot dry rock geothermal energy. Renew Energy 74:37–48. https://doi.org/10.1016/j.renene.2014.07.056
Chen J, Jiang F (2016) A numerical study of EGS heat extraction process based on a thermal non-equilibrium model for heat transfer in subsurface porous heat reservoir. Int J Heat Mass Transf 52(2):255–267. https://doi.org/10.1007/s00231-015-1554-y
Cheng Y (2009) Boundary element analysis of the stress distribution around multiple fractures: implications for the spacing of perforation clusters of hydraulically fractured horizontal wells. In: SPE Eastern Regional Meeting, Charleston, West Virginia, USA
Cladouhos TT, Clyne M, Nichols M, Petty S, Osborn WL, Nofziger L (2011) Newberry Volcano EGS Demonstration stimulation modeling. GRC Trans 35:317–322
Cloetingh SAPL, Van Wees JD, Ziegler PA, Lenkey L, Beekman F, Tesauro M, Bonté D (2010) Lithosphere tectonics and thermo-mechanical properties: an integrated modelling approach for Enhanced Geothermal Systems exploration in Europe. Earth-Sci Rev 102(3–4):159–206. https://doi.org/10.1016/j.earscirev.2010.05.003
Cuenot N, Dorbath C, Dorbath L (2008) Analysis of the microseismicity induced by fluid injections at the EGS site of Soultz-sous-Forêts (Alsace, France): implications for the characterization of the geothermal reservoir properties. Pure Appl Geophys 165(5):797–828. https://doi.org/10.1007/s00024-008-0335-7
Cuenot N, Dorbath C, Frogneux M, Langet N (2010) Microseismic activity induced under circulation conditions at the EGS Project of Soultz-sous-Forêts (France). In: Proceedings world geothermal conference, Bali, Indonesia
Cuss RJ, Wiseall AC, Hennissen JAI, Waters CN, Kemp SJ, Ougier-Simonin A, Holyoake S, Haslam RB (2015) Hydraulic fracturing: a review of theory and field experience. British Geological Survey Open Report, OR/15/066
Dash ZV, Dreesen DS, Walter F, House L (1985) The massive hydraulic fracture of Fenton Hill HDR Well EE-3. In: International Symposium on Geothermal Energy, Geothermal Resources Council, Kailua-Kona, Hawaii, USA
Dash ZV, Aguilar RG, Dennis BR, Dreesen DS, Fehler MC, Hendron RH, House LS, Ito H, Kelkar SM, Malzahn MV (1989) ICFT: an initial closed-loop flow test of the Fenton Hill Phase II HDR reservoir (No. LA-11498-HDR). Los Alamos National Lab. NM (USA)
Davatzes N, Hickmann S, Zemach E, Spielman P, Robertson-Tait A, Drakos P, Lutz S, Rose P, Moore J, Majer E, KennedyM, Stacey R, Swyer M (2012) Structural and geomechanical constraints in designing an EGS: example at Desert Peak Geothermal Field, Nevada. Oral presentation presented at ICEGS 2012, Freiburg, 25 May 2012
Davies R, Foulger G, Bindley A, Styles P (2013) Induced seismicity and hydraulic fracturing for the recovery of hydrocarbons. Mar Pet Geol 45:171–185. https://doi.org/10.1016/j.marpetgeo.2013.03.016
De Barros L, Daniel G, Guglielmi Y, Rivet D, Caron H, Payre X, Gourlay M (2016) Fault structure, stress, or pressure control of the seismicity in shale? Insights from a controlled experiment of fluid-induced fault re-activation. J Geophys Res Solid Earth 121(6):4506–4522. https://doi.org/10.1002/2015JB012633
De Simone S, Carrera J, Vilarrasa V (2017) Superposition approach to understand triggering mechanisms of post-injection induced seismicity. Geothermics 70:85–97. https://doi.org/10.1016/j.geothermics.2017.05.011
Deichmann N, Giardini D (2009) Earthquakes induced by the stimulation of an enhanced geothermal system below Basel (Switzerland). Seismol Res Lett 80(5):784–798. https://doi.org/10.1785/gssrl.80.5.784
Deichmann N, Kraft T, Evans KF (2014) Identification of faults activated during the stimulation of the Basel geothermal project from cluster analysis and focal mechanisms of the larger magnitude events. Geothermics 52:84–97. https://doi.org/10.1016/j.geothermics.2014.04.001
Dempsey D, Kelkar S, Hickman S, Davatzes N, Moos D (2015) Modeling shear stimulation of the EGS well desert peak 27–15 Using a coupled thermal-hydrological-mechanical simulator. Int J Rock Mech Min Sci 78:190–206. https://doi.org/10.1016/j.ijrmms.2015.06.003
Den Hartog SAM, Niemeijer AR, Spiers CJ (2012a) New constraints on megathrust slip stability under subduction zone P-T conditions. Earth Planet Sci Lett 353–354:240–252. https://doi.org/10.1016/j.epsl.2012.08.022
Den Hartog SAM, Peach CJ, de Winter DAM, Spiers CJ, Shimamoto T (2012b) Frictional properties of megathrust fault gouges at low sliding velocities: new data on effects of normal stress and temperature. J Struct Geol 38:156–171. https://doi.org/10.1016/j.jsg.2011.12.001
Detournay E (2016) Mechanics of hydraulic fractures. Annu Rev Fluid Mech 48:311–339. https://doi.org/10.1146/annurev-fluid-010814-014736
Dezayes C, Genter A (2008) Large-scale fracture network based on Soultz borehole data. In: EHDRA Scientific Conference, Proceedings of the EHDRA scientific

conference 24–25 September 2008. Soultz-sous-Forêts, France

Dèzes P, Schmid SM, Ziegler PA (2004) Evolution of the European Cenozoic Rift System: interaction of the Alpine and Pyrenean orogens with their foreland lithosphere. Tectonophysics 389(1–2):1–33. https://doi.org/10.1016/j.tecto.2004.06.011

Di Y, Tang H (2018) Simulation of multistage hydraulic fracturing in unconventional reservoirs using displacement discontinuity method (DDM). In: Wu YS (ed) Hydraulic Fracture Modeling. Gulf Professional Publishing, Houston, pp 41–74. https://doi.org/10.1016/B978-0-12-812998-2.00003-5

Dieterich JH (1978) Time-dependent friction and the mechanics of stick-slip. Pure Appl Geophys 116:790–806. https://doi.org/10.1007/978-3-0348-7182-2_15

Dinske C, Shapiro SA (2013) Seismotectonic state of reservoirs inferred from magnitude distributions of fluid-induced seismicity. J Seismol 17(1):13–25. https://doi.org/10.1007/s10950-012-9292-9

Dorbath L, Cuenot N, Genter A, Frogneux M (2009) Seismic response of the fractured and faulted granite of Soultz-sous-Forêts (France) to 5 km deep massive water injections. Geophys J Int 177(2):653–675. https://doi.org/10.1111/j.1365-246X.2009.04030.x

Duchane D, Brown D (2002) Hot dry rock (HDR) geothermal energy research and development at Fenton Hill, New Mexico. Geo-Heat Centre Q Bull 13–19

Dyer BC, Schanz U, Ladner F, Häring MO, Spillman T (2008) Microseismic imaging of a geothermal reservoir stimulation. Lead Edge 27(7):856–869. https://doi.org/10.1190/1.2954024

Economides MJ, Nolte KG (1989) Reservoir stimulation, vol 2. Wiley, Englewood Cliffs, NJ

Ellsworth WL (2013) Injection-induced earthquakes. Science 341(6142):1225942. https://doi.org/10.1126/science.1225942

Ellsworth WL, Giardini D, Townend J, Ge S, Shimamoto T (2019) Triggering of the Pohang, Korea, earthquake (M_w 5.5) by enhanced geothermal system stimulation. Seismol Res Lett 90(5):1844–1858. https://doi.org/10.1785/0220190102

Elsworth D, Spiers CJ, Niemeijer AR (2016) Understanding induced seismicity. Science 354(6318):1380–1381. https://doi.org/10.1126/science.aal2584

Erarslan N, Williams DJ (2012) Mechanism of rock fatigue damage in terms of fracturing rocks. Int J Fatigue 43:76–89. https://doi.org/10.1016/j.ijfatigue.2012.02.008

Evans KF, Moriya H, Niitsuma H, Jones RH, Phillips WS, Genter A et al (2005) Microseismicity and permeability enhancement of hydrogeologic structures during massive fluid injections into granite at 3 km depth at the Soultz HDR site. Geophys J Int 160(1):388–412. https://doi.org/10.1111/j.1365-246X.2004.02474.x

Evans KF, Zappone A, Kraft T, Deichmann N, Moia F (2012) A survey of the induced seismic responses to fluid injection in geothermal and CO_2 reservoirs in Europe. Geothermics 41:30–54. https://doi.org/10.1016/j.geothermics.2011.08.002

Eyre TS, Eaton DW, Garagash DI, Zecevic M, Venieri M, Weir R, Lawton DC (2019) The role of aseismic slip in hydraulic fracturing–induced seismicity. Sci Adv 5(8):eaav7172. https://doi.org/10.1126/sciadv.aav7172

Fang Y, Elsworth D, Wang C, Ishibashi T, Fitts JP (2017) Frictional stability-permeability relationships for fractures in shales. J Geophys Res Solid Earth 122(3):1760–1776. https://doi.org/10.1002/2016JB013435

Farkas MP, Hofmann H, Zimmermann G, Zang A, Bethmann F, Meier P, Cottrell M, Josephson N (2021) Hydromechanical analysis of the second hydraulic stimulation in well PX-1 at the Pohang fractured geothermal reservoir, South Korea. Geothermics 89:101990. https://doi.org/10.1016/j.geothermics.2020.101990

Fast C, Holman GB, Covlin RJ (1977) The application of massive hydraulic fracturing to the tight muddy "J'' formation, Wattenberg Field, Colorado. J Pet Technol 29(01):10–11. https://doi.org/10.2118/5624-PA

Fehler MC (1989) Stress control of seismicity patterns observed during hydraulic fracturing experiments at the Fenton Hill hot dry rock geothermal energy site, New Mexico. Int J Rock Mech Min Sci Geomech Abstr 26(3–4):211–219. https://doi.org/10.1016/0148-9062(89)91971-2

Fink J, Heim E, Klitzsch N (2022) State of the art in deep geothermal energy in Europe: with focus on direct heating. Springer International Publishing, Cham

Fisher MK, Heinze JR, Harris CD, Davidson BM, Wright CA, Dunn KP (2004) Optimizing horizontal completion techniques in the Barnett shale using microseismic fracture mapping. In: SPE Annual technical conference and exhibition, Houston, Texas, USA

Foulger GR, Wilson MP, Gluyas JG, Julian BR, Davies RJ (2018) Global review of human-induced earthquakes. Earth-Sci Rev 178:438–514. https://doi.org/10.1016/j.earscirev.2017.07.008

Gai S, Nie Z, Yi X, Zou Y, Zhang Z (2020) Study on the interference law of staged fracturing crack propagation in horizontal wells of tight reservoirs. ACS Omega 5(18):10327–10338. https://doi.org/10.1021/acsomega.9b04423

Gale JF, Reed RM, Holder J (2007) Natural fractures in the Barnett Shale and their importance for hydraulic fracture treatments. Am Assoc Pet Geol Bull 91(4):603–622. https://doi.org/10.1306/11010606061

Galis M, Ampuero JP, Mai PM, Cappa F (2017) Induced seismicity provides insight into why earthquake ruptures stop. Sci Adv 3(12):eaap7528. https://doi.org/10.1126/sciadv.aap7528

Gan Q, Lei Q (2020) Induced fault reactivation by thermal perturbation in enhanced geothermal systems. Geothermics 86:101814. https://doi.org/10.1016/j.geothermics.2020.101814

Garcia-Aristizabal A (2018) Modelling fluid-induced seismicity rates associated with fluid injections: examples related to fracture stimulations in geothermal areas. Geophys J Int 215(1):471–493. https://doi.org/10.1093/gji/ggy284

Gaucher E, Schoenball M, Heidbach O, Zang A, Fokker PA, van Wees JD, Kohl T (2015) Induced seismicity in geothermal reservoirs: a review of forecasting approaches. Renew Sust Energy Rev 52:1473–1490. https://doi.org/10.1016/j.rser.2015.08.026

Geertsma J, De Klerk F (1969) A rapid method of predicting width and extent of hydraulically induced fractures. J Pet Technol 21(12):1571–1581. https://doi.org/10.2118/2458-PA

Genter A, Cuenot N, Goerke X, Bernd M, Sanjuan B, Scheiber J (2012) Status of the Soultz geothermal project during exploitation between 2010 and 2012. In: Proceedings of the 37th Workshop on Geothermal Reservoir engineering. Stanford University, CA

Genter A, Traineau H (1996) Analysis of macroscopic fractures in granite in the HDR geothermal well EPS-1, Soultz-sous-Forêts, France. J Volcanol Geotherm Res 72(1–2):121–141. https://doi.org/10.1016/0377-0273(95)00070-4

Gérard A, Baumgärtner J, Baria R (1997) An attempt towards a conceptual model derived from 1993-1996 hydraulic operations at Soultz. In: Proceedings of NEDO international geothermal synposium, Sendai, 2, pp 329–341

Geyer JF, Nemat-Nasser S (1982) Experimental investigation of thermally induced interacting cracks in brittle solids. Int J Solids Struct 18(4):349–356. https://doi.org/10.1016/0020-7683(82)90059-2

Ghamgosar M, Erarslan N (2016) Experimental and numerical studies on development of fracture process zone (FPZ) in rocks under cyclic and static loading. Rock Mech Rock Eng 49(3):893–908. https://doi.org/10.1007/s00603-015-0793-z

Ghassemi A (2012) A review of some rock mechanics issues in geothermal reservoir development. Geotech Geol Eng 30(3):647–664. https://doi.org/10.1007/s10706-012-9508-3

Giardini D (2009) Geothermal quake risks must be faced. Nature 462:848–849. https://doi.org/10.1038/462848a

Gong F, Guo T, Sun W, Li Z, Yang B, Chen Y, Qu Z (2020) Evaluation of geothermal energy extraction in Enhanced Geothermal System (EGS) with multiple fracturing horizontal wells (MFHW). Renew Energy 151:1339–1351. https://doi.org/10.1016/j.renene.2019.11.134

Grecksch G, Jung R, Tischner T, Weidler R (2003) Hydraulic fracturing at the European HDR/HFR test site Soultz-sous-Forêts (France)-a conceptual model. In: Proceedings of the European geothermal conference. Leibniz Institute for Applied Geosciences GGA, Germany

Grigoli F, Cesca S, Rinaldi AP, Manconi A, Lopez-Comino JA, Clinton JF et al (2018) The November 2017 M_w 5.5 Pohang earthquake: A possible case of induced seismicity in South Korea. Science 360(6392):1003–1006. https://doi.org/10.1126/science.aat2010

Guglielmi Y, Cappa F, Avouac JP, Henry P, Elsworth D (2015) Seismicity triggered by fluid injection-induced aseismic slip. Science 348(6240):1224–1226. https://doi.org/10.1126/science.aab0476

Guo B, Fu P, Hao Y, Peters CA, Carrigan CR (2016) Thermal drawdown-induced flow channeling in a single fracture in EGS. Geothermics 61:46–62. https://doi.org/10.1016/j.geothermics.2016.01.004

Haimson BC, Kim CM (1991) Mechanical behaviour of rock under cyclic fatigue. Rock Mech Rock Eng 3:845–863

Häring MO, Schanz U, Ladner F, Dyer BC (2008) Characterisation of the Basel 1 enhanced geothermal system. Geothermics 37(5):469–495. https://doi.org/10.1016/j.geothermics.2008.06.002

He C, Yao W, Wang Z, Zhou Y (2006) Strength and stability of frictional sliding of gabbro gouge at elevated temperatures. Tectonophysics 427(1–4):217–229. https://doi.org/10.1016/j.tecto.2006.05.023

Hébert R, Ledésert B, Genter A, Bartier D, Dezayes C (2011) Mineralprecipitation in geothermal reservoir: the study case of calcite in theSoultz-sous-Forêts enhanced geothermal system. In: 36rd workshop ongeothermal reservoir engineering, SGP-TR-191

Henninges J, Brandt W, Erbas K, Moeck I, Saadat A, Reinsch T, Zimmermann G (2012) Downhole monitoring during hydraulic experiments at the in-situ geothermal lab Groß Schönebeck. In: Proceedings of the thirty-seventh workshop on geothermal reservoir engineering. Stanford University, Stanford, 30 Jan 1-Feb 2012

Hillers GT, Vuorinen TA, Uski MR, Kortström JT, Mäntyniemi PB, Tiira T, Malin PE, Saarno T (2020) The 2018 geothermal reservoir stimulation in Espoo/Helsinki, Southern Finland: Seismic network anatomy and data features. Seismol Res Lett 91(2A):770–786. https://doi.org/10.1785/0220190253

Hofmann H, Zimmermann G, Zang A, Min KB (2018) Cyclic soft stimulation (CSS): a new fluid injection protocol and traffic light system to mitigate seismic risks of hydraulic stimulation treatments. Geotherm Energy 6:27. https://doi.org/10.1186/s40517-018-0114-3

Hofmann H, Zimmermann G, Farkas M, Huenges E, Zang A, Leonhardt M, Kwiatek G, Martinez-Garzon P, Bohnhoff M, Min KB, Fokker P (2019) First field application of cyclic soft stimulation at the Pohang Enhanced Geothermal System site in Korea. Geophys J Int 217(2):926–949. https://doi.org/10.1093/gji/ggz058

Hogarth RA, Bour D (2015) Flow performance of the Habanero EGS closed loop. In: Proceedings of world geothermal congress, Melbourne, Australia

Hogarth RA, Holl HG, McMahon A (2013a) Production, injection and closed-loop testing at Habanero EGS project. In: Proceedings, 35th New Zealand Geothermal Workshop, Rotorua, New Zealand

Hogarth RA, Holl HG, McMahon A (2013b) Flow testing results from Habanero EGS Project. In: Proceedings 6th Australian geothermal energy conference, Brisbane, pp 21–28

Hogarth R, Holl HG (2017) Lessons learned from the Habanero EGS Project. Geotherm Resour Counc Trans 41:13

Hölker A, Graf R (2005) Modelling the seismograms of microseismic events at potential observation stations for the evaluation of alternative observation network configurations. Report prepared for the Deep Heat Mining (DHM) Project Basel on behalf of Geothermal Explorers Ltd. Pratteln, Switzerland, p 32

Holl H, Barton C (2015) Habanero field-structure and state of stress. In: Proceedings the world geothermal congress, 19–25 April, Melbourne, Australia

Hong TK, Lee J, Park S, Kim W (2022) Major influencing factors for the nucleation of the 15 November 2017 M_w 5.5 Pohang earthquake. Phys Earth Planet Inter 323:106833. https://doi.org/10.1016/j.pepi.2021.106833

Horváth F, Musitz B, Balázs A, Végh A, Uhrin A, Nádor A, Koroknai B, Pap N, Tóth T, Wórum G (2015) Evolution of the Pannonian basin and its geothermal resources. Geothermics 53:328–352. https://doi.org/10.1016/j.geothermics.2014.07.009

Huenges E, Hurter S, Saadat A, Köhler S, Trautwein U (2002) The in-situ geothermal laboratory Groß Schönebeck: learning to use low permeability aquifers for geothermal power. In: Proceedings 27th stanford geothermal workshop, pp 78–81

Humphreys B, Hodson-Clarke A, Hogarth R (2014) Habanero Geothermal Project Field Development Plan. COM-FN-OT-PLN-01166

Ikari MJ, Saffer DM, Marone C (2007) Effect of hydration state on the frictional properties of montmorillonite-based fault gouge. J Geophys Res Solid Earth 112:B06423. https://doi.org/10.1029/2006JB004748

Ikari MJ, Marone C, Saffer DM (2011) On the relation between fault strength and frictional stability. Geology 39(1):83–86. https://doi.org/10.1130/G31416.1

Ito H (2003) Inferred role of natural fractures, veins, and breccias in development of the artificial geothermal reservoir at the Ogachi Hot Dry Rock site, Japan. J Geophys Res 108:B92426. https://doi.org/10.1029/2001JB001671

Ito T, Hayashi K (2003) Role of stress-controlled flow pathways in HDR geothermal reservoirs. Pure Appl Geophys 160(5):1103–1124. https://doi.org/10.1007/PL00012563

Izadi G, Gaither M, Cruz L, Baba C, Moos D, Fu P (2015) Fully 3D hydraulic fracturing model: optimizing sequence fracture stimulation in horizontal wells. In: 49th US Rock mechanics/geomechanics symposium, San Francisco, California, USA, ARMA-2015–119

Jia Y, Fang Y, Elsworth D, Wu W (2020) Slip velocity dependence of friction-permeability response of shale fractures. Rock Mech Rock Eng 53:2109–2121. https://doi.org/10.1007/s00603-019-02036-8

Jiang F, Chen J, Huang W, Luo L (2014) A three-dimensional transient model for EGS subsurface thermo-hydraulic process. Energy 72:300–310. https://doi.org/10.1016/j.energy.2014.05.038

Jung R, Ortiz A (2007) Analyse eines hydraulischen Injektionstests und eines massiven Wasserfrac-Tests in der Geothermiebohrung Basel-1. Institut für Geowissenschaftliche Gemeinschaftsaufgaben Hannover (Germany) report to Geopower Basel AG for the Swiss Deep Heat Mining Project Basel, pp 20

Jung R, Rummel F, Jupe A, Bertozzi A, Heinemann B, Wallroth T (1996) Large scale hydraulic injections in the granitic basement in the European HDR programme at Soultz, France. In Proceedings of the 3rd international HDR forum, Santa Fe, pp 75–76

Jung R, Weidler R (2000) A conceptual model for the stimulation process of the HDR- system at Soultz. Geotherm Resour Counc Trans 24:143–147

Jupe AJ, Green ASP, Wallroth T (1992) Induced microseismicity and reservoir growth at the Fjällbacka hot dry rocks project, Sweden. Int J Rock Mech Min Sci Geomech Abstr 29(4):343–354. https://doi.org/10.1016/0148-9062(92)90511-W

Kaieda H, Ito H, Kiho K, Suzuki K, Suenaga H, Shin K (2005) Review of the Ogachi HDR project in Japan. In: Proceedings of the world geothermal congress 2005, Antalya

Kaieda H, Sasaki S, Wyborn D (2010) Comparison of characteristics of micro-earthquakes observed during hydraulic stimulation operations in Ogachi, Hijiori and Cooper Basin HDR projects. In: Proceedings of the world geothermal congress 2010, Bali

Kang JQ, Zhu JB, Zhao J (2019) A review of mechanisms of induced earthquakes: from a view of rock mechanics. Geomech Geophys Geo-Energy Geo-Resour 5:171–196. https://doi.org/10.1007/s40948-018-00102-z

Kennedy BM, Pruess K, Lippmann MJ, Majer EL, Rose PE, Adams M, Roberston-Tait A, Moller N, Weare J, Clutter T, Brown DW (2010) A History of Geothermal Energy Research and Development in the United States. Reservoir Engineering 1976–2006. Office of Energy Efficiency and Renewable Energy (EERE), Washington, DC (United States). https://doi.org/10.2172/1218859

Kiel OM (1977) The Kiel process reservoir stimulation by dendritic fracturing. Soc. Pet. Eng. SPE 6984

Kim H, Xie L, Min KB, Bae S, Stephansson O (2017) Integrated in situ stress estimation by hydraulic fracturing, borehole observations and numerical analysis at the EXP-1 borehole in Pohang, Korea. Rock Mech Rock Eng 50(12):3141–3155. https://doi.org/10.1007/s00603-017-1284-1

Kim KH, Ree JH, Kim Y, Kim S, Kang SY, Seo W (2018a) Assessing whether the 2017 M_w 5.4 Pohang earthquake in South Korea was an induced event. Science 360(6392):1007–1009. https://doi.org/10.1126/science.aat6081

Kim KI, Min KB, Kim KY, Choi JW, Yoon KS, Yoon WS et al (2018b) Protocol for induced microseismicity in the first enhanced geothermal systems project in Pohang, Korea. Renew Sust Energy Rev 91:1182–1191. https://doi.org/10.1016/j.rser.2018.04.062

Kim KI, Yoo H, Park S, Yim J et al (2022) Induced and triggered seismicity by immediate stress transfer and delayed fluid migration in a fractured geothermal reservoir at Pohang, South Korea. Int J Rock Mech Min Sci 153:105098. https://doi.org/10.1016/j.ijrmms.2022.105098

King G (2010) Thirty years of gas shale fracturing: what have we learned? SPE 133456, paper presented at the SPE Annual Technical Conference and Exhibition, Florence, Italy

Knoblauch TA, Trutnevyte E (2018) Siting enhanced geothermal systems (EGS): Heat benefits versus induced seismicity risks from an investor and societal perspective. Energy 164:1311–1325. https://doi.org/10.1016/j.energy.2018.04.129

Koh J, Roshan H, Rahman SS (2011) A numerical study on the long term thermo-poroelastic effects of cold water injection into naturally fractured geothermal reservoirs. Comput Geotech 38(5):669–682. https://doi.org/10.1016/j.compgeo.2011.03.007

Kohl T, Mégel T (2007) Predictive modeling of reservoir response to hydraulic stimulations at the European EGS site Soultz-sous-Forêts. Int J Rock Mech Min Sci 44(8):1118–1131. https://doi.org/10.1016/j.ijrmms.2007.07.022

Korean Government Commission (2019) Summary report of the Korean Government Commission on relations between the 2017 Pohang Earthquake and EGS Project. Geological Society of Korea, Seoul, South Korea

Kosakowski G, Berkowitz B, Scher H (2001) Analysis of field observations of tracer transport in a fractured till. J Contam Hydrol 47(1):29–51. https://doi.org/10.1016/S0169-7722(00)00140-6

Kraft T, Deichmann N (2014) High-precision relocation and focal mechanism of the injection-induced seismicity at the Basel EGS. Geothermics 52:59–73. https://doi.org/10.1016/j.geothermics.2014.05.014

Krietsch H, Gischig VS, Doetsch J, Evans KF, Villiger L, Jalali M et al (2020) Hydro-mechanical processes and their influence on the stimulation effected volume: Observations from a decameter-scale hydraulic stimulation project. Solid Earth Discuss 11(5):1699–1729. https://doi.org/10.5194/se-11-1699-2020

Kukkonen IT, PenttiM (2021) St1 Deep Heat Project: Geothermal energy to the district heating network in Espoo. In: IOP conference series: earth and environmental science, vol 703(1), IOP Publishing, p 012035

Kumano Y, Moriya H, Asanuma H, Soma N, Kaieda H, Tazuka K et al (2005) Interpretation of reservoir creation process at Cooper Basin, Australia by acoustic emission. J Acoust Emiss 23:129–135

Kumar D, Ghassemi A (2016) Hydraulic stimulation of multiple horizontal wells for EGS reservoir creation. In: GRC proceedings, Sacramento, CA, pp 373–381

Kumar D, Ghassemi A (2019) Multistage hydraulic fracturing of EGS wells with application to FORGE. In: Proceedings, 44th workshop on geothermal reservoir engineering, Stanford University, Stanford, California, SGP-TR-214

Kwiatek G, Bohnhoff M, Dresen G, Schulze A, Schulte T, Zimmermann G, Huenges E (2010) Microseismicity induced during fluid-injection: a case study from the geothermal site at Groß Schönebeck, North German Basin. Acta Geophys 58(6):995–1020. https://doi.org/10.2478/s11600-010-0032-7

Kwiatek G, Saarno T, Ader T, Bluemle F, Bohnhoff M, Chendorain M et al (2019) Controlling fluid-induced seismicity during a 6.1-km-deep geothermal stimulation in Finland. Sci Adv 5(5):eaav7224. https://doi.org/10.1126/sciadv.aav7224

Ladner F, Häring MO (2009) Hydraulic characteristics of the basel 1 enhanced geothermal system. Geotherm Resour Counc Trans 33:199–204

Laubscher H (2001) Plate interactions at the southern end of the Rhine graben. Tectonophysics 343(1–2):1–19. https://doi.org/10.1016/S0040-1951(01)00193-7

Ledésert B, Hebert R, Genter A, Bartier D, Clauer N, Grall C (2010) Fractures, hydrothermal alterations and permeability in the Soultz Enhanced Geothermal System. CR Geosci 342(7–8):607–615. https://doi.org/10.1016/j.crte.2009.09.011

Ledésert BA, Hébert RL (2012) The Soultz-sous-Forêts enhanced geothermal system: a granitic basement used as a heat exchanger to produce electricity. Heat Exchanges-Basic Design Appl 477–504

Ledingham P, Cotton L, Law R (2019) The united downs deep geothermal power project. In: Proceedings of the 44th workshop on geothermal reservoir engineering, Stanford University, Stanford, CA, USA, pp 11–13

Lei Q, Tsang CF (2022) Numerical study of fluid injection-induced deformation and seismicity in a mature fault zone with a low-permeability fault core bounded by a densely fractured damage zone. Geomech Energy Environ. 31:100277. https://doi.org/10.1016/j.gete.2021.100277

Lee Y, Park S, Kim J, Kim HC, Koo MH (2010) Geothermal resource assessment in Korea. Renew Sustain Energy Rev 14(8):2392–2400. https://doi.org/10.1016/j.rser.2010.05.003

Lee KK, Ellsworth WL, Giardini D, Townend J, Ge S, Shimamoto T et al (2019) Managing injection-induced seismic risks. Science 364(6442):730–732. https://doi.org/10.1126/science.aax1878

Lee TJ, Song Y (2008) Lesson learned from low-temperature geothermal development in Pohang, Korea. In: Proceedings of the 8th Asian geothermal symposium, pp 101–106

Lei Q, Doonechaly NG, Tsang CF (2021) Modelling fluid injection-induced fracture activation, damage growth, seismicity occurrence and connectivity change in naturally fractured rocks. Int J Rock Mech Min Sci 138:104598. https://doi.org/10.1016/j.ijrmms.2020.104598

Lei Q, Tsang CF (2022) Numerical study of fluid injection-induced deformation and seismicity in a mature fault zonewith a low-permeability fault core bounded by a densely fractured damage zone. Geomech Energy Environ31:100277. https://doi.org/10.1016/j.gete.2021.100277

Leonhardt M, Kwiatek G, Martínez-Garzón P, Bohnhoff M, Saarno T, Heikkinen P, Dresen G (2021) Seismicity during and after stimulation of a 6.1 km deep enhanced geothermal system in Helsinki, Finland. Solid Earth 12(3):581–594. https://doi.org/10.5194/se-12-581-2021

Li N, Xie H, Hu J et al (2022) A critical review of the experimental and theoretical research on cyclic hydraulic fracturing for geothermal reservoir stimulation. Geomech Geophys Geo-Energ Geo-Resour 8:7. https://doi.org/10.1007/s40948-021-00309-7

Lim H, Deng K, Kim YH, Ree JH, Son TR, Kim KH (2020) The 2017 M_w 5.5 Pohang earthquake, South Korea, and poroelastic stress changes associated with fluid injection. J Geophys Res Solid Earth 125(6):e2019JB019134. https://doi.org/10.1029/2019JB019134

Liu J, Wang Z, Shi W, Tan X (2020) Experiments on the thermally enhanced permeability of tight rocks: a potential thermal stimulation method for Enhanced Geothermal Systems. Energy Sources Recovery Util Environ Eff 2020:1–14. https://doi.org/10.1080/15567036.2020.1745332

Lopez-Comino JA, Cesca S, Heimann S, Grigoli F, Milkereit C, Dahm T, Zang A (2017) Characterization of hydraulic fractures growth during the Äspö Hard Rock Laboratory experiment (Sweden). Rock Mech Rock Eng 50(11):2985–3001. https://doi.org/10.1007/s00603-017-1285-0

Lu SM (2018) A global review of enhanced geothermal system (EGS). Renew Sustain Energy Rev 81:2902–2921. https://doi.org/10.1016/j.rser.2017.06.097

Luginbuhl M, Rundle JB, Turcotte DL (2019) Statistical physics models for aftershocks and induced seismicity. Philos Trans Royal Soc a 377(2136):20170397. https://doi.org/10.1098/rsta.2017.0397

Lutz SJ, Zutshi A, Robertson-Tait A, Drakos P, Zemach E (2011) Lithologies, hydrothermal alteration, and rock mechanical properties in wells 15–12 and BCH-3, Bradys hot springs geothermal field, Nevada. Geotherm Resour Counc Trans 35:469–476

Majer EL, Baria R, Stark M, Oates S, Bommer J, Smith B, Asanuma H (2007) Induced seismicity associated with enhanced geothermal systems. Geothermics 36(3):185–222. https://doi.org/10.1016/j.geothermics.2007.03.003

Marone C, Raleigh CB, Scholz CH (1990) Frictional behavior and constitutive modeling of simulated fault gouge. J Geophys Res Solid Earth 95(B5):7007–7025. https://doi.org/10.1029/JB095iB05p07007

McClure MW (2015) Generation of large post injection-induced seismic events by backflow from dead-end faults and fractures. Geophys Res Lett 42(16):6647–6654. https://doi.org/10.1002/2015GL065028

McClure MW, Horne RN (2011) Investigation of injection-induced seismicity using a coupled fluid flow and rate/state friction model. Geophysics 76(6):WC181–WC198. https://doi.org/10.1190/geo2011-0064.1

McClure MW, Horne RN (2013a) Discrete fracture network modeling of hydraulic stimulation: coupling flow and geomechanics. Springer Science & Business Media, Berlin

McClure MW, Horne RN (2014a) An investigation of stimulation mechanisms in Enhanced Geothermal Systems. Int J Rock Mech Min Sci 72:242–260. https://doi.org/10.1016/j.ijrmms.2014.07.011

McClure MW, Horne RN (2014b) Correlations between formation properties and induced seismicity during high pressure injection into granitic rock. Eng Geol 175:74–80. https://doi.org/10.1016/j.enggeo.2014.03.015

McClure MW, Horne RN (2013b) Conditions required for shear stimulation in EGS. In: Proceedings of the 2013b European geothermal congress, Pisa, Italy

McClure MW, Horne RN (2013c) Is pure shear stimulation always the mechanism of stimulation in EGS? In: Proceedings, thirty-eight workshop on geothermal reservoir engineering, Stanford University, Stanford, CA, SGP-TR-198

McClure MW (2012) Modeling and characterization of hydraulic stimulation and induced seismicity in geothermal and shale gas reservoirs. Doctoral dissertation, Stanford University

McGarr A (2014) Maximum magnitude earthquakes induced by fluid injection. J Geophys Res Solid Earth 119(2):1008–1019. https://doi.org/10.1002/2013JB010597

McGarr A, Bekins B, Burkardt N, Dewey J, Earle P, Ellsworth W et al (2015) Coping with earthquakes induced by fluid injection. Science 347(6224):830–831. https://doi.org/10.1126/science.aaa0494

McGarr A, Barbour AJ, Majer E L (2018) Reasons to doubt the 15 November 2017 Pohang, South Korea, earthquakes were induced. In: AGU Fall Meeting Abstracts, vol 2018, pp S23B-0515

A McGarr EL Majer R Skoumal (2019) Why the M5.5 Pohang, South Korea, main shock was likely not caused by a nearby Enhanced Geothermal System (EGS) project. In: AGU Fall meeting abstracts, vol 2019. pp S14C–08

Méheust Y, Schmittbuhl J (2000) Flow enhancement of a rough fracture. Geophys Res Lett 27(18):2989–2992. https://doi.org/10.1029/1999GL008464

Meixner TJ, Gunn PJ, Boucher RK, Yeates TN, Richardson LM, Frears RA (2000) The nature of the basement to the Cooper Basin region, South Australia. Explor Geophys 31(2):24–32. https://doi.org/10.1071/EG00024

Meyer BR, Bazan LW (2011) A discrete fracture network model for hydraulically induced fractures-theory, parametric and case studies. In: Proceedings SPE hydraulic fracturing technology conference and exhibition, The Woodlands, Texas, USA, SPE 140514

Mills T, Humphreys B (2013) Habanero pilot project-Australia's first EGS power plant. In: Proceedings, 35th New Zealand geothermal workshop, Rotorua, New Zealand

Moore PW, Pearson RA (1989) Production logging results. Hot Dry Rock Geothermal Energy: Phase 2B Final Report of the Camborne School of Mines Project, edited by RH Parker, Pergamon Press, Oxford

Moore J, McLennan J, Allis R, Pankow K, Simmons S et al (2018) The Utah frontier observatory for geothermal research (FORGE): results of recent drilling and geoscientific surveys. In: Geothermal Resources Council 42nd Annual Meeting-Geothermal Energy, GRC

Moore J, McLennan J, Allis R, Pankow K, Simmons S et al (2019) The utah frontier observatory for research in geothermal energy (FORGE): an international laboratory for enhanced geothermal system technology development

Moore DE, Lockner DA (2004) Crystallographic controls on the frictional behavior of dry and water-saturated sheet structure minerals. J Geophys Res Solid Earth 109(B3):B03401. https://doi.org/10.1029/2003JB002582

Moreno L, Tsang CF (1994) Flow channeling in strongly heterogeneous porous media: a numerical study. Water Resour Res 30(5):1421–1430. https://doi.org/10.1029/93WR02978

Moriya H, Niitsuma H, Baria R (2003) Estimation of fine scale structures in Soultz HDR reservoir by using microseismic multiplets. In: Proceedings of the 28th workshop on geothermal reservoir engineering, Stanford University, CA

Morrill J, Miskimins JL (2012) Optimization of hydraulic fracture spacing in unconventional shales. In: SPE hydraulic fracturing technology conference, The Woodlands, Texas, USA, SPE-152595-MS. https://doi.org/10.2118/152595-MS

Morrow CA, Moore DE, Lockner DA (2000) The effect of mineral bond strength and adsorbed water on fault gouge frictional strength. Geophys Res Lett 27(6):815–818. https://doi.org/10.1029/1999GL008401

Mukuhira Y, Asanuma H, Niitsuma H, Häring MO (2013) Characteristics of large-magnitude microseismic events recorded during and after stimulation of a geothermal

reservoir at Basel, Switzerland. Geothermics 45:1–17. https://doi.org/10.1016/j.geothermics.2012.07.005

Mukuhira Y, Dinske C, Asanuma H, Ito T, Häring MO (2017) Pore pressure behavior at the shut-in phase and causality of large induced seismicity at Basel, Switzerland. J Geophys Res Solid Earth 122(1):411–435. https://doi.org/10.1002/2016JB013338

Murphy HD, Fehler MC (1986) Hydraulic fracturing of jointed formations (No. LA-UR-85-3701; CONF-860325-1). Los Alamos National Lab. NM (USA)

Nagel NB, Sanchez-Nagel M (2011) Stress shadowing and microseismic events: A numerical evaluation. In SPE annual technical conference and exhibition, Denver, Colorado, USA, SPE-147363-MS. https://doi.org/10.2118/147363-MS

Nagel NB, Gil I, Sanchez-Nagel M, Damjanac B (2011) Simulating hydraulic fracturing in real fractured rocks -Overcoming the limits of pseudo3D models. In: SPE hydraulic fracturing technology conference, The Woodlands, Texas, USA, SPE-140480-MS. https://doi.org/10.2118/140480-MS

Nagel N, Zhang F, Sanchez-Nagel M, Lee B (2013) Quantitative evaluation of completion techniques on influencing shale fracture 'complexity'. In: ISRM international conference for effective and sustainable hydraulic fracturing, ISRM-ICHF-2013-036

Neretnieks I (1987) Channeling effects in flow and transport in fractured rocks-Some recent observations and models. In: Proceedings of GEOVAL-87, Stockholm, Sweden

Niemeijer AR, Collettini C (2013) Frictional properties of a low-angle normal fault under in situ conditions: thermally-activated velocity weakening. Pure Appl Geophys 171(10):2641–2664. https://doi.org/10.1007/s00024-013-0759-6

Norbeck JH, McClure MW, Horne RN (2018) Field observations at the Fenton Hill enhanced geothermal system test site support mixed-mechanism stimulation. Geothermics 74:135–149. https://doi.org/10.1016/j.geothermics.2018.03.003

Nordgren RP (1972) Propagation of a vertical hydraulic fracture. Soc Pet Eng J 12(4):306–314. https://doi.org/10.2118/3009-PA

Olasolo P, Juárez MC, Morales MP, Liarte IA (2016) Enhanced geothermal systems (EGS): a review. Renew Sustain Energy Rev 56:133–144. https://doi.org/10.1016/j.rser.2015.11.031

Olson JE (2008) Multi-fracture propagation modeling: Applications to hydraulic fracturing in shales and tight gas sands. In: 42nd U.S. rock mechanics symposium (USRMS), San Francisco, California, ARMA-08-327

Palmer ID, Moschovidis ZA, Cameron JR (2007) Modeling shear failure and stimulation of the Barnett Shale after hydraulic fracturing. In: SPE hydraulic fracturing technology conference, College Station, Texas, USA, SPE-106113-MS. https://doi.org/10.2118/106113-MS

Pan SY, Gao M, Shah KJ, Zheng J, Pei SL, Chiang PC (2019) Establishment of enhanced geothermal energy utilization plans: barriers and strategies. Renew Energy 132:19–32. https://doi.org/10.1016/j.renene.2018.07.126

Pandey SN, Vishal V, Chaudhuri A (2018) Geothermal reservoir modeling in a coupled thermo-hydro-mechanical-chemical approach: a review. Earth-Sci Rev 185:1157–1169. https://doi.org/10.1016/j.earscirev.2018.09.004

Park S, Kim KI, Xie L, Yoo H, Min KB, Kim M et al (2020) Observations and analyses of the first two hydraulic stimulations in the Pohang geothermal development site, South Korea. Geothermics 88:101905. https://doi.org/10.1016/j.geothermics.2020.101905

Parker R (1999) The rosemanowes HDR project 1983–1991. Geothermics 28(4–5):603–615. https://doi.org/10.1016/S0375-6505(99)00031-0

Parotidis M, Shapiro SA, Rothert E (2004) Back front of seismicity induced after termination of borehole fluid injection. Geophys Res Lett 31(2):L02612. https://doi.org/10.1029/2003GL018987

Patel SM, Sondergeld CH, Rai CS (2017) Laboratory studies of hydraulic fracturing by cyclic injection. Int J Rock Mech Min Sci 95:8–15. https://doi.org/10.1016/j.ijrmms.2017.03.008

Pearson C (1981) The relationship between micro seismicity and high pore pressures during hydraulic stimulation experiments in low permeability granitic rocks. J Geophys Res Solid Earth 86(B9):7855–7864. https://doi.org/10.1029/JB086iB09p07855

Perkins TK, Kern LR (1961) Widths of hydraulic fractures. J Pet Technol 13(9):937–949. https://doi.org/10.2118/89-PA

Pine RJ, Batchelor AS (1984) Downward migration of shearing in jointed rock during hydraulic injections. Int J Rock Mech Min Sci Geomech Abstr 21(5):249–263. https://doi.org/10.1016/0148-9062(84)92681-0

Portier S, Vuataz FD, Nami P, Sanjuan B, Gérard A (2009) Chemical stimulation techniques for geothermal wells: experiments on the three-well EGS system at Soultz-sous-Forêts, France. Geothermics 38(4):349–359. https://doi.org/10.1016/j.geothermics.2009.07.001

Portier S, Andre L, Vuataz F (2007) Review on chemical stimulation techniques in oil industry and applications to geothermal systems. Technical report in enhanced geothermal innovative network for Europe. CREGE - Centre for Geothermal Research, Neuchâtel; 2007

Rachez X, Gentier S (2010) 3D-hydromechanical behavior of a stimulated fractured rock mass. In: Proceedings world geothermal conference, Bali, Indonesia

Rafiee M, Soliman MY, Pirayesh E (2012) Hydraulic fracturing design and optimization: a modification to zipper frac. In: SPE annual technical conference and exhibition, San Antonio, Texas, USA, SPE-159786-MS. https://doi.org/10.2118/159786-MS

Rathnaweera TD, Wu W, Ji Y, Gamage RP (2020) Understanding injection-induced seismicity in enhanced geothermal systems: From the coupled thermo-hydro-mechanical-chemical process to anthropogenic earthquake prediction. Earth-Sci Rev 205:103182. https://doi.org/10.1016/j.earscirev.2020.103182

Ravier G, Seibel O, Pratiwi AS, Mouchot J, Genter A, Ragnarsdóttir KR, Sengelen X (2019) Towards an optimized operation of the EGS Soultz-sous-Forêts power plant (Upper Rhine Graben, France). In: Proceedings of the European geothermal congress, Den Haag, Netherlands

Riahi A, Damjanac B (2013) Numerical study of hydro-shearing in geothermal reservoirs with a pre-existing discrete fracture network. In: Proceedings of the 38th workshop on geothermal reservoir engineering, Stanford, CA, pp 11–13

Riffault J, Dempsey D, Karra S, Archer R (2018) Microseismicity cloud can be substantially larger than the associated stimulated fracture volume: the case of the Paralana Enhanced Geothermal System. J Geophys Res Solid Earth 123:6845–6870. https://doi.org/10.1029/2017JB015299

Rinaldi AP, Rutqvist J (2019) Joint opening or hydroshearing? Analyzing a fracture zone stimulation at Fenton Hill. Geothermics 77:83–98. https://doi.org/10.1016/j.geothermics.2018.08.006

Rogers S, Elmo D, Dunphy R, Bearinger D (2010) Understanding hydraulic fracture geometry and interactions in the Horn River Basin through DFN and numerical modeling. In: Canadian Unconventional Resources and International Petroleum Conference, Calgary, Alberta, Canada, SPE-137488-MS. https://doi.org/10.2118/137488-MS

Romero AE Jr, McEvilly TV, Majer EL, Vasco D (1995) Characterization of the geothermal system beneath the Northwest Geysers steam field, California, from seismicity and velocity patterns. Geothermics 24(4):471–487. https://doi.org/10.1016/0375-6505(95)00003-9

Rosberg JE, Erlström M (2019) Evaluation of the Lund deep geothermal exploration project in the Romeleåsen Fault Zone, South Sweden: a case study. Geotherm Energy 7(1):10. https://doi.org/10.1186/s40517-019-0126-7

Roussel NP, Sharma MM (2011) Optimizing fracture spacing and sequencing in horizontal-well fracturing. SPE Prod Oper 26(2):173–184. https://doi.org/10.2118/127986-PA

Rubinstein JL, Mahani AB (2015) Myths and facts on wastewater injection, hydraulic fracturing, enhanced oil recovery, and induced seismicity. Seismol Res Lett 86(4):1060–1067. https://doi.org/10.1785/0220150067

Ruina A (1983) Slip instability and state variable friction laws. J Geophys Res Solid Earth 88(B12):10359–10370. https://doi.org/10.1029/JB088iB12p10359

Rutqvist J, Stephansson O (2003) The role of hydromechanical coupling in fractured rock engineering. Hydrogeol J 11(1):7–40. https://doi.org/10.1007/s10040-002-0241-5

Rutqvist J, Freifeld B, Min KB, Elsworth D, Tsang Y (2008) Analysis of thermally induced changes in fractured rock permeability during 8 years of heating and cooling at the Yucca Mountain Drift Scale Test. Int J Rock Mech Min Sci 45(8):1373–1389. https://doi.org/10.1016/j.ijrmms.2008.01.016

Schaefer F, Heinig S (2011) Geothermal project GeneSys, hannover-facies model of the wealden water storage reservoir. In: 1st EAGE sustainable earth sciences (SES) conference and exhibition, cp-268–00110. https://doi.org/10.3997/2214-4609.20144182

Schill E, Genter A, Cuenot N, Kohl T (2017) Hydraulic performance history at the Soultz EGS reservoirs from stimulation and long-term circulation tests. Geothermics 70:110–124. https://doi.org/10.1016/j.geothermics.2017.06.003

Schoenball M, Baujard C, Kohl T, Dorbath L (2012) The role of triggering by static stress transfer during geothermal reservoir stimulation. J Geophys Res Solid Earth 117(B9):B09307. https://doi.org/10.1029/2012JB009304

Schultz R, Skoumal RJ, Brudzinski MR, Eaton D, Baptie B, Ellsworth W (2020) Hydraulic fracturing-induced seismicity. Rev Geophys 58(3):e2019RG000695. https://doi.org/10.1029/2019RG000695

Scuderi MM, Collettini C (2016) The role of fluid pressure in induced versus triggered seismicity: insights from rock deformation experiments on carbonates. Sci Rep 6(1):24852. https://doi.org/10.1038/srep24852

Segall P, Lu S (2015) Injection-induced seismicity: poroelastic and earthquake nucleation effects. J Geophys Res Solid Earth 120(7):5082–5103. https://doi.org/10.1002/2015JB012060

Shapiro SA, Dinske C (2009) Fluid-induced seismicity: pressure diffusion and hydraulic fracturing. Geophys Prospect 57(2):301–310. https://doi.org/10.1111/j.1365-2478.2008.00770.x

Shapiro SA, Krüger OS, Dinske C, Langenbruch C (2011) Magnitudes of induced earthquakes and geometric scales of fluid-stimulated rock volumes. Geophysics 76(6):WC55–WC63. https://doi.org/10.1190/geo2010-0349.1

Shimamoto T, Logan JM (1981) Effects of simulated fault gouge on the sliding behavior of Tennessee sandstone: nonclay gouges. J Geophys Res Solid Earth 86(B4):2902–2914. https://doi.org/10.1029/JB086iB04p02902

Singh I, Miskimins JL (2010) A numerical study of the effects of packer-induced stresses and stress shadowing on fracture initiation and stimulation of horizontal wells. In: Canadian unconventional resources and international petroleum conference, Calgary, Alberta, Canada, SPE-136856-MS. https://doi.org/10.2118/136856-MS

Smith CF, Hendrickson AR (1965) Hydrofluoric acid stimulation of sandstone reservoirs. J Pet Technol 17(2):215–222. https://doi.org/10.2118/980-PA

Sneddon IN, Elliot HA (1946) The opening of a Griffith crack under internal pressure. Q Appl Math 4(3):262–267

Soma N, Asanuma H, Kaieda H, Tezuka K, Wyborn D, Niitsuma H (2004) On site mapping of microseismicity at Cooper Basin, Australia HDR project by the Japanese team. In Proceedings, twenty-ninth workshop on geothermal reservoir engineering, Stanford University, CA, USA

Suckale J (2009) Induced seismicity in hydrocarbon fields. Adv Geophys 51:55–106. https://doi.org/10.1016/S0065-2687(09)05107-3

Summers R, Byerlee J (1977) A note on the effect of fault gouge composition on the stability of frictional sliding. Int J Rock Mech Min Sci Geomech Abstr 14(3):155–160. https://doi.org/10.1016/0148-9062(77)90007-9

Taghichian A, Zaman M, Devegowda D (2014) Stress shadow size and aperture of hydraulic fractures in unconventional shales. J Pet Sci Eng 124:209–221. https://doi.org/10.1016/j.petrol.2014.09.034

Tang H, Winterfeld PH, Wu YS, Huang ZQ, Di Y, Pan Z, Zhang J (2016) Integrated simulation of multi-stage hydraulic fracturing in unconventional reservoirs. J Nat

Gas Sci Eng 36:875–892. https://doi.org/10.1016/j.jngse.2016.11.018

Tao Q (2010) Numerical modeling of fracture permeability change in naturally fractured reservoirs using a fully coupled displacement discontinuity method. Doctoral dissertation, Texas A&M University

Tembe S, Lockner DA, Wong TF (2010) Effect of clay content and mineralogy on frictional sliding behavior of simulated gouges: Binary and ternary mixtures of quartz, illite, and montmorillonite. J Geophys Res Solid Earth 115(B3):B03416. https://doi.org/10.1029/2009JB006383

Tenzer H (2001) Development of hot dry rock technology. Geo-Heat Center Q Bull. 22:14–22

Tester JW, Murphy HD, Grigsby CO, Robinson BA, Potter RM (1986) Fractured geothermal reservoir growth induced by heat extraction (No. LA-UR-86-903; CONF-8604136-2). Los Alamos National Lab. NM (USA)

Tester JW, Brown DW, Potter RM (1989) Hot dry rock geothermal energy: a new energy agenda for the 21st Century. Technical report, Los Alamos National Lab. NM (USA)

Tester JW, Anderson BJ, Batchelor AS, Blackwell DD, DiPippo R, Drake EM, Garnish J, Livesay B, Moore MC, Nichols K, Petty S (2006) The future of geothermal energy. Massachusetts Institute of Technology, 358

Tischner T, Schindler M, Jung R, Nami P (2007) HDR project Soultz: Hydraulic and seismic observations during stimulation of the 3 deep wells by massive water injections. In Proceedings, 32nd workshop on Geothermal Engineering, Stanford University, Stanford, CA, USA

Tsang CF, Neretnieks I (1998) Flow channeling in heterogeneous fractured rocks. Rev Geophys 36(2):275–298. https://doi.org/10.1029/97RG03319

Tsang YW, Tsang CF (1989) Flow channeling in a single fracture as a two-dimensional strongly heterogeneous permeable medium. Water Resour Res 25(9):2076–2080. https://doi.org/10.1029/WR025i009p02076

Valley B, Evans KF (2006) Stress state at Soultz-sous-Forêts to 5 km depth from wellbore failure and hydraulic observations. In: Proceedings, 32nd workshop on geothermal reservoir engineering, Stanford University, Stanford, CA, USA, pp 329–338

Van der Elst NJ, Page MT, Weiser DA, Goebel TH, Hosseini SM (2016) Induced earthquake magnitudes are as large as (statistically) expected. J Geophys Res Solid Earth 121(6):4575–4590. https://doi.org/10.1002/2016JB012818

Veatch RW (1983) Overview of current hydraulic fracturing design and treatment technology–part 1. J Pet Technol 35(4):677–687. https://doi.org/10.2118/10039-PA

Verberne BA, He C, Spiers CJ (2010) Frictional properties of sedimentary rocks and natural fault gouge from the Longmen Shan fault zone, Sichuan, China. Seismol Soc Am Bull 100(5B):2767–2790. https://doi.org/10.1785/0120090287

Verberne BA, Niemeijer AR, De Bresser JH, Spiers CJ (2015) Mechanical behavior and microstructure of simulated calcite fault gouge sheared at 20–600 °C: Implications for natural faults in limestones. J Geophys Res Solid Earth 120(12):8169–8196. https://doi.org/10.1002/2015JB012292

Vermylen J, Zoback MD (2011) Hydraulic fracturing, microseismic magnitudes, and stress evolution in the Barnett Shale, Texas, USA. In SPE hydraulic fracturing technology conference, The Woodlands, Texas, USA, SPE-140507-MS. https://doi.org/10.2118/140507-MS

Vidal J, Genter A (2018) Overview of naturally permeable fractured reservoirs in the central and southern Upper Rhine Graben: Insights from geothermal wells. Geothermics 74:57–73. https://doi.org/10.1016/j.geothermics.2018.02.003

Warpinski NR, Du J, Zimmer U (2012) Measurements of hydraulic-fracture-induced seismicity in gas shales. SPE Prod Oper 27(3):240–252. https://doi.org/10.2118/151597-PA

Warpinski NR, Wolhart SL, Wright CA (2001) Analysis and prediction of microseismicity induced by hydraulic fracturing. In: SPE annual technical conference and exhibition, New Orleans, Louisiana, USA, SPE-71649-MS. https://doi.org/10.2118/71649-MS

Waters GA, Dean BK, Downie RC, Kerrihard KJ, Austbo L, McPherson B (2009) Simultaneous hydraulic fracturing of adjacent horizontal wells in the Woodford Shale. In: SPE hydraulic fracturing technology conference, The Woodlands, Texas, USA, SPE-119635-MS. https://doi.org/10.2118/119635-MS

Westaway R, Burnside NM (2019) Fault "corrosion" by fluid Injection: a potential cause of the November 2017 55 Korean Earthquake. Geofluids 2019. https://doi.org/10.1155/2019/1280721

Willis-Richards J, Watanabe K, Takahashi H (1996) Progress toward a stochastic rock mechanics model of engineered geothermal systemsJ. J Geophys Res Solid Earth 101(B8):17481–17496. https://doi.org/10.1029/96JB00882

Wong SW, Geilikman M, Xu G (2013) Interaction of multiple hydraulic fractures in horizontal wells. In SPE unconventional gas conference and exhibition, Muscat, Oman, SPE-163982-MS. https://doi.org/10.2118/163982-MS

Woo JU, Kim M, Sheen DH et al (2019) An in-depth seismological analysis revealing a causal link between the 2017 M_W 5.5 Pohang earthquake and EGS project. J Geophys Res Solid Earth 124(12):13060–13078. https://doi.org/10.1029/2019JB018368

Wyss R, Rybach L (2010) Developing deep geothermal resources in Switzerland. In: Proceedings of the 2010 world geothermal congress. Bali, Indonesia, p 4

Xing P, Damjanac B, Moore J, McLennan J (2022) Flowback test analyses at the utah frontier observatory for research in geothermal energy (FORGE) site. Rock Mech Rock Eng 55(5):3023–3040. https://doi.org/10.1007/s00603-021-02604-x

Xu J, Zhai C, Qin L (2017) Mechanism and application of pulse hydraulic fracturing in improving drainage of coalbed methane. J Nat Gas Sci Eng 40:79–90. https://doi.org/10.1016/j.jngse.2017.02.012

Yamamoto K, Shimamoto T, Sukemura S (2004) Multiple fracture propagation model for a three-dimensional hydraulic fracturing simulator. Int J Geomech 4(1):46–57. https://doi.org/10.1061/(ASCE)1532-3641(2004)4:1(46)

Yao S, Zeng F, Liu H, Zhao G (2012) A semi-analytical model for multi-stage fractured horizontal wells. In: SPE Canadian unconventional resources conference. https://doi.org/10.2118/162784-MS

Yeo IW, Brown MRM, Ge S, Lee KK (2020) Causal mechanism of injection-induced earthquakes through the

M_w 5.5 Pohang earthquake case study. Nat Commun 11(1):2614. https://doi.org/10.1038/s41467-020-16408-0

Yin Q, Liu R, Jing H, Su H, Yu L, He L (2019) Experimental study of nonlinear flow behaviors through fractured rock samples after high-temperature exposure. Rock Mech Rock Eng 52(9):2963–2983. https://doi.org/10.1007/s00603-019-1741-0

Yin Q, Jing H, Liu R, Su H, Yu L, Han G (2020) Pore characteristics and nonlinear flow behaviors of granite exposed to high temperature. Bull Eng Geol Environ 79(3):1239–1257. https://doi.org/10.1007/s10064-019-01628-6

Yin Q, Wu J, Zhu C, He M, Meng Q, Jing H (2021a) Shear mechanical responses of sandstone exposed to high temperature under constant normal stiffness boundary conditions. Geomech Geophys Geo-Energy Geo-Resour 7:35. https://doi.org/10.1007/s40948-021-00234-9

Yin Q, Wu J, Zhu C, Wang Q, Zhang Q, Jing H, Xie J (2021b) The role of multiple heating and water cooling cycles on physical and mechanical responses of granite rocks. Geomech Geophys Geo-Energy Geo-Resour 7:69. https://doi.org/10.1007/s40948-021-00267-0

Zang A, Wagner FC, Stanchits S, Janssen C, Dresen G (2000) Fracture process zone in granite. J Geophys Res Solid Earth 105(B10):23651–23661. https://doi.org/10.1029/2000JB900239

Zang A, Stanchits S, Dresen G (2002) Acoustic emission controlled triaxial rock fracture and friction tests. In: Dyskin AV, Hu X, Sahouryeh E (eds) Structural integrity and fracture. Swets & Zeitlinger, Lisse, pp 289–294

Zang A, Yoon JS, Stephansson O, Heidbach O (2013) Fatigue hydraulic fracturing by cyclic reservoir treatment enhances permeability and reduces induced seismicity. Geophys J Int 195(2):1282–1287. https://doi.org/10.1093/gji/ggt301

Zang A, Oye V, Jousset P, Deichmann N, Gritto R, McGarr A et al (2014) Analysis of induced seismicity in geothermal reservoirs-an overview. Geothermics 52:6–21. https://doi.org/10.1016/j.geothermics.2014.06.005

Zang A, Stephansson O, Stenberg L, Plenkers K, Specht S, Milkereit C et al (2017) Hydraulic fracture monitoring in hard rock at 410 m depth with an advanced fluid-injection protocol and extensive sensor array. Geophys J Int 208(2):790–813. https://doi.org/10.1093/gji/ggw430

Zang A, Zimmermann G, Hofmann H, Stephansson O, Min KB, Kim KY (2019) How to reduce fluid-injection-induced seismicity. Rock Mech Rock Eng 52(2):475–493. https://doi.org/10.1007/s00603-018-1467-4

Zangeneh N, Eberhardt E, Bustin RM (2015) Investigation of the influence of stress shadows on horizontal hydraulic fractures from adjacent lateral wells. J Unconv Oil Gas Resour 9:54–64. https://doi.org/10.1016/j.juogr.2014.11.001

Zhou X, Ghassemi A (2011) Three-dimensional poroelastic analysis of a pressurized natural fracture. Int J Rock Mech Min Sci 48(4):527–534. https://doi.org/10.1016/j.ijrmms.2011.02.002

Zhou J, Zeng Y, Jiang T, Zhang B (2018) Laboratory scale research on the impact of stress shadow and natural fractures on fracture geometry during horizontal multi-staged fracturing in shale. Int J Rock Mech Min Sci 107:282–287. https://doi.org/10.1016/j.ijrmms.2018.03.007

Zhuang L, Jung SG, Diaz M, Kim KY, Hofmann H, Min KB et al (2020) Laboratory true triaxial hydraulic fracturing of granite under six fluid injection schemes and grain-scale fracture observations. Rock Mech Rock Eng 53(10):4329–4344. https://doi.org/10.1007/s00603-020-02170-8

Zhuang L, Kim KY, Jung SG, Diaz MB, Min KB, Park S, Zang A, Stephansson O, Zimmerman G, Yoon JS (2016) Laboratory study on cyclic hydraulic fracturing of Pocheon granite in Korea. In: 50th U.S. rock mechanics/geomechanics symposium, Houston, Texas, USA, ARMA-2016-163

Ziegler M, Valley B, Evans KF (2015) Characterization of natural fractures and fracture zones of the Basel EGS reservoir inferred from geophysical logging of the Basel-1 well. In: Proceedings world geothermal congress 2015, Melbourne, Australia, pp 19–25

Zimmermann G, Reinicke A (2010) Hydraulic stimulation of a deep sandstone reservoir to develop an Enhanced Geothermal System: laboratory and field experiments. Geothermics 39(1):70–77. https://doi.org/10.1016/j.geothermics.2009.12.003

Zimmermann G, Reinicke A, Brandt W, Blöcker G, Milsch H, Holl HG, Moeck I, Schulte T, Saadat A, Huenges E (2008) Results of stimulation treatments at the geothermal reserach wells in Gross Schönebeck. Proceedings 33rd Workshop on Geothermal Reservoir Engineering. Stanford University, Stanford, CA, USA, pp 96–100

Zimmermann G, Moeck I, Blöcher G (2010) Cyclic waterfrac stimulation to develop an enhanced geothermal system (EGS): conceptual design and experimental results. Geothermics 39(1):59–69. https://doi.org/10.1016/j.geothermics.2009.10.003

Zimmermann G, Blöcher G, Reinicke A, Brandt W (2011) Rock specific hydraulic fracturing and matrix acidizing to enhance a geothermal system-concepts and field results. Tectonophysics 503(1–2):146–154. https://doi.org/10.1016/j.tecto.2010.09.026

Zimmermann G, Zang A, Stephansson O, Klee G, Semiková H (2019) Permeability enhancement and fracture development of hydraulic in situ experiments in the Äspö Hard Rock Laboratory, Sweden. Rock Mech Rock Eng 52:495–515. https://doi.org/10.1007/s00603-018-1499-9

Zoback MD (2010) Reservoir geomechanics. Cambridge University Press, Cambridge, UK

Zoback MD (2012) Managing the seismic risk posed by wastewater disposal. Earth Magazine, pp 38–43